UNIVERSITY OF CALIFORNIA, MERCED

Climatic Controls on Deep Soil Carbon and Nitrogen Dynamics

A dissertation submitted in partial satisfaction of the requirements for the degree Doctor of Philosophy

in

Environmental Systems

by

Kimber Candice Moreland

Committee in charge:

Asmeret Asefaw Berhe, Chair
Stephen C. Hart
Teamrat Ghezzhei
Anthony O'Geen

2020

The Dissertation of Kimber Candice Moreland is approved, and it is acceptable in quality and form for publication on microfilm and electronically:

Asmeret Asefaw Berhe, Chair

Stephen C. Hart

Teamrat Ghezzehei

Anthony O'Geen

University of California, Merced

2020

TABLE OF CONTENTS

LIST OF FIGURES

LIST OF TABLES

ACKNOWLEDGEMENTS

Without the help of 100's of people, I could not have told the stories on this research. I'm massively appreciative of the expertise, help, presence, and love of others in order to do effective research. A massive thank you to Asmeret Asefaw Berhe who has taught me how precious and powerful soil is and has helped me to see my purpose on the planet to help protect soils. She has taught me the value of soil and how our lives and our Earth depend on healthy soils. She has also been a role model to me in how to speak up for what is right even when that is really difficult to do.

Thank you, Karis McFarlane, for believing in me and my science questions. For welcoming me into your lab and for being my science role model in soil carbon research. I am also appreciative of being a part of CAMS and learning from everyone in this group.

Thank you, Stephen Hart, who has taught me integrity in research and how to be meticulous for good work to be published. He has also taught me the kind of example I want to be in my own future lab.

Thank you, Teamrat Ghezzehei, for leading by example in Zen and asking oneself really tough questions in order to create effective science. Your words have a ripple effect on me, and I will carry them throughout my life.

Thank you, Anthony O'Geen for your endless knowledge and understanding of the sites and for helping to dig deep. I also appreciate your support and encouragement throughout this process.

Thank you, Morgan Barnes, for the continued sacrifice in helping to ensure sampling, classification, teaching me mixed effect models, and the extensive data we have collected together. Morgan has also taught me to be a better scientist and believe in myself and I consider her my truest friend.

Thank you, Nicholas Dove, for help with collected the samples, data and for always being a wealth of knowledge, especially in statistics. You also helped me to see my growth and become the person I am today.

Thank you to the numerous people who have helped Morgan and I obtain all this excellent data and samples specifically, Erin Stacy, Michelle Gilmore, Oscar Elias, Susan Glasser, Florence Lucey, and Veronika Ullmann. We could not have done this without you.

Thank you, Tania Gonzalez, for your support for the past six years with my mental health. You were my rock and guidance in the hardest time of my life. I am forever grateful for our conversations and for you helping me to become who I am today.

Thank you, Taylor Broek, Ben Sulman, Fernanda Santos, Allegra Meyer, Kari Finstad, Alex Hedgpeth, and Rebecca Abney for your guidance and leading by example in how to become an excellent junior scientist.

Lastly, thank you the SSCZO funding and sites that I am privileged and honored to have sampled and told the stories of. This is just the beginning of my relationship with soil, of whom I consider a friend, and am inspired to spend the rest of my life protecting.

Funding for this work was provided by the U.S. National Science Foundation, through the Southern Sierra Critical Zone Observatory, Award number: EAR-1331939; and University of California Lab Fees Research Fellowship, Award number: LGF-18-488060/SCW1447 from DOE-BER-TES

CURRICULUM VITAE

Kimber Moreland

University of California, Merced

5200 N Lake Rd, Merced, CA 95340

kmoreland@ucmerced.edu

EDUCATION

University of California, Merced: Ph.D. in Environmental Systems

Adviser: Asmeret Asefaw Berhe 2014-2020

Committee: Teamrat Ghezzehei, Stephen Hart, Anthony O' Geen

Regis University: B.S. Biology

Emphasis in Ecology and Evolution 2008-2012

PUBLICATIONS

Santos, F., Abney, R., Barnes, M., Jin, L., **Moreland, K**., Bogie, N., Sulman, B., Ghezzehei, T. A., Berhe, A. A. (2019). The role of soil physical properties for determining biogeochemical responses to soil warming. *In:* Ecosystem Consequences of Soil Warming: Microbes, Vegetation, Fauna and Soil Biogeochemistry. Editor: Jacqueline Mohan

Tian, Z., Moreland, K., McFarlane, K., Hart, SC., Bales, R., Hartsough, P., O'Geen, A. Berhe, AA. Deep in the critical zone: weathered bedrock represents a large, potentially active pool of soil carbon. (In Review, PNAS)*Dual first author

Reed, C., Berhe, AA., **Moreland, K.,** Wilcox, J., Sullivan, B. (2020). Restoring function: positive responses of carbon and nitrogen to 20 years of hydrologic restoration in montane meadows. (In Review, Ecological Applications)

Manuscripts in preparation

Moreland, K., McFarlane, K., Berhe, AA. (2020). Climatic controls on deep soil organic carbon stabilization in the critical zone. (Submit August 2020)

Moreland, K., A. Berhe, AA. Modeling of climatic impacts on forest soil nitrogen storage from topsoil to bedrock. (Submit August 2020)

CONFERENCE PRESENTATIONS

Moreland, K., McFarlane, K., Berhe, AA., O'Geen, A. 2020. Oral. Deep Subsurface Δ14C partitioning among a bioclimatic gradient. LLNL Biogeochemistry meeting. Livermore, CA

Moreland, K., McFarlane, K., Berhe, AA., O'Geen, A. 2019. Oral. Climatic controls on deep soil organic carbon persistence across a bioclimatic gradient in California. American Geochemical Union. USA

Moreland, K., 2019. Guest lecturer. Soil nutrients and cycling. Soil Science Course. University of California, Merced. USA

Moreland, K., McFarlane, K., Berhe, AA., O'Geen, A. 2019. Poster. Deep Subsurface Δ14C partitioning among a bioclimatic gradient. European Geochemical Conference. Austria

Moreland, K., Tian, Z., Berhe, AA., O'Geen, A. 2019. Poster. CZ Subsoil Carbon: subsoil and regolith constitute significant and dynamic pool of Carbon. Soil Science Society of America Annual Conference. San Diego, CA

Moreland, K., Tian, Z., Berhe, AA., O'Geen, A. 2018. Poster. CZ Subsoil Carbon: subsoil and regolith constitute significant and dynamic pool of Carbon. Annual Southern Sierra Nevada Critical Zone Observatory Meeting. Berkeley, CA.

Moreland, K., Tian, Z., Berhe, AA., O'Geen, A. 2018. Poster. Deep Soil Carbon in the Critical Zone: Climatic influences on the amount and chemical composition of carbon in weathered bedrock. 21st World Congress of Soil Science. 2018

Moreland, K. 2018. BIOTAQ Soil Science Module. Oral. Yosemite High School, CA.

Moreland, K., Tian, Z., Berhe, AA., O'Geen, A. 2018. Oral. Deep Soil Carbon in the Critical Zone: Climatic influences on the amount and chemical composition of carbon in weathered bedrock. Environmental Lunch Seminar, UCM

Moreland, K., Tian, Z., Berhe, AA., O'Geen, A. 2018. Oral. Deep Soil Carbon in the Critical Zone: Climatic influences on the amount and chemical composition of carbon in weathered bedrock. American Geochemical Union. New Orleans, LA.

Moreland, K., Tian, Z., Berhe, AA., O'Geen, A. 2017. Poster. Deep Soil Carbon in the Critical Zone: Climatic influences on the amount and chemical composition of carbon in weathered bedrock. Annual Southern Sierra Nevada Critical Zone Observatory Meeting. CA.

Berhe, AA., **Moreland, K.,** O'Geen, A., 2017. Poster. Deep Coil Carbon in the Critical Zone: amount and nature of carbon in weathered bedrock, and its implication for soil carbon inventory. Critical Zone Science: Current Advances and Future Opportunities. Arlington, VA.

Moreland, K. 2017. Imposter Syndrome, Mental Health, Interpersonal Issues in Graduate School. Oral. Engineering Department Professional Seminar, Merced, CA.

Moreland, K. 2017. BIOTAQ Soil Science Module. Oral. Yosemite High School, CA.

Moreland, K, and AA. Berhe, Fogel, M., O'Geen, A. 2016. Poster. Climatic Controls on Deep Soil Organic Matter in the Critical Zone. Goldschmidt, Yokohama, Japan.

Moreland, K, and AA. Berhe, Fogel, M., O'Geen, A. 2016. Poster. Climatic Controls on Deep Soil Organic Matter in the Critical Zone. Southern Sierra Critical Zone Inter-Annual Meeting, CA

Moreland, K. and C. Kleier. 2012. Poster. Observational flooding effects on Rhizophora mangle. Ecological Society of America Annual Meeting, Portland, OR

Moreland, K. and C. Kleier. 2012. Poster. Observational flooding effects on Rhizophora mangle. SPARC competition, Denver, CO

GRANTS & AWARDS

2020-LLNL Lab directed research directive **($600,000)**

2020-UCM ES Summer Fellowship **($7,000)**

2018-2020 DOE-UC Lab Fees In-Residence Graduate Fellowship **($138,000)**

2018-IUSS Wilford Gardner Travel Fellowship **($1,000)**

2018-Student Nominated Outstanding Graduate Student, UCM

2018-DOE Office of Science Graduate Student Research Award **($38,000)** *

2017-UCM Interdisciplinary Small Grants Program **($3,000)**

2017- UCM ES Professional Development Fellowship **($1,000)**

2017- 2018 CAMS Student Training Fellowship **($10,000)**

2017-GSA Sponsored Event Fund for BIOTAQ **($588)**

2017-GSA Sponsored Event Fund for ESEE **($112)**

2017-Environmental Systems Summer Fellow **($4,300)**

2016-17 Graduate Student Association-Graduate Organization Fund **($400)**

2014-2017 National Science Foundation award through the Critical Zone Award

2016 Environmental Systems Summer Fellow **($6,000)**

2014-15 Science Across Virtual Institutes CZO summer funding **($6,000)**

2013 Regis University Research and Scholarship Council **($5,000)**

2010-2012 Regis University Deans List

2011-SPARC research grant- Regis University **($500)**

2011-1st place SPARC Poster Presentation Award **($80)**

2009-2nd place Hope Illuminated Writing Contest Award

*Awarded, but not accepted because UC Lab Fees Fellowship was awarded first.

LEADERSHIP & SERVICE

2020-"Skype-A-Scientist" leader of section for soil science
2019-LLNL CAMS Elected Writing Group Leader
2017-2019 Environmental Systems Program planning committee
2017-Merced STEAM Center scientist for "Ask-A-Scientist" science fair competition
2017-2019 BiotaQ Outreach Program President
2017-UCM STEM Resource Center, GirlCode Workshop- Leading a sub-section for soils
2017-SSCZO Outreach-taught 20 students about soil science
2017-Lead Naturalist Training on the UCM Vernal Pool Reserve
2016-2018 Elected President of Environmental System Chapter of George Wright Society
2015-Present Women in STEM Mentor/Mentee Program
2015-Present BiotaQ Project Module Co-Founder and Presenter
2014-2018 Elected Environmental Systems Graduate Representative
2013- Regis University Research and Scholarship Council
2013-Regis University Mentoring Project Mentee
2012 RegisCorps Leadership Member
2009-2012 Regis University CHOICES Mentor/Mentee
2009-2012-Regis University SPARC Member

TEACHING EXPERIENCE

UC Merced Teaching Assistant

Soil Science (ESS170L/ES292 30L) 2017

Guest lectures

Fundamentals of soil science (ESS 170) 2019

PROFESSIONAL AFFLIATIONS

American Geophysical Union

Soil Science Society of America

Ecological Society of America

Earth Science Women's Network

Women in Science, Technology, Engineering, and Math

PROFESSIONAL SERVICE

SSSA Meeting Co-Organizer and Moderator of Deep, Wide, and Alive: Expanding Our View of Soils in a Changing Environment — 2019

TECHNICAL SKILLS

Equipment: Certified Operator of LLNL-CAMS NEC 1-MV tandem mass accelerator, High Field Nuclear Magnetic Resonance Spectrometer (liquid-state NMR), CHNO Elemental Analyzer with auto-sampler and Isotopic Mass Spectrometer (^{13}C and ^{15}N), Fourier Transformed Infrared Spectroscopy (DRIFT and ATR), and CO_2 Gas Chromatograph.

Data analyses/coding: Extensive experience with R-programming (linear and nonlinear models (mixed effect/polynomial), SoilR, graphic representation of data in R. ^{14}C data collection, reductions, reporting.

Lab Experience: Extensive wet chemistry experience, density fractionation, low level ^{14}C sample preparation, basic soil analysis (pH, texture, moisture, root separations, soil pit characterization, color, CEC, conductivity, bulk density (hydrometer, plaster cast, etc.), chemical/lab safety, ^{13}C and ^{15}N soil, plant, and root stable isotope preparation.

Field Experience: Extensive soil pit and auguring sampling down to 10 m in depth. Co-lead management and organization of a team with UC-Davis to dig and sample over 20 soil pits in grassland and forested areas. Plant identification, sampling (soil, dust, vegetation, root, water, and microbial sampling), navigation.

ABSTRACT

The soil system stores more carbon than the atmosphere and biosphere combined. However, until recently, most studies on soil organic matter dynamics had focused on near surface soil organic carbon (C) dynamics with relatively little attention devoted to determining how much C and nitrogen (N) is stored in deep soil layers, and how climate influences deep soil organic C and N dynamics. Hence, our understanding of how climate influences the mechanisms that regulate the magnitude and direction of changes in deep soil organic matter remain incomplete. In my dissertation research, I studied soils that developed under four different climatic regimes along an elevation gradient on the western slopes of the Sierra Nevada in California (site of the Southern Sierra Critical Zone Observatory). Using soil samples that were collected from the surface down to bedrock contact (that extended to more than 10 m below the surface), I determined how climate regulates deep soil organic carbon and nitrogen stocks, chemical composition of organic matter, mean residence times of soil carbon and nitrogen at depth; and conducted statistical analyses to determine how variability of climate along the SSCZO bio-climosequence is related to a range of climatic variables. In the first chapter, I found that up to 78% of soil C is stored below a 0.3-m depth, with up to 29% of total C stored in saprock below 1.5 m. A conservative global scaling of these results illustrates that deep regolith stores over 200 Pg of organic carbon quantifying a previously unrealized organic carbon pool in the Earth system. In the second chapter, I dug deeper into C stabilization mechanisms and how climate impacts distribution of C in free and mineral protected pools of soil C. I discovered that the radiocarbon concentration of C in the topsoil and subsoil free particulate and

subsoil mineral associated fractions had a statistically significant relationship with climate. However, the aggregate protected pool of C was not influenced by climate, suggesting that the free particulate and subsoil mineral associated fractions of subsoil C are vulnerable to changes in climate. The third chapter focused on dynamics of soil N in topsoil compared to subsoils and shows that climate imposes important controls on N in topsoil and subsoil free particulate and occluded fractions. The mineral associated N was not found to be sensitive to changes in climate. Overall, my dissertation research demonstrated both indirect and direct mechanisms through which climate can impact soil C and N dynamics from the topsoil to bedrock contact. I presented substantial evidence to refute the long-held assumption that subsoil organic matter does not respond to changes in atmospheric climate.

CHAPTER 1: INTRODUCTION

BACKGROUND

Deep soil layers (below 30 cm or below the A-horizon) can account for up to 70% of the carbon (C) stored in soils (Tian et al. In review). Decomposition of deep soil organic matter (SOM) contributes to surface carbon dioxide efflux, and is controlled by climate, soil physico-chemical properties, and geomorphology of the landscapes and associated hydrology. However, much uncertainty remains in our quantification and process-level understanding of how climate impacts soil C stability and stabilization mechanisms, especially in the subsoil (Rumpel and Kögel-Knabner 2011). My dissertation research investigated climatic controls on near-surface compared to deep soil organic carbon (SOC) and nitrogen (N) storage, stability, stabilization mechanisms, and chemical composition down to 10 meters below the surface in the National Science Foundation-funded Southern Sierra Nevada Critical Zone (SSCZO). Instead of focusing on topsoil or lab incubations that last relatively short periods of time, I investigated the role of ambient climate, in controlling vertical (from topsoil to 10 meters) distribution and persistence on soil organic C (SOC) and total nitrogen (N) cycling in temperate ecosystems along the SSCZO bio-climosequence in an observational study.

Until recently, subsoil C and N dynamics has been the focus of a very limited number of climate or climate change-related studies even though the estimated global average soil thickness is 2 m, with some soils extending past 50 m (Shangguan et al. 2017). By some accounts, 60% of all SOC is found in the subsoil and that pool of, older C (compared to SOM in near-surface soil layers), is vulnerable to loss with increased temperatures

(Jobbágy and Jackson 2000; Rumpel and Kögel-Knabner 2011; Hicks Pries et al. 2017). Generally, with increased depth, SOM concentration decreases and its stability increases, as inferred from radiocarbon-based turnover rates and decomposition rates derived from incubation experiments (Eusterhues et al. 2003). Even though previous studies had documented that decomposition is slower in the subsoil, recent studies have been showing that subsoil SOM is vulnerable to loss and can have important contributions to changes in greenhouse gas effluxes from the soil system in the atmosphere (Rumpel and Kögel-Knabner 2011). Depending on the season, 30%-80% of surface CO_2 efflux could come from deep soil layers (Rumpel and Kögel-Knabner 2011; Berhe et al. 2008). But it remains hard to extrapolate these studies to larger scales as few studies have investigated relevant factors (*e.g.,* C amount, distribution, mineralogical controls, and stability) at depths greater than 1 m. To the best of my knowledge, only a small number of previous studies have quantified C or N amount, distribution, composition, and/or stability in subsoil, in particular in C horizons (Rumpel and Kögel-Knabner 2011). Even less attention has been paid to improving our mechanistic understanding of SOM dynamics across a range of climates (i.e., soil thicknesses, and physical and chemical properties). It is both timely and critical to improve our understanding of key differences in C and N cycling that emerge with depth as deep soils are common and have large contribution to soil C and N stocks globally.

Subsoil OM can be a mixture of new and old SOM, that is rendered relatively stable due to burial, aggregation, its disconnection with decomposers, and chemical association with soil minerals (Marin-Spiotta et al. 2014; Rumpel 2004). Aggregate formation and burial

provide physical stability (physical separation from microbes) for OC. Soils with higher degree of aggregation have been shown to have slower turnover times for SOC (Moni et al. 2010). Soil burial (process, rate, sediment material) is an important physical mechanism for stabilizing SOC at depth particularly in depositional landform positions (Marin-Spiotta et al. 2014). SOC can also form chemical bonds with mineral surfaces. Chemical interaction of organic matter with the mineral phase, in particular amorphous iron (Fe) and aluminum (Al) oxides, was reported to be the main stabilization mechanism in acidic and near-neutral soils and in temperate forests and grassland soils (Rasmussen et al. 2005). According to Eusterhues et al. (2005), the amount of non-oxidizable C present in soil samples from different depths along the soil profile correlated to the ^{14}C activity of the sample, suggesting that SOM in subsoil horizons becomes older, when a greater proportion of SOM is associated with the mineral phase. Understanding climatic effects on these stabilization mechanisms is critical to fully understand how soil C stability will respond to future changes in climate.

Climate change influences on the stability of soil C has been a growing area of study, but investigation of SOC stability in the subsoil has so far been rare (Rumpel and Kögel-Knabner 2011). Subsoil OC stability depends on supply of fresh input (via dissolved organic C by leaching) to stimulate microbial mineralization (Fontaine et al. 2007). The OC becomes vulnerable via the priming effect where microbes mineralized C that was 2,567 years old. Other studies also have found that substrates limit subsoil OM mineralization through a variety of physical and chemical stabilization mechanisms (Marschner et al. 2008). Typically, soils with a longer seasonal duration of moisture

likely increase SOC content whereas drier soils (or frequent wetting/drying) likely reduce the SOC content (Horwath, 2015). Future climate change could cause less of this new OM input to reach the subsoil due to increased temperatures, higher evaporation, and drought. On the other hand, increased or intense rainfall events could periodically stimulate loss of that slower cycling pool of OC (Fontaine et al. 2007). Several important questions remain unanswered, including how changes in temperature and precipitation will influence the stabilization mechanisms of subsoil OC.

Uncertainty surrounding the SOC warming response increases with soil depth because the temperature sensitivity of subsoil OC stability is unknown (Rumpel and Kögel-Knabner 2011). Over the next century, subsoils are projected to warm at roughly the same rate as surface soils (Hicks Pries et al. 2017). Global average soil temperature is predicted to warm the entire profile by 4 °C by 2100 ((IPCC) Intergovernmental Panel on Climate Change 2014). Observed that mineralization of subsoil C may be much more sensitive to temperature change than those of topsoil C (Fierer et al. 2003). One study showed that OC in the subsoil, with residence times in the order of 1000 years, contributed to 20-25% of whole profile soil respiration and up to 10% of the warming response with 4 degree increase in temperature (Hicks Pries et al. 2017). Others showed that a subsurface soil was more susceptible to loss by nutrient inputs and temperature increases (Fierer et al. 2003), while at least one study found that subsurface soil was less responsive to temperature increases compared to the upper horizons (MacDonald et al. 1995). Generally, decomposition and turnover rates used in most previous studies were derived from incubation experiments in the lab and are typically covered around 1 m of

soil depth. There is now a great need for obtaining robust estimates of climatic influences on the stability of subsoil C *in situ* and accounting of the entire soil profile.

The mean residence time of SOC was observed to increase with soil depth (studied up to 1 m), but limited information exists about the composition of the predominantly old OM in B and C horizons, where interaction with the mineral phase is likely the dominant stabilization mechanism (Hemingway et al. 2019; Kaiser et al. 2012). Soil formation processes and root litter input were shown to be crucial factors determining the chemical composition of mineral subsoils (Rumpel et al. 2002). Few studies have investigated the fate of OM compounds in subsoil C with special reference to climate. Aromatic compounds and clay in the B horizons have been assumed to protect polysaccharides against microbial degradation (Schmidt et al. 2000; Schmidt and Kogel-Knabner 2002). However, these studies concentrated on selected soil horizons. Therefore, I investigated the fate of the organic chemical compounds by studying the distribution and composition of OM from the topsoil to depth of 10 m along a bio-climosequence.

Most soil N is in organic molecules that make up soil organic matter (SOM) hence the distribution of the N parallels SOM (Weil and Brady 2016). N is a major nutrient controlling the microbial functioning, plant growth, and the cycling of SOM making it as one of the most important and complex biomolecules to understand (Chapin et al. 2011; LeBauer and Treseder 2008; Houlton and Morford 2015). Globally, soils store up to 50% of N below 30 cm (Batjes 1996), however the current depth of studies is to 23 cm in four prominent soil science journals (Yost and Hartemink 2020). Most studies focus on the topsoil N and therefore are missing subsoil N dynamics, especially when it comes to

understanding how climate controls these N dynamics with depth. Since N cycling influences C sequestration by limiting plant growth, understanding whole profile N accumulation and stability and how it will change with climate is imperative to understand how C sequestration will respond to changes in projected climate (Knocker et al., 2011). My dissertation research improves understanding about how climate is likely impact soil N across the entire soil profile.

To address the above discussed knowledge gaps, my dissertation research examined the effect of climate on the chemical structure, stability, and stabilization mechanisms of the entire profile OC and N to a maximum depth of 10 m. My study took place across the four sites along the National Science Foundation-funded Southern Sierra Critical Zone Observatory (SSCZO) that spans from 405 to 3,000 m.a.s.l. elevation gradient in the Southern Sierra Nevada in California. The soils I studied developed in temperate ecosystems with a Mediterranean-type climate. Vegetation (primary production) changes with elevation due to climate (increases in precipitation and soil water storage). Climate ultimately controls the soil physico-chemical properties and OM concentrations. The SSCZO gradient is particularly well-suited to address the research questions I outline below as it is located along an elevation transect that allows a space-for-time substitution approach to infer the effect of climate change on SOC and N dynamics by comparing data from sites across the elevation gradient.

RESEARCH OBJECTIVES AND HYPOTHESES

The overall objective of my dissertation research is to investigate how climate regulates subsoil OC and N dynamics. My research uses a range of advanced analytical

approaches from soil science, biogeochemistry, and ecology to address focused research questions on climatic effects on SOM chemical composition, stability, and stabilization mechanisms. In study systems located on the western Sierra Nevada bio-climosequence, my dissertation research specifically answers the following questions:

1. How does climate influence whole profile OC and total N (TN) stocks, stability, and stabilization mechanisms?
2. How is the chemical composition of subsoil SOM related to climate?

My dissertation research built upon previous findings of the SSCZO collaboration to improve our understanding of C and N cycling in the critical zone. In particular, my studies provided novel findings that will enables a whole soil C accounting (including O/A to C horizons) and improved mechanistic understanding of SOM dynamics across a range of climates (i.e., soil thicknesses, and physical and chemical properties).

DISSERTATION CHAPTERS

This dissertation is split into the following three chapters:

Chapter 1: *Deep in the critical zone: weathered bedrock represents a large, potentially active pool of soil carbon*

The first chapter focuses on climatic impacts on bulk soil organic C stock, stability and chemical composition. The study used soil samples from topsoil all the way down to bedrock contact along the SSCZO bio-climosequence to demonstrate that C storage in weathered bedrock (Cr horizon, also known as saprock) to determine how much weathered bedrock contributes to soil's carbon storage potential. Further investigation using combination of radiocarbon and Fourier-transformed infrared spectroscopy (FTIR)

was used to determine if old SOM in weathered bedrock is more processed than C in near-surface soil layers. Results presented in this chapter also quantify the potential vulnerability of C in weathered bedrock to changes in climate. This chapter concludes with a global extrapolation of OC in weathered bedrock to determine significance of C storage in deep regolith to global soil C stock. This manuscript is in revision for *Proceedings of the National Academies of Science.*

Chapter 2: *Climatic controls on deep soil organic carbon distribution and persistence*

The second chapter is focused on how climate along the SSCZO bio-climosequence influences distribution of C in soil and persistence of SOC in the different pools. I conducted density fractionation samples (A and B horizon) to separate soil C into three pools: free light (debris inside and outside aggregates, fLF), occluded (oLF), and heavy fractions (OM bound to minerals, HF). The fractionation of soils in to fLF, oLF, and HF isolates SOM that is stabilized by three distinct mechanisms that are presumed to stabilized OM to different extent, and whose effectiveness are based on underlying soil and chemical properties. I quantified mean residence time (MRT) of SOC in each of the fractions, and their variability with depth, using radiocarbon. Furthermore, I used FTIR spectroscopy to determine functional group-level bulk SOM composition and extent of decomposition. A mixed effect model was used to determine climatic impacts on OC held within each fraction and how that changed from the topsoil to the subsoil. I plan to submit this manuscript to *Biogeosciences*.

Chapter 3: *Climatic controls on soil nitrogen stock, distribution, composition, and persistence in deep vs. near-surface soil layers*

The third chapter focuses on climatic impacts on soil N dynamics deep soil layers. Results presented in this chapter present whole profile total soil N stock and how climate influence N in the soil versus the saprock. Then, I determined distribution of soil N in the density fractions to investigate how N is partitioned in soil, and if climate imposes more control on its partitioning in subsoil. Lastly, I analyzed at the stable isotopic $\delta_{15}N$ composition of the fractions, roots, aboveground biomass, weathered bedrock, and the bulk samples to look at ecosystem cycling of N and $\delta_{15}N$ trends with depth. I used a first order kinetic one pool steady state model of soil N in combination with the radiocarbon data to estimate mean accumulation rate and turnover time of N in soil profiles along the bio-climosequence. Furthermore, I used mixed effect model to investigate the climatic impacts on N in the fractions for the topsoil vs. subsoil. I plan to submit this manuscript to *Biogeochemistry*.

SIGNIFIGANCE

Subsoil represents a major, previously unexplored reservoir of soil C. My dissertation research was, as far as I can tell, the first major effort to determine how climate regulates subsoil OC and N storage, chemical composition, stability, and stabilization mechanisms by considering the entire soil profile, from the topsoil to bedrock contact. With the current average soil sampling depth being restricted to the top 23 cm (Yost and Hartemink 2020), we had a long way to go in order to fully understand soil C and N dynamics at depth. By conducting this research along the western slope of the Sierra Nevada bio-climosequence, I was able to investigate climatic effects on subsoil SOM dynamics that is missing from current literature while keeping the other soil

forming factors constant. Understanding how climate influences subsoil C and N dynamics is critical when considering that most subsoils are characterized as having high-mean residence times of as much as several thousand years and as storing more than half of the total soil C stocks. Furthermore, accurate accounting of subsoil C and N storage, chemical composition, and persistence will likely have profound implications for accurate accounting of rates of terrestrial sequestration of atmospheric CO_2, identification of the sources of CO_2 efflux at the soil surface, and improving our understanding of the overall vulnerability/stability of SOC under anticipated climate change. Beyond the scientific contributions, findings from my dissertation research are also likely to inform policy discussions around natural climate change and bio-engineering solutions, including climate-smart land management practices that seek to increase the amount of C that soils can sequester from the atmosphere. Results from my dissertation research will also be critical for future soil C and Earth System models, to enable them to make more informed mathematical functions of how C storage, stability, and vulnerability to loss vary instead of continuing to reply on parameterization of deep soil C and N dynamics that is based on results observed from shallow soil layers. Most importantly, the results from this dissertation will be a call to action for soil scientists to dig deeper in order to better understand the dynamic world of soils.

REFERENCES

Batjes, N.H. 1996. Total carbon and nitrogen in the soils of the world. *European journal of soil science* 47(2), pp. 151–163.

Berhe, A.A., Harden, J.W., Torn, M.S. and Harte, J. 2008. Linking soil organic matter dynamics and erosion-induced terrestrial carbon sequestration at different landform positions. *Journal of Geophysical Research* 113(G4).

Chapin, F.S., Matson, P.A. and Vitousek, P.M. 2011. *Principles of Terrestrial Ecosystem Ecology*. New York, NY: Springer New York.

Eusterhues, K., Rumpel, C., Kleber, M. and Kögel-Knabner, I. 2003. Stabilisation of soil organic matter by interactions with minerals as revealed by mineral dissolution and oxidative degradation. *Organic geochemistry* 34(12), pp. 1591–1600.

Fierer, N., Allen, A.S., Schimel, J.P. and Holden, P.A. 2003. Controls on microbial CO2 production: a comparison of surface and subsurface soil horizons. *Global Change Biology* 9(9), pp. 1322–1332.

Fontaine, S., Barot, S., Barré, P., Bdioui, N., Mary, B. and Rumpel, C. 2007. Stability of organic carbon in deep soil layers controlled by fresh carbon supply. *Nature* 450(7167), pp. 277–280.

Hemingway, J.D., Rothman, D.H., Grant, K.E., et al. 2019. Mineral protection regulates long-term global preservation of natural organic carbon. *Nature* 570(7760), pp. 228–231.

Hicks Pries, C.E., Castanha, C., Porras, R.C. and Torn, M.S. 2017. The whole-soil carbon flux in response to warming. *Science* 355(6332), pp. 1420–1423.

Horwath, W. 2015. Carbon Cycling. In: *Soil microbiology, ecology and biochemistry*. Elsevier, pp. 339–382.

Houlton, B.Z. and Morford, S.L. 2015. A new synthesis for terrestrial nitrogen inputs. *SOIL* 1(1), pp. 381–397.

(IPCC) Intergovernmental Panel on Climate Change ed. 2014. *Climate Change 2013 - The Physical Science Basis*. 1st ed. Cambridge, UK and New York, NY, USA: Cambridge University Press.

Jobbágy, E.G. and Jackson, R.B. 2000. The vertical distribution of soil organic carbon and its relation to climate and vegetation. *Ecological Applications*.

Kaiser, M., Ellerbrock, R.H., Wulf, M., Dultz, S., Hierath, C. and Sommer, M. 2012. The influence of mineral characteristics on organic matter content, composition, and stability of topsoils under long-term arable and forest land use. *Journal of Geophysical Research* 117(G2).

LeBauer, D.S. and Treseder, K.K. 2008. Nitrogen limitation of net primary productivity in terrestrial ecosystems is globally distributed. *Ecology* 89(2), pp. 371–379.

MacDonald, N.W., Zak, D.R. and Pregitzer, K.S. 1995. Temperature effects on kinetics of microbial respiration and net nitrogen and sulfur mineralization. *Soil Science Society of America Journal* 59(1), pp. 233–240.

Marin-Spiotta, E., Chaopricha, N.T., Plante, A.F., et al. 2014. Long-term stabilization of deep soil carbon by fire and burial during early Holocene climate change. *Nature Geoscience* 7(6), pp. 428–432.

Marschner, B., Brodowski, S., Dreves, A., et al. 2008. How relevant is recalcitrance for the stabilization of organic matter in soils? *Journal of Plant Nutrition and Soil Science* 171(1), pp. 91–110.

Moni, C., Rumpel, C., Virto, I., Chabbi, A. and Chenu, C. 2010. Relative importance of sorption versus aggregation for organic matter storage in subsoil horizons of two contrasting soils. *European journal of soil science* 61(6), pp. 958–969.

Rasmussen, C., Torn, M.S. and Southard, R.J. 2005. Mineral assemblage and aggregates control carbon dynamics in a california conifer forest. *Soil Science Society of America Journal* 69(6), p. 1711.

Rumpel, C. 2004. Location and chemical composition of stabilized organic carbon in topsoil and subsoil horizons of two acid forest soils. *Soil Biology and Biochemistry* 36(1), pp. 177–190.

Rumpel, C. and Kögel-Knabner, I. 2011. Deep soil organic matter—a key but poorly understood component of terrestrial C cycle. *Plant and soil* 338(1–2), pp. 143–158.

Rumpel, C., Kögel-Knabner, I. and Bruhn, F. 2002. Vertical distribution, age, and chemical composition of organic carbon in two forest soils of different pedogenesis. *Organic geochemistry* 33(10), pp. 1131–1142.

Schmidt, M.W.I., Knicker, H. and Kögel-Knabner, I. 2000. Organic matter accumulating in Aeh and Bh horizons of a Podzol — chemical characterization in primary organo-mineral associations. *Organic geochemistry* 31(7–8), pp. 727–734.

Schmidt, M.W.I. and Kogel-, I. 2002. Organic matter in particle-size fractions from A and

B horizons of a Haplic Alisol. *European journal of soil science* 53(3), pp. 383–391.

Shangguan, W., Hengl, T., Mendes de Jesus, J., Yuan, H. and Dai, Y. 2017. Mapping the global depth to bedrock for land surface modeling. *Journal of Advances in Modeling Earth Systems* 9(1), pp. 65–88.

Weil, R. and Brady, N. 2016. *The Nature And Properties Of Soils (15th Edition)*. 15th ed. Columbus: Pearson.

Yost, J.L. and Hartemink, A.E. 2020. How deep is the soil studied – an analysis of four soil science journals. *Plant and soil*.

Tian, Z ., Moreland, K., O'Geen, A., et al. In review. Deep in the critical zone: weathered bedrockrepresents a large and potentially active pool of soil carbon.

CHAPTER 2: DEEP IN THE CRITICAL ZONE: WEATHERED BEDROCK REPRESENTS A LARGE, POTENTIALLY ACTIVE POOL OF SOIL CARBON

ABSTRACT

Large uncertainty remains in the spatial distribution of deep soil carbon storage and how climate controls belowground C. Here, we present whole-regolith carbon stocks, radiocarbon age, and chemical composition down to 10-m. Up to 78% of soil C is stored below a 0.3-m depth, with up to 29% of total carbon stored in saprock below 1.5 m. A conservative global scaling found that deep regolith stores over 200 Pg of organic carbon. Radiocarbon, spectroscopy, and isotopic analyses revealed that deep soil and weathered bedrock carbon is a combination of both relatively fresh material and older, more decomposed carbon. Collectively, this work illustrates that carbon in saprock represent a massive, previously unrealized carbon pool, that is potentially susceptible to losses caused by changes in climate.

INTRODUCTION

Soil is the largest terrestrial carbon (C) reservoir on Earth, storing over 3000 Pg organic carbon (OC) (Le Quéré et al., 2014). Up to 60% of terrestrial soil OC is found in subsoil layers (from depths between 0.3 to 1.0 m), but few studies report soil OC data below a 1.0 m depth (Jobbágy & Jackson 2000; Richter & Markewitz 1995; Jackson et al., 2002; Harper & Tibbet, 2013). Subsoil OC is typically old with residence times on the order of 1000 years or more (Marin-Spiotta et al., 2011). Despite its long residence time, subsoil OC is projected to become more susceptible to loss, and could account for 25% of soil respiration under conditions that are expected to occur with climate warming (Hicks-Preis et al., 2018). Restriction of soil OC stock estimates to the upper layers of soil has been leading to underestimation of global soil OC stocks and limits our understanding of how regolith OC responds to changes in climate.

Organic C storage, persistence, chemical composition, and stabilization mechanisms are fundamentally distinct in surface soil and subsoil. Compared to subsoil, OC concentration in near-surface soil horizons is typically higher with shorter mean residence times (Jobbágy & Jackson 2000; Chabbi et al., 2009). The rate of organic matter (OM) decomposition is slower in subsoil compared to topsoil, largely due to lower concentration of OC and lower microbial abundance, as well as and physico-chemical differences (burial, aggregation, high degree of organo-mineral association) (Rumpel & Kögel-Knabner, 2011; Chabbi et al., 2009; Schrumpf et al., 2013). However, despite its persistence, OC in subsoils can be vulnerable to mineralization due to changes in climate

(Jobbágy & Jackson 2000; Chabbi et al., 2009; Melillo et al., 2002; Davidson & Janssens, 2006; Berhe et al., 2007), including warming (Hicks-Pries et al., 2018). Little is known about the dynamics of SOC in regolith because it is hidden deep below the Earth's surface. This imposes unique sampling challenges and requires substitutions of space-for-climate, in the form of a bioclimatic gradient, to assess the susceptibility of deep SOC to climate change.

We investigated the distribution, stability, and chemical composition of OM in regolith to the depth of hard bedrock, that included the mineral soil and saprock (maintains the original rock texture but is porous and friable; total regolith spanning 2-10 m) along a 2300-m bio-climosequence in the southern Sierra Nevada in California (Fig. 2-1; Table 2-4). Climate gradients, with increasing elevation include decreasing temperature, and increasing precipitation and deep water percolation, (calculated as the difference between precipitation and evapotranspiration). We used the Southern Sierra Nevada Critical Zone Observatory to infer the effect of climate on OC, a site particularly well suited to address these research objectives as it is located along a well-characterized elevation transect with soils ranging from Entisols to Alfisols, representing a range of soil properties and vegetation cover. Analysis of OC down to 10 m enabled us to conduct a whole-regolith OC accounting and derive mechanistic understanding of OM dynamics across a range of environmental conditions (i.e., soil thicknesses, physical and chemical properties, vegetation, and soil types).

MATERIALS AND METHODS

SITES DESCRIPTION

The four study sites were located along an elevation transect, from 405 m to 2700 m, on the western slope of the southern Sierra Nevada, California. Vegetation changes with elevation in response to changes in climate (Table 2-2). All the sites experience a Mediterranean-type climate with cool, moist winters, and warm, dry summers. Soils have formed from granitic bedrock. The granitic substrate across the sites is hypothesized to be of comparable age with the exception of the highest elevation site where bedrock was scoured by glaciers during the last glacial maximum (Giger & Schmitt et al., 1983).

REGOLITH SAMPLING

A total of thirty-six regolith profiles were analyzed (Table 2-3): three Geoprobe cores (a hydraulic coring device, Model DT22) and four pits excavated by a backhoe were sampled at the oak savannah site (405 m); five Geoprobe cores, five hand augers, and five pits were sampled at the ponderosa pine/oak forest site (1160 m); five Geoprobe cores, one hand auger, and four pits were sampled at the mixed-conifer forest site (2015 m); and four pits were excavated at the subalpine forest site (2700 m). To collect regolith cores, a Geoprobe sampler was used from the soil surface to depth of refusal. Hand augering (with a depth limitation of 7.6 m) was used at a subset of sites that could not be accessed by the Geoprobe vehicle. Geoprobe and hand auger samples at adjacent locations were compared to ensure that there was no sampling effect on OC distributions.

Soil pits were sampled by genetic horizons and samples were collected at 20 to 50 cm intervals by the Geoprobe and hand-auger. Regolith was partitioned into soil and saprock.

Saprock was identified as having brittle consistency and rock fabric (Graham et al., 2010). With hand augers, the depth of transition from soil to saprock was identified in the field by a change in color and consistency. Within saprock, layers were identified based on color and fabric features including mineral grain size and orientation.

CARBON AND NITROGEN ANALYSES

Soil and saprock materials were air-dried, gently crushed by a rolling pin, and sieved (2 mm mesh openings). Percentage of fine-earth fraction (< 2 mm) and coarse earth fraction (> 2 mm) were measured based on air-dry mass. The coarse fraction was assumed to have no OC. Gravimetric water content was determined on air-dried subsamples by drying overnight at 105 °C. Total C and N concentration (%) of the fine-earth fraction was determined on samples ground to pass a 180- μm sieve and analyzed by dry combustion (Costech Analytical ECS 4010 instrument, Costech Analytical Technologies, Inc., Valencia, CA). The average signal detected from samples of low concentration (354 ± 162 (s.d.0), n=10) was significantly larger than the blank (15 ± 14 (s.d.), n=9). Most samples had pH values below 6.0, so we assumed no inorganic C was present in these samples. However, we pretreated a subset of samples having the highest pH values (6.8-7.0) with hydrochloric acid and in all cases the acid pretreatment did not result in a significant reduction in total C. Hence, total C was equivalent to total organic C in our samples.

Bulk density of soil and saprock was measured using the core method (Dane et al., 2002). Three core samples were taken in each horizon from three soil profiles and averaged. They were oven-dried at 105 °C and the > 2 mm fraction and roots were removed. Bulk density of lower saprock was measured by cutting an exact volume from the bottom 5-cm of each core, which was sampled by the Geoprobe at 1 m depth intervals and oven-dried at 105 °C.

Total OC inventory (C_S, kg C m^{-2}) was calculated from total OC concentration (C, g kg^{-1}), thickness of the sample layers (d_C, cm) and mean bulk density (ρ_b, Mg/m^3), with correction for the weight percent of coarse earth fraction (Eq. 2-1).

$$C_s = \sum C \times d_c \times \rho_b \times 100 \quad (2\text{-}1)$$

Total OC density (C_d, kg C m^{-3}) was calculated by OC concentration of total regolith thickness, soil thickness (d, cm), and saprock thickness (Eq. 2-2).

$$C_d = C_s / \sum d \quad (2\text{-}2)$$

Multiple depth profiles (see Table 2-4 for n) of OC were aggregated over 0.10-m depth intervals to create an average OC depth profile (Fig. 2-2) using the R package Algorithms for Quantitative Pedology (AQP). Polynomial and linear regression models were performed to explore possible correlations between the climatic parameters (temperature, precipitation, and deep water percolation) and C_s and C_d. The square of the correlation

coefficient (adjusted R_2) was calculated by the "Pearson" method on individual soil and saprock samples, and significance of regression model was evaluated by p-value ≤ 0.001. All analysis and graphs were conducted in R version 3.3.

DIFFUSE REFLECTANCE INFRARED FOURIER TRANSFORM (DRIFT) SPECTROSCOPIC ANALYSES

Soil and saprock subsamples were analyzed for OM composition via Diffuse Reflectance Infrared Fourier Transform spectroscopy. Mid-IR spectra (400 to 4000 cm^{-1}) were recorded using an IR spectrophotometer (Bruker IFS 66v/s, Ettlingen, Germany) and a Praying Mantis DRIFT sampler (Harrick Scientific Corporation, Ossining, NY). Before analysis, all samples were finely ground to a powder consistency using a ball mill (SPEX Sample Prep Mixer Mill 8000C, Metuchen, NJ, USA) and then dried at 60 °C for 24 hours; oven-dried samples were kept in a desiccator prior to analyses. Finely ground and oven-dried potassium bromide (Aldrich Chemical Company, Saint Louis, MO, USA, FT-IR grade) was used as a background reference for all FTIR analyses. We used 500 background scans and 500 sample scans with a 4 cm^{-1} resolution. All spectra were tangentially baseline corrected. Peak areas were calculated that corresponded to local baselines to remove impacts from larger spectral features and tails (Kalbitz & Kaiser 2008). Using "approxfun" and "integrate" functions in R version 0.98.1028, the areas of peaks were calculated by subtracting the area of the baseline between each endpoint (Hall et al., 2018).

Several studies have used ratios of specific spectral bands to study chemical composition of soil OM (Artz et al., 2006; Calderón et al., 2006; Ellerbrock et al., 2005). The FTIR spectra were analyzed to determine level of OM transformation that is derived from decomposition using a ratio of peak heights at areas of interest. Peaks heights at 2925 and 2850 cm^{-1} (spanning 2898–2976 and 2839–2870 cm^{-1}) indicate aliphatic C–H asymmetric and symmetric stretches. Peak heights at 1648 cm^{-1} (spanning 1570–1710 cm^{-1}) indicate C=O stretch of amides, quinones, and ketones, with constituents coming from C=C. A clearly distinguishable shoulder at 1512 cm^{-1} (spanning 1500–1550 cm^{-1}) is indicative of the aromatic C=C stretch. A pronounced peak at 1400 cm^{-1} (spanning 1360–1450 cm^{-1}) reflects the carboxylate C–O (COO) stretch. Ratios of these areas of peak heights were used as an index for degree of OM processing during decomposition (Kaiser et al., 2012; Ryals et al., 2014).

RADIOCARBON ANALYSIS

Radiocarbon analyses was conducted on soil samples after sealed-tube combustion of OC to CO_2 (with CuO and Ag) that was then reduced onto Fe powder in the presence of H_2 (Vogel et al. 1984). Radiocarbon values were measured in 2018 on the Van de Graaff FN accelerator mass spectrometer at the Center for Accelerator Mass Spectrometry at the Lawrence Livermore National Laboratory. Organic matter $\delta^{13}C$ values were determined at the University of California Merced using a DELTA V Plus Isotope Ratio Mass Spectrometer (Thermo Fisher Scientific, Inc., Waltham, MA, USA). Radiocarbon isotopic values were corrected for mass-dependent fractionation with measured $\delta^{13}C$

values and were reported in Δ-notation corrected for ^{14}C decay since 1950 (Stuiver & Polach et al., 1977).

ESTIMATING THE GLOBAL REGOLITH OC POOL

A global scenario of regolith C was created from the World Soil Information Service (WoSIS) database (Batjes et al., 2016). Soil OC content and bulk density, corrected by coarse fraction percent, were used to calculate the C stock (Eq. 2-1) for four different conditions: 1. all soils in the database to a depth of 2.5 m or bedrock, whichever was shallower (6,947 soil profiles); 2. the C stock in the upper 1 m (6,947 soil profiles); 3. a hypothetical C stock assuming a saprock thickness of 4 m where the C concentration of the lower most depth was allocated to the entire theoretical (4 m) thickness; and 4. an entire regolith thickness (soil plus the theoretical saprock defined above). The land area for estimation of a global regolith OC pool was determined by aggregating climatic and lithological classes from the global ecological land unit (ELUs) database (Sayre et al., 2014) using ArcGIS. We created a scenario where thickness of regolith was 5 m under all rock types, which represented the mean thickness across the SSCZO gradient. The global area of estimation was limited to bioclimatic conditions that were conceivably warm and wet enough to have the capacity to form a thick regolith across all bedrock types (sedimentary, metamorphic and igneous). Thus, very cold environments and arid environments were excluded from this scenario. The scenario was further constrained to show the C stock in these bioclimates on igneous intrusive rocks (plutonic rocks) that more closely reflected the conditions of our measurements.

The soil OC pool was calculated by accumulated OC stock and land area (Eq. 2-3):

$$C_i = C_s \times A \tag{2-3}$$

where C_i is total OC inventory, C_s is accumulated OC stock, A is land area.

The saprock OC pool was calculated by depth-weighted OC density, regolith thickness, and land area (Eq. 2-4):

$$C_i = C_d \times d \times A \tag{2-4}$$

where C_d is depth-weighted OC density, d is thickness of regolith.

DRIFT-FTIR MINERAL CONTENT TESTING

DRIFT-FTIR was analyzed on regolith and soil samples before and after organic matter removal (by ashing in a muffle furnace) to subtract out the mineral signature to help determine if the regolith sample results showed evidence of mineral interference and if the regolith samples were too low in C to show peaks in the targeted areas. Samples were ashed with the furnace at 430 °C for 8 hours. This is an extra precaution to confirm the integrity of the results. All of the samples used for the ponderosa pine site (35 samples) from the pit and geoprobe samples were ashed with the furnace at 430 °C for 8 hours. Bulk soil and regolith results were compared with post-ashing samples and were analyzed in the same manner as all of the other samples. The bulk samples and post-ashing samples look almost identical with only minor differences in peak ratios of interest. This illustrates that even though regolith is low in OM the peaks do represent the OC in those samples and the mineral portion does not impact the OM peaks.

RESULTS

Variability in OC concentration was low in saprock (Fig. 2-2; s.d.: 0.15-0.94 g/kg, n=27) suggesting that the effect of climate on deep regolith OC storage is primarily through its effect on thickness, not concentration of deep OC. Climate along the western slope of the southern Sierra Nevada exerts strong controls on weathering and net primary productivity (NPP) (Dahlgren et al., 1997). Plant productivity and weathering are limited by low precipitation in the lowest elevation oak savannah ecosystem, and low temperature and historic glaciation in the high-elevation subalpine forest ecosystem. Middle elevation sites (ponderosa pine/oak and mixed-conifer forests) have climatic conditions optimal for chemical weathering (Tian et al., 2019; Dixon et al., 2009) (regolith thickening) and NPP (Kelly et al., 2016). Regolith thickness ranged from 1.0 to 10.7 m across the climosequence and was thickest at the middle elevations (Fig. 2-1). Soil OC concentration and inventory were highest at the mid-elevation sites, where NPP is not limited by climate (Kelly et al., 2016; Goulden et al., 2014). Average OC concentration decreased from 26 g/kg in surface soil (A horizon) to 0.2 g/kg in deep saprock. The range in OC concentration in saprock was consistent with previous studies (0.3 - 0.4 g/kg) in Australia where regolith thicknesses ranges from 5 to 38 m, and in eastern USA with regolith depths of 6 m (Richter & Markewitz, 1995; Harper & Tibbet, 2013).

While soils exhibited the largest OC inventory at every site, saprock accounted for a substantial proportion (over 25%) of total OC stock at mid-elevations (Fig 2-1). In soil, OC stock increased with elevation to a maximum of 19 kg OC m^{-2} in mixed-conifer forest (2015 m), but decreased to 11 kg OC m^{-2} in subalpine forest (2700 m) to levels

near that of ponderosa pine/oak forest (13 kg OC m^{-2}; Fig. 2-1; Table 2-4). The relative proportion of OC stock in soil (compared to saprock) decreased from oak savannah (405 m), ponderosa pine forest (1160 m) to mixed coniferous forest (2015 m) except in subalpine forest (2700 m), because this site did not have deep regolith (Fig. 2-1). The proportion of OC stock in saprock had an opposite trend to that of soil; increasing with elevation in saprock; decreasing with elevation in soil (Fig. 2-1). This trend reflects the thicker saprock at the two mid-elevation sites.

ORGANIC CARBON STORAGE IN SOIL AND SAPROCK

While deep saprock $\Delta^{14}C$ values suggest, on average, relatively old OC is present in saprock, fluctuations with depth imply a mixture of old and younger OM. This result is likely due to the mean $\Delta^{14}C$ value of OM in saprock having input of relatively newer OM from overlying soil layers via downward percolation of dissolved organic matter (DOM), and deep regolith exploration of roots and mycorrhizae. Across all sites, topsoil (A-horizon) $\Delta^{14}C$ values indicated that soil OC was dominantly composed of modern OM ($\Delta^{14}C$ -70 to 120‰, Fig. 2-2b). At all sites, $\Delta^{14}C$ of OC became increasingly lower with depth. Surprisingly, the lowest $\Delta^{14}C$ value (-921‰ or 20,300 y BP average radiocarbon age) was found in saprock at 6 m depth in mixed-conifer forest site, while younger OC in saprock was found at 9.5 m depth (-456‰ or 4,800 y BP average radiocarbon age).

CHEMICAL COMPOSITION TO INFER PROCESSING OF ORGANIC MATTER IN SOIL VS. REGOLITH

Ratios of peak areas derived from Diffuse Reflectance Infrared Fourier Transform (DRIFT) spectroscopy were used to infer abundance of chemical functional groups, and biochemical proxies for decomposition-related processing of OM (Kaiser et al. 2012). We computed these ratios following methods outlined in Hall et al. (2018). Interestingly, at all sites, some samples below 2 m show similar ratios to topsoil (Fig. 2-2). This suggests that in places old OC in deep regolith is not necessarily more decomposed than it is in overlying soil. There was little change in the ratio of C=C/COO (Fig. 2-2d) for all sites, except for a few samples in mixed conifer pine/oak forest that have high C=C/COO ratios (~175 m) overlying relatively low ratios (~5.5 and 7 m; Fig. 2-2d). There was a gradual decrease in both C-H/COO (Fig. 2-2f) and C-H/C=O (Fig. 2-2g) with depth for all sites. There were sharp increases in these peaks in both of the mid-elevation sites at multiple points in soil and saprock. Infrequent sharp increases in this relationship, especially for ponderosa pine/oak forest and mixed conifer forest at mid-elevation sites, likely suggest presence of OM that is more plant/root derived in nature (Hall et al., 2019; Ryals et al., 2014). These attributes are further confirmed by the slight increase in the C=C/C=O (Fig. 2-2e) with depth. It is also interesting to note that soil OM chemical composition in the oak savannah is distinct from other sites, suggesting vegetation type/root depth plays a role in distribution and transformations of OM in soil.

The C:N mass ratio decreased slightly with depth and aligns with FTIR indices of decomposition (Fig. 2-2). We observed a decreasing trend in C:N ratio with depth, except

at the oak savannah site, suggesting that OM in deep regolith is more processed OM than in topsoil (Rumpel & Kögel-Knabner, 2011; Batjes, 2016), or consists of mineral-associated SOM that typically has a low C:N ratio (von Lützow et al., 2007). However, C:N values show variability with depth, possibly reflecting a mixture of OM processed to different degrees in saprock. It is also possible that variability in C:N ratio with depth is due to the nature of vegetation. Given the radiocarbon abundance of deep C, at around 4-m depth for mid-elevation sites, it is possible that deep C:N ratios reflect a past vegetation type. For example, analysis of pollen records and packrat middens indicate a sagebrush steppe existed at mid-elevations in the Sierra during the last glacial maximum, and the transition from steppe to forest is believed to have occurred about 10,000 years ago (Anderson, 1990; 1996; Woolfenden et al., 1996).

SOURCE OF DEEP C

At the SSCZO, previous studies have shown that roots extend into saprock through fractures to access deep water (Bales et al., 2011; Stone & Kalisz, 1991; Hubbert et al., 2001; O'Geen et al., 2018). Roots may extend to the base of the regolith profile to access water directly or with mycorrhizal hyphae that are associated with tree and chaparral roots (Witty et al., 2003; Egerton-Warburton et al., 2003). Considering the very old OM found in regolith, dead roots or root exudates could be a major source of this old OM as previous studies have shown that root derived OM can be preferentially retained by minerals (Bird & Torn 2006; Rasse et al., 2006), and can be more protected and readily stabilized in soil than other sources of OM (Denef & Six, 2006). In addition, this OM in saprock lacks readily available OC sources and constant cool temperatures at depth limiting microbial

activity and is likely to be protected by physical separation from soil microbes, and mineral protection (Salome et al., 2010). In soils derived from granitic parent material, soil OC enters saprock via deep percolation through the coarse overlying soil layers and via preferential flow paths created by rock fracturing during physical and biogeochemical weathering processes. If otherwise easily decomposable dissolved organic matter (DOM) leaches down the soil profile, it can persist in regolith for longer periods of time if it forms chemical association with secondary minerals. For example, if DOM is sorbed on surfaces of secondary minerals or it (co-)precipitates with aluminum (Al) and iron (Fe) oxides it can persist for long periods of time (Kalbitz & Kaiser 2008). However, regolith in the Sierra Nevada displays minimal degree of alteration by chemical weathering. The clay content is below 8% and the pedogenic iron concentration (dithionite extractable Fe) is well below that of overlying soil (Tian et al., 2019). Reactive soil constituents that can provide physical or chemical stabilization to OM in saprock are not uniformly distributed with depth. Elevated levels of secondary weathering products capable of stabilizing OC have been shown to be concentrated in zones around roots and fractures within saprock (Frazier & Graham, 2000). Hence, it is possible that stabilization of OM through association with soil minerals is limited to patches around roots and rock fractures.

CLIMATE SENSITIVITY OF DEEP C

An important question is how climate influences deep OC. To address this question, we tested the variability of soil and saprock OC storage with changes in MAT, MAP, and DWP across the SSCZO bioclimatic gradient. Soil OC inventory (kg C m^{-2}) and density (kg C m^{-3}) has a positive correlation with MAP and DWP and was negatively correlated

with MAT (Fig. 2-3). Correlations between soil OC and climatic variables reflected peak storage at mid elevations where temperatures were mild and precipitation was relatively high. Correlations were nonlinear likely because NPP is limited in subalpine forest by low temperatures (Goulden & Bales 2014). Correlation between soil OC and climate variables is consistent with other studies across different climatic life zones (Post et al., 1982). Regression analysis shows that MAT explained more variability in OC inventory than other climatic variables tested (Fig. 2-3), suggesting that OC storage in soils is vulnerable to climate warming. The inventory of OC trends in saprock was similar to soil, however, OC density in saprock had a slightly different climatic response (Fig. 2-3).

Changes in OC density and inventory across the climate gradient reveal an intricate role of deep regolith in C cycling. Overall, we observed different amounts of deep OC in regolith at four climatic zones, with highest OC storage at mid-elevations (Fig. 2-3 a-c) where climate is most conducive to weathering (i.e., regolith thickening) and NPP is high. With a slope near zero, OC density (g m^{-3}) in saprock (Fig. 2-3 d-f) was insensitive to differences in climate. Uniformity of OC density in saprock across the gradient may be a result of the climatic effect being dampened by cool, stable temperatures at depth relative to soils, which experience dynamic swings in temperature and moisture (Tian et al., 2019). In deep regolith, year-round cool temperatures coupled with low microbial activity (Rumpel, C. & Kögel-Knabner, 2011; Chabbi et al., 2009) provides evidence to explain why old and new OC (OC input from dissolved OM and roots) coexist along with data suggesting fresh and highly degraded C mixtures (Fig. 2-2).

Climate can affect OC inventory in deep regolith indirectly through thickening of the weathering profile. This is indicated by positive linear correlations between climatic variables and OC inventory (kg C m^{-2}) of saprock (Fig. 2-3a-c). Mid-elevation sites have thicker regolith due to climatic regimes that favor weathering (wetter and kinetically favorable temperatures), transforming bedrock into a friable and porous parent material that can accommodate roots and percolating DOC (Dahlgren et al., 1997; Tian et al., 2019; Graham et al., 2010).

GLOBAL EXTENT OF DEEP SOIL OC STORAGE IN REGOLITH

We developed a conservative global estimate of OC stock in deep regolith from the World Soil Information Service (WoSIS) database and global ecological land units (Sayre et al., 2014) to evaluate the potential magnitude of deep C relative to the global terrestrial OC budget. The global area of estimation was limited to bioclimatic conditions that were conceivably warm and wet enough to form a relatively thick regolith (5 m) across all rock types. Thus, very cold environments and arid environments were excluded from this scenario. To more closely mimic conditions of our measurements, the scenario was further constrained to show the OC stock in igneous intrusive rocks (plutonic rocks). The scenario demonstrates that subsoil and saprock OC can account for a significant fraction of the "hidden" OC sink in the global OC budget (Table 2-1). The hypothetical OC inventory for saprock in all rock types was on average 201 Pg (s.d. 257 Pg), in excess of the unbalanced global OC budget (118 Pg) (Houghton et al., 2007); although the median value was 79 Pg. Considering only igneous intrusive rocks (plutonics) in this global scenario saprock accounted for an average of 28 Pg C.

CONCLUSION

Our findings demonstrate that regolith thickness, which is governed in part by climate, directly influences deep OC inventory and indirectly influences OC cycling. The large stock of persistent OC in saprock represents a previously unexplored pool of OC in the Earth system. Our analysis provides a deeper understanding of the processes regulating OC input, storage, and turnover to improve estimations of the true capacity of the critical zone to store OC and the vulnerability of deep OC to changes in climate. Overall, we observed significant and varying amounts of deep OC at the four climatic zones, with the highest OC storage occurring at mid elevations where climate is most conducive to weathering and NPP.

Over the next century, subsoils are projected to warm at roughly the same rate as surface soils. Global average soil temperature is predicted to warm the entire profile by 4°C by 2100 (Metz et al., 2007). The effect of a temperature increase on C cycling is less certain in deep saprock, were temperature swings are muted and OC is isolated from high rates of microbial activity. However, our results show that OC in saprock is a mixture of relatively young and old OM that has experienced different degrees of decomposition. If relatively younger OM is entering saprock and diluting the old OM pools (see supplemental information), then climatic factors are likely to influence not only the amount, but also the composition and persistence of OM in regolith. Specifically, temperature exerts a strong control on regolith OC storage and dynamics through both its effects on plant productivity and OC input into the deep regolith. Our study provides compelling evidence to justify further investigations in different ecosystems of soil and

deep regolith OC sensitivity to changes in temperature critical for predictions of future response of terrestrial OC to climate (Carvalhais et al., 2014).

ACKNOWLEDGEMENTS

Funding: U.S. National Science Foundation, through the Southern Sierra Critical Zone Observatory, Grant/Award number: EAR-1331939; and UC Lab Fees Research Fellowship, Award number: LGF-18-488060/SCW1447 from DOE-BER-TES

REFERENCES

Anderson, R. S. Holocene forest development and paleoclimates within the central Sierra Nevada, California. *The Journal of Ecology*, 470-489 (1990).

Anderson, R. S. Postglacial biogeography of Sierra lodgepole pine (Pinus contorta var. murrayana) in California. *Ecoscience* 3, 343-351 (1996).

Artz, R. R. E., Chapman, S. J. & Campbell, C. D. Substrate utilization profiles of microbial communities in peat are depth dependent and correlate with whole soil FTIR profiles. *Soil Biology and Biochemistry* 38, 2958-2962 (2006).

Bales, R. C. *et al.* Soil moisture response to snowmelt and rainfall in a Sierra Nevada mixed-conifer forest. *Vadose Zone Journal* 10, 786-799 (2011).

Batjes, N. H. Harmonized soil property values for broad-scale modelling (WISE30sec) with estimates of global soil carbon stocks. *Geoderma* 269, 61-68 (2016).

Beaudette, D. E., Roudier, P. & O'Geen, A. T. Algorithms for quantitative pedology: a toolkit for soil scientists. *Computers & Geosciences* 52, 258-268 (2013).

Berhe, A. A., Harte, J., Harden, J. W. & Torn, M. S. The significance of the erosion-induced terrestrial carbon sink. *BioScience* 57, 337-346 (2007).

Bird, J. A. & Torn, M. S. Fine roots vs. needles: a comparison of 13 C and 15 N dynamics in a ponderosa pine forest soil. *Biogeochemistry* 79, 361-382 (2006).

Calderón, F. J., McCarty, G. W. & Reeves Iii, J. B. Pyrolysis-MS and FT-IR analysis of fresh and decomposed dairy manure. *Journal of analytical and applied pyrolysis* 76, 14-23 (2006).

Carvalhais, N. *et al.* Global covariation of carbon turnover times with climate in terrestrial ecosystems. *Nature* 514, 213-217 (2014).

Chabbi, A., Kögel-Knabner, I. & Rumpel, C. Stabilized carbon in subsoil horizons is located in spatially distinct parts of the soil profile. *Soil Biology and Biochemistry* 41, 256-261 (2009).

Dahlgren, R. A., Boettinger, J. L., Huntington, G. L. & Amundson, R. G. Soil development along an elevational transect in the western Sierra Nevada, California. *Geoderma* 78, 207-236 (1997).

Dane, J. H., Topp, G. C. & Campbell, G. S. *Methods of soil analysis physical methods*. (2002).

Davidson, E. A. & Janssens, I. A. Temperature sensitivity of soil carbon decomposition and feedbacks to climate change. *Nature* 440, 165-173 (2006).

Denef, K. & Six, J. Contributions of incorporated residue and living roots to aggregate-associated and microbial carbon in two soils with different clay mineralogy. *European Journal of Soil Science* 57, 774-786 (2006).

Dixon, J. L., Heimsath, A. M. & Amundson, R. The critical role of climate and saprolite weathering in landscape evolution. *Earth Surface Processes and Landforms* 34, 1507-1521 (2009).

Egerton-Warburton, L. M., Graham, R. C. & Hubbert, K. R. Spatial variability in mycorrhizal hyphae and nutrient and water availability in a soil-weathered bedrock profile. *Plant and Soil* 249, 331-342 (2003).

Ellerbrock, R. H., & Gerke, H. H. Characterizing organic matter of soil aggregate coatings and biopores by Fourier transform infrared spectroscopy. *European Journal of Soil Science 55*(2), 219–228 (2004).

Ellerbrock, R. H., Kersebaum, K. C. & Kaiser, M. Isolation and characterization of soil organic matter fractions different in solubility as a possibility to evaluate and to improve C-pools in C-turnover models. *Archives of Agronomy and Soil Science* 51, 209-219 (2005).

Frazier, C. S. & Graham, R. C. Pedogenic transformation of fractured granitic bedrock, southern California. *Soil Science Society of America Journal* 64, 2057-2069 (2000).

Giger, D. R. & Schmitt, G. J. Soil survey of the Sierra National Forest area, California. *United States Department of Agriculture (USDA) Forest Service Publication, Clovis* (1983).

Goulden, M. L. & Bales, R. C. Mountain runoff vulnerability to increased evapotranspiration with vegetation expansion. *Proceedings of the National Academy of Sciences* 111, 14071-14075 (2014).

Graham, R. C., Rossi, A. M. & Hubbert, K. R. Rock to regolith conversion: Producing hospitable substrates for terrestrial ecosystems. *GSA today* 20, 4-9 (2010).

Hall, S. J., Berhe, A. A. & Thompson, A. Order from disorder: do soil organic matter composition and turnover co-vary with iron phase crystallinity? *Biogeochemistry* 140, 93-110 (2018).

Harper, R. J. & Tibbett, M. The hidden organic carbon in deep mineral soils. *Plant and Soil* 368, 641-648 (2013).

Harrison, R. B., Footen, P. W. & Strahm, B. D. Deep soil horizons: contribution and importance to soil carbon pools and in assessing whole-ecosystem response to management and global change. *Forest Science* 57, 67-76 (2011). 19

Hicks-Pries, C. E., Castanha, C., Porras, R., Phillips, C. & Torn, M. S. Response to Comment on" The whole-soil carbon flux in response to warming". *Science* 359 (2018).

Houghton, R. A. Balancing the global carbon budget. *Annu. Rev. Earth Planet. Sci.* 35, 313-347 (2007).

Hubbert, K. R., Beyers, J. L. & Graham, R. C. Roles of weathered bedrock and soil in seasonal water relations of Pinus jeffreyi and Arctostaphylos patula. *Canadian Journal of Forest Research* 31, 1947-1957 (2001).

Hubbert, K. R., Graham, R. C. & Anderson, M. A. Soil and weathered bedrock: Components of a Jeffrey pine plantation substrate. *Soil Science Society of America Journal* 65, 1255-1262 (2001).

International Panel on Climate Change (IPCC) (2007). Contribution of Working Group III to the Fourth Assessment Report of the Intergovernmental Panel on Climate Change, 2007. B. Metz, O.R. Davidson, P.R. Bosch, R. Dave, L.A. Meyer (eds). Cambridge University Press, Cambridge, UK and New York, NY, USA.

Jackson, R. B., Banner, J. L., Jobbágy, E. G., Pockman, W. T. & Wall, D. H. Ecosystem carbon loss with woody plant invasion of grasslands. *Nature* 418, 623-626 (2002).

Jobbágy, E. G. & Jackson, R. B. The vertical distribution of soil organic carbon and its relation to climate and vegetation. *Ecological applications* 10, 423-436 (2000).

Kaiser, M., Berhe, A. A., Sommer, M. & Kleber, M. Application of ultrasound to disperse soil aggregates of high mechanical stability. *Journal of Plant Nutrition and Soil Science* 175, 521-526 (2012).

Kalbitz, K. & Kaiser, K. Contribution of dissolved organic matter to carbon storage in forest mineral soils. *Journal of Plant Nutrition and Soil Science* 171, 52-60 (2008).

Kelly, A. E. & Goulden, M. L. A montane Mediterranean climate supports year-round photosynthesis and high forest biomass. *Tree physiology* 36, 459-468 (2016).

Le Quéré, C. *et al.* Global carbon budget 2014. *Earth System Science Data* 7, 47–85 (2015).

Marin-Spiotta, E., Chadwick, O. A., Kramer, M. & Carbone, M. S. Carbon delivery to deep mineral horizons in Hawaiian rain forest soils. *Journal of Geophysical Research: Biogeosciences* 116 (2011).

Melillo, J. M. *et al.* Soil warming and carbon-cycle feedbacks to the climate system. *Science* 298, 2173-2176 (2002).

O'Geen, A. T. *et al.* Southern Sierra Critical Zone Observatory and Kings River Experimental Watersheds: A synthesis of measurements, new insights, and future directions. *Vadose Zone Journal* 17 (2018).

Post, W. M., Emanuel, W. R., Zinke, P. J. & Stangenberger, A. G. Soil carbon pools and world life zones. *Nature* 298, 156-159 (1982).

Rasse, D. P., Mulder, J., Moni, C. & Chenu, C. Carbon turnover kinetics with depth in a French loamy soil. *Soil Science Society of America Journal* 70, 2097-2105 (2006).

Richter, D. D. & Markewitz, D. How deep is soil? *BioScience* 45, 600-609 (1995).

Ryals, R., Kaiser, M., Torn, M. S., Berhe, A. A. & Silver, W. L. Impacts of organic matter amendments on carbon and nitrogen dynamics in grassland soils. *Soil Biology and Biochemistry* 68, 52-61 (2014).

Rumpel, C. & Kögel-Knabner, I. Deep soil organic matter—a key but poorly understood component of terrestrial C cycle. *Plant and soil* 338, 143-158 (2011).

Salome, C., Nunan, N., Pouteau, V., Lerch, T. Z. & Chenu, C. Carbon dynamics in topsoil and in subsoil may be controlled by different regulatory mechanisms. *Global Change Biology* 16, 416-426 (2010).

Sayre, R. *et al. A new map of global ecological land units—an ecophysiographic stratification approach*. (Association of American Geographers, 2014).

Schrumpf, M. *et al.* Storage and stability of organic carbon in soils as related to depth, occlusion within aggregates, and attachment to minerals. *Biogeosciences* 10, 1675-1691 (2013).

Stone, E. L. & Kalisz, P. J. On the maximum extent of tree roots. *Forest Ecology and Management* 46, 59-102 (1991).

Stuiver, M. & Polach, H. A. Discussion reporting of 14 C data. *Radiocarbon* 19, 355-363 (1977).

Tian, Z., Hartsough, P. C. & O'Geen, A. T. Lithologic, Climatic and Depth Controls on Critical Zone Transformations. *Soil Science Society of America Journal* 83, 437-447 (2019).

Vogel, J. S., Southon, J. R., Nelson, D. E. & Brown, T. A. Performance of catalytically condensed carbon for use in accelerator mass spectrometry. *Nuclear Instruments and Methods in Physics Research Section B: Beam Interactions with Materials and Atoms* 5, 289-293 (1984).

von Lützow, M. *et al.* SOM fractionation methods: relevance to functional pools and to stabilization mechanisms. *Soil Biology and Biochemistry* 39, 2183-2207 (2007). 20

Wang, Y., Li, Y., Ye, X., Chu, Y. & Wang, X. Profile storage of organic/inorganic carbon in soil: From forest to desert. *Science of the Total Environment* 408, 1925-1931 (2010).

Witty, J. H., Graham, R. C., Hubbert, K. R., Doolittle, J. A. & Wald, J. A. Contributions of water supply from the weathered bedrock zone to forest soil quality. *Geoderma* 114, 389-400 (2003).

Woolfenden, W. B. Quaternary Vegetation History. Sierra Nevada Ecosystem Project: Final Report to Congress, vol II, Assessments and scientific basis for management options. 47-70 (Centers for Water and Wildland Resources, Davis, University of California, 1996).

FIGURES

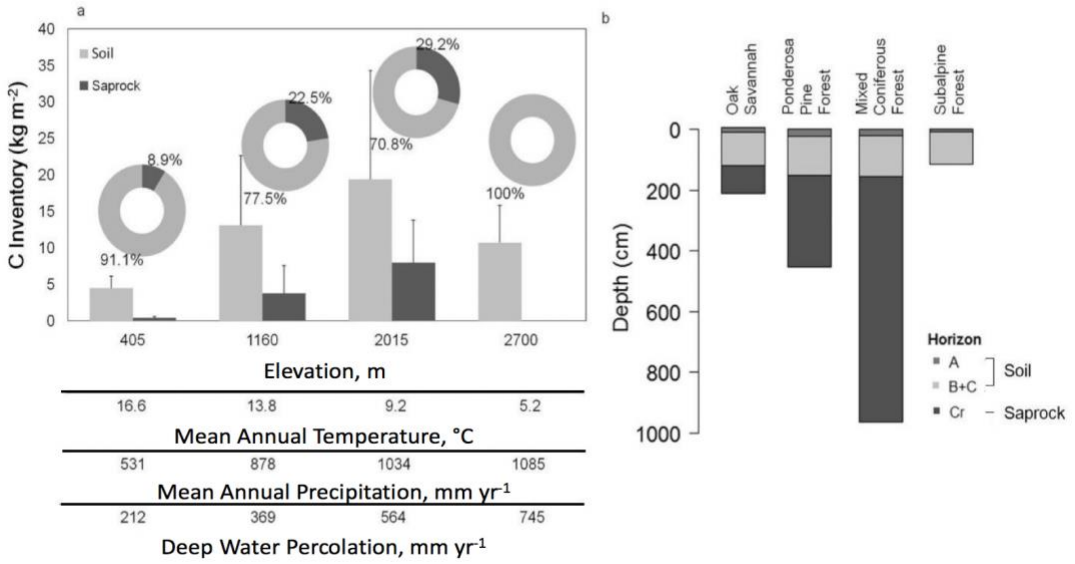

Figure 0-1 Allocation of organic carbon (OC) in soil and saprock across the bioclimatic gradient along the western slope of the southern Sierra Nevada. (a) Bar chart represents the OC pool (error bars are standard deviations, N=48) in soil and saprock. Pie charts represent the proportion of OC stock in soil and saprock among the four study sites: oak savannah (405 m, ponderosa pine/oak forest (ll60 m), mixed-conifer forest (2015 m), and subalpine forest (2700 m); (b) mean thickness of soil and saprock at each study site (Table 2-3).

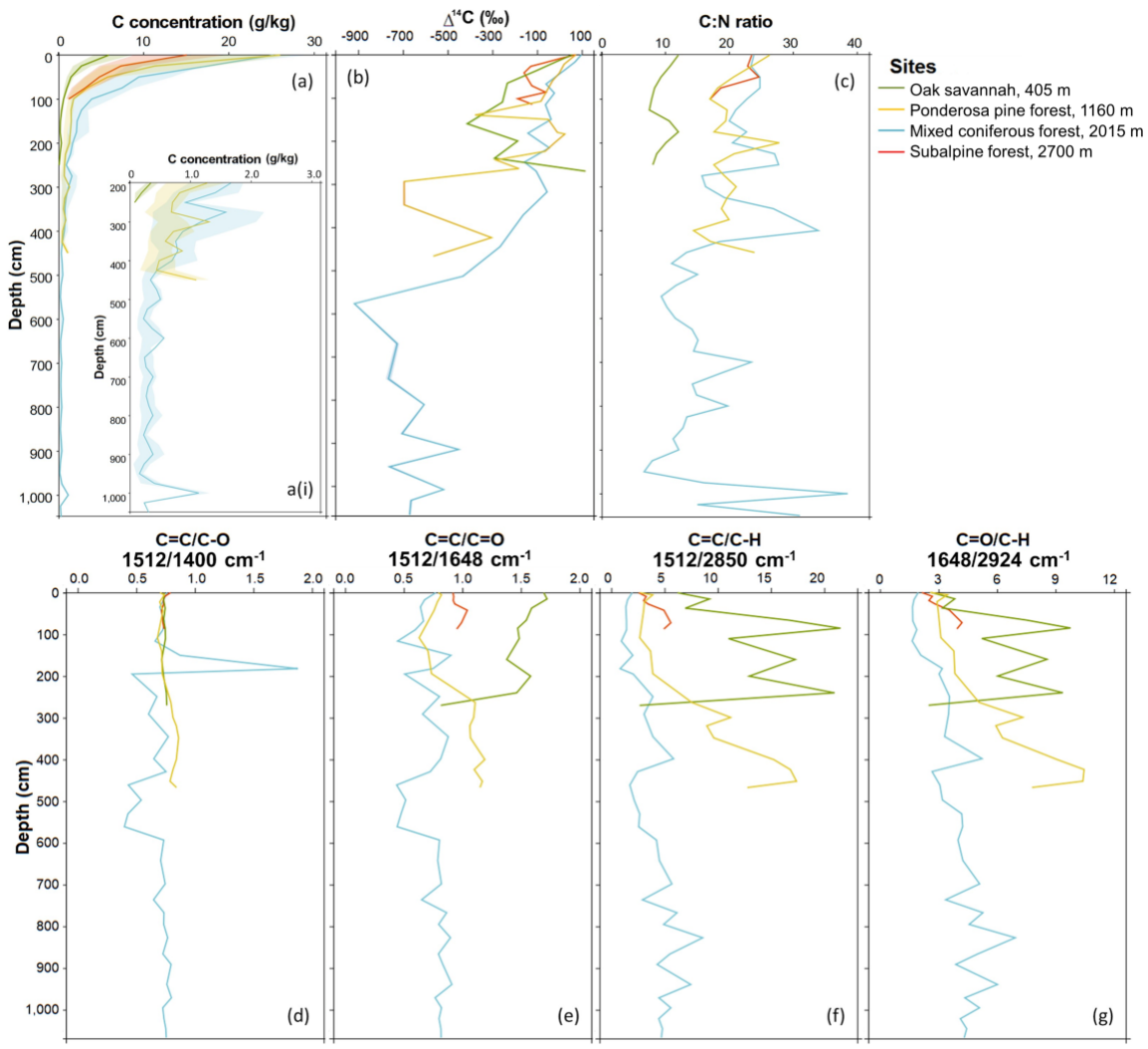

Figure 0-2. Depth profiles across the bio-climatic gradient of: (a) total organic carbon (OC) concentration (%, n = 77); (a(i)) a rescaled portion (2 – 10 m) of the profile data to visualize the low OC trends; (b) radiocarbon $\Delta^{14}C$ (‰); (c) carbon to nitrogen (C:N) mass ratio; (d) the ratios of integrated areas of C=C of aromatic rings to carboxylate COO- (1512 cm^{-1}/1400 cm^{-1}); (e) the ratios of C=C of aromatic rings to C=O of amides, quinones, and ketones (1512 cm^{-1}/1648 cm^{-1}); (f) the ratio of aliphatic C-H to carboxylate COO ((2850 + 2925cm^{-1})/1400 cm^{-1}); and (g) the ratio of aliphatic C-H to C=O of amides, quinones, and ketones to aliphatic C-H ((2850 + 2925 cm^{-1})/1648 cm^{-1}). Solid

color lines represent the mean value; transparent color shading (a) represents the values from first quartile to third quartile.

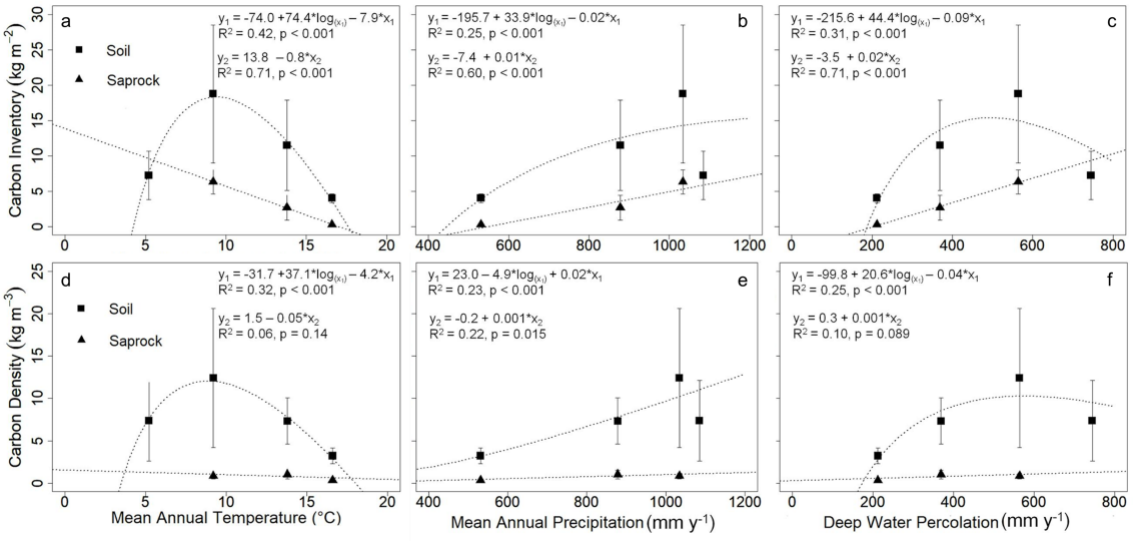

Figure 0-3 Correlations between climate variables (a) mean annual air temperature , (b) mean annual precipitation , and (c) deep water percolation, and carbon inventory, and climate variables (d) mean annual temperature, (e) mean annual precipitation, and (f) deep water percolation, and C density in soil and saprock. Note the highest elevation site did not contain saprock. Points are mean values; error bars represent the standard deviation; n = 55 for soil, n = 22 for saprock; y_1 and x_1 represent regressions of soil, y_2 and x_2 represent regressions of saprock.

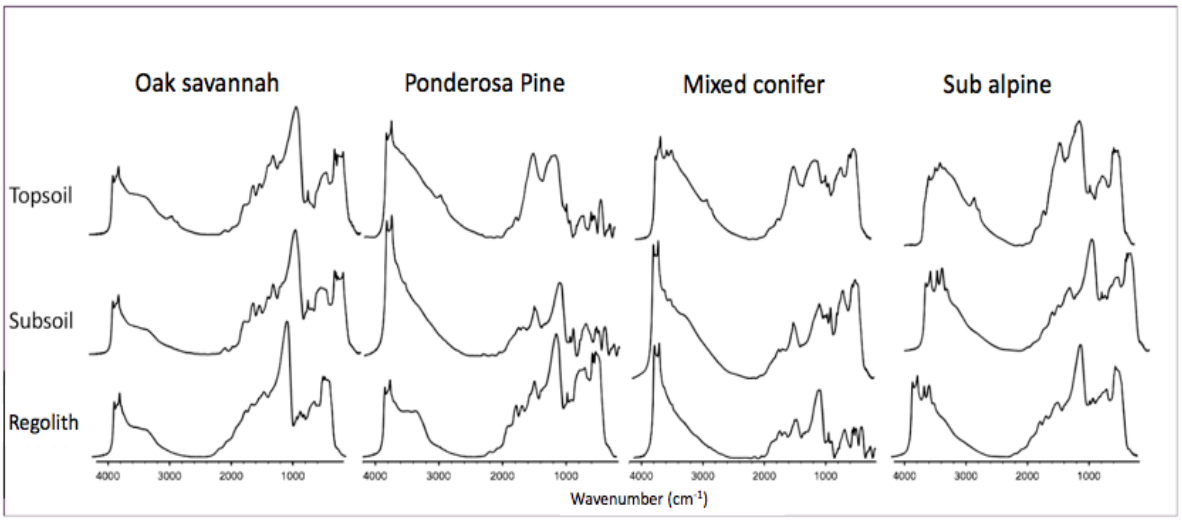

FIGURE 2-4 Representative of FTIR-DRIFT spectra of the topsoil (A horizon), subsoil (BC horizon), and the deepest regolith sample. From left to right depth is 270 cm, 467 cm, 1067 cm, and 102+ cm, from the lowest elevation to the highest elevation site.

TABLES

Table 0-1 Global scaling of OC stock in regolith.

Carbon pool	All regolith types[1]			Plutonics[2]		
	Mean	Median	s.d.[3]	Mean	Median	s.d.[3]
Soil, 0-1 m	120	73	174	13	9	13
Soil, 0.0-2.5 m	157	85	242	15	10	20
Saprock, 1-5 m	201	79	257	28	11	36
Regolith, 0-5 m	321	152	310	41	20	38

1. Estimated area of 52.7 million m^2. Area includes major climate environments that are conceivably warm and wet enough to be relevant to OC inventory, namely: cold very wet, cold wet, cold moist, cold semi-dry, cool wet, cool moist, cool semi-dry, warm moist, warm semi-dry, hot very wet, hot wet, hot moist, hot semi-dry, very hot very wet, very hot wet, very hot moist, and very hot semi dry.

2. Estimated area of 7.3 million m^2. Area includes igneous intrusive rock type within the above climate zones that are relevant to our study environment, namely: acidic plutonics, intermediate plutonics, and basic plutonics.

3. Analysis of 6,947 soil profiles from the World Soil Information Service (WoSIS) database were used.

Table 0-2 Site characteristics along a granitic-derived elevation gradient in the Sierra Nevada, California.

Location Name	Elevation	Mean Annual Min/Max Temperature[1]	Mean Annual Precipitation[2]	Soil Taxonomy[3]	Vegetation Communities[1]
Oak savannah	405	9.3~23.5	531	Coarse-loamy, mixed, active, thermic Mollic Haploxeralfs	Blue oak (*Quercus douglasii)*, interior live oak (*Quercus wislizeni*), gray pine (*Pinus sabiniana*), California Buckeye (*Aesculus californica*), poison oak (*Toxicodendron diversilobum*) and annual grasses
Ponderosa pine/oak forest	1160	5.5~18.0	878	Fine-loamy, mixed, semiactive, mesic Ultic Haploxeralfs	Mix of Ponderosa Pine (*Pinus ponderosa*) with oak (*Quercus kelloggii*)
Mixed-conifer forest	2015	2.7~14.8	1034	Coarse-loamy, mixed, superactive, frigid Humic Dystroxerepts	Mix of white fir (*Abies concolor*), Ponderosa pine (*Pinus ponderosa*), Sugar pine (*Pinus lambertiana*) and incense cedar (*Calocedrus decurrens*)
Subalpine forest	2700	-1.9~10.2	1078	Sandy-skeletal, mixed,	Lodgepole Pine (*Pinus contorta*) and Western

					Typic Cryorthents	White Pine (*Pinus monticola*)

1 Data from Southern Sierra CZO website http://criticalzone.org/sierra/infrastructure/field-areas-sierra/

2 Mean annual precipitation is extracted from PRISM database in 1981-2010

3 Major soil units are identified from Web Soil Survey

Table 2-3 Thickness of soil and saprock along an elevation transect of the Sierra Nevada, California. (0.15-0.94 g kg^{-1})

Vegetation communities (elevation)	Mean soil thickness (m)	Mean saprock thickness (m)	Mean regolith thickness (m)
Oak savannah (405 m)	1.23 (n = 7)	0.67 (n = 4)	1.62 (n = 7)
Ponderosa pine/oak forest (1160 m)	1.53 (n = 15)	2.45 (n = 10)	4.06 (n = 10)
Mixed-conifer forest (2015 m)	1.54 (n = 10)	7.55 (n = 6)	9.41 (n = 6)
Subalpine forest (2700 m)	1.00 (n = 4)	0.00 (n = 4)	1.00 (n = 4)
Mean±standard error	1.33±0.13 (n = 4)	2.67±1.71 (n = 4)	4.02±1.91 (n = 4)

Table 2-4. Carbon stock (kg C m^{-2}) in soil and saprock along an elevation gradient of the Sierra Nevada, California.

Vegetation communities (elevation)	Soil			Saprock		
	Mean	Median	s.d.	Mean	Median	s.d.
	kg C m^{-2}					
Oak savannah (405 m)	4.51 (n=15)	4.41	1.64	0.44 (n=6)	0.44	0.17
Ponderosa pine/oak forest (1160 m)	13.10 (n=20)	10.38	9.58	3.81 (n=10)	2.77	3.80
Mixed-conifer forest (2015 m)	19.40 (n=14)	15.67	14.93	7.99 (n=6)	4.33	5.80
Subalpine forest (2700 m)	10.70 (n=6)	9.60	5.16	NA	NA	NA

Table 3-5. Bulk density (Mg m^{-3}) in pedogenic horizons of regolith profiles along an elevation gradient of the Sierra Nevada, California.

Depth	Bulk Density		
cm (pedogenic horizon)	Mg m^{-3}		
Oak savannah (405 m)	Minimum	Median	Maximum
0-15 (A)	1.38	1.41	1.69
15-65 (B_{w1})	1.43	1.65	1.80
65-123 (B_{w2})	1.52	1.67	1.83
123-145 (C_1)	1.52	1.56	1.67
145-270 (C_2/C_r)	1.56	1.69	1.80
Ponderosa pine/oak forest (1160 m)	Minimum	Median	Maximum
0-25 (O/A)	0.78	0.93	1.07
25-50 (B_{w1})	1.01	1.16	1.28
50-70 (B_{w2}/B_{t1})	1.08	1.24	1.38
70-110 (B_{t2})	1.08	1.14	1.43
110-153 (B_{t3}/BC)	1.12	1.16	1.64

153-220 (C_{r1})	1.19	1.21	1.22
220-300 (C_{r2})	1.06	1.42	1.60
300-400 (C_{r3})	1.35	1.55	2.12
400-467 (C_{r4})	1.27	1.67	1.84
Mixed-conifer forest (2015 m)	Minimum	Median	Maximum
0-15 (O/A)	0.64	0.84	1.15
15-30 (BA)	0.91	1.20	1.21
30-60 (B_{w1})	1.23	1.33	1.34
60-100 (B_{w2})	1.07	1.34	1.55
100-154 (BC/C)	1.13	1.21	1.55
154-200 (C_{r1})	1.20	1.22	1.43
200-300 (C_{r2})	1.23	1.51	1.69
300-400 (C_{r3})	1.35	1.56	1.83
400-500 (C_{r4})	1.54	1.66	1.89
500-600 (C_{r5})	1.44	1.59	1.87
600-700 (C_{r6})	1.48	1.60	1.95

700-800 (C_{r7})	1.55	1.59	2.12
800-900 (C_{r8})	1.48	1.66	1.94
900-1000 (C_{r9})	1.58	1.70	1.72
1000-1067 (C_{r10})	1.64	1.66	1.67
Subalpine forest (2700 m)	Minimum	Median	Maximum
0-10 (O/A)	1.08	1.28	1.45
10-20 (AB/B_{w1})	1.00	1.28	1.48
20-30 (B_{w2})	1.26	1.40	1.66
30-50 (B_{w3})	1.34	1.39	1.66
50-90 (BC/C_1)	1.52	1.59	1.79
90-115 (C_2)	1.06	1.12	1.36

Table 3-6. Carbon density (kg C m^{-3}) in soil and saprock.

Vegetation communities (elevation)	Soil			Saprock		
	Mean	Median	s.d.	Mean	Median	s.d.
	kg C m^{-3}					
Oak savannah (405 m)	3.67 (n=15)	3.58	1.33	0.48 (n=6)	0.47	0.19
Ponderosa pine/oak forest (1160 m)	8.56 (n=20)	5.79	6.26	1.27 (n=10)	0.92	1.27
Mixed-conifer forest (2015 m)	12.60 (n=14)	10.17	9.70	0.99 (n=6)	0.54	0.72
Subalpine forest (2700 m)	9.30 (n=6)	8.34	4.49	NA	NA	NA

Table 3-7. C storage proportions of different zones in the entire regolith.

Vegetation communities (elevation)	Proportion of C storage in the entire regolith (%)				
	A horizon	0-50 cm	0 - 100 cm	Soil	Weathered bedrock
Oak savannah (405 m)	32.0	66.2	86.5	91.1	8.9
Ponderosa pine/oak forest (1160 m)	35.5	54.7	71.1	77.5	22.5
Mixed-conifer forest (2015 m)	18.6	42.3	62.6	70.8	29.2
Subalpine forest (2700 m)	20.0	69.8	98.0	100	NA
Mean±standard error	26.5±4.2	58.3±6.2	79.6±7.9	84.9±6.6	20.2±6.0

CHAPTER 3: CLIMATIC CONTROLS ON DEEP SOIL ORGANIC CARBON DISTRIBUTION AND PERSISTENCE

ABSTRACT

Soil stores more carbon (C) than the atmosphere and vegetation combined and plays a major role in regulating greenhouse gas fluxes between land and the atmosphere. However, most of our current knowledge on soil C dynamics is mainly based on observations from topsoil (to 23 cm), yet the average global soil thickness is greater than 2 m. Large uncertainty remains in our quantification of the spatial distribution of deep soil C storage and process-level understanding of climatic controls on belowground C storage. Using a bio-climosequence in the Sierra Nevada, techniques including density fractionation, Fourier transformed infrared spectroscopy, and radiocarbon were used to understand climatic controls on deep soil organic C distribution, persistence, and chemical composition. We illustrate that SOC partitioning, persistence, and carbon:nitrogen (C:N) ratio of the density fractions varied the most in the transition from moisture-limited oak savannah to energy-limited conifer forests and finally to temperature-limited subalpine forest. Soil C in the oak savannah site had the lowest C concentration, lowest $\Delta^{14}C$ value, lowest C:N ratio, highest aromatic:aliphatic ratio in the mineral associated heavy fraction pool (HF), and highest concentration of the total soil C is in the HF. Results illustrate that these moisture-limited ecosystems store very persistent, microbially processed C that it associated with minerals in the topsoil and subsoil. As elevation increased, we found more C in the free light and occluded light fraction suggesting that physical association of OM with soil minerals (including through

aggregation) plays important role in C persistence in locations with higher plant productivity. We tested mean annual temperature, mean annual precipitation, deep water percolation, actual evapotranspiration, and gross primary productivity on the radiocarbon values of the density fraction pools in the topsoil and subsoil. The results indicate that actual evapotranspiration and gross primary productivity accounted for a significant amount of variability in the persistence of free particulate C suggesting that this labile pool is most vulnerable to changes in climate. Variability in the persistence of the topsoil mineral associated HF was also significantly correlated to actual evapotranspiration and gross primary productivity, suggesting that this fraction is vulnerable to loss by changes in climate. Overall, deep soil organic carbon distribution and persistence varies as a function of direct and indirect influences of soil properties, including regolith thickness and vegetation, that is ultimately governed by climate.

INTRODUCTION

Currently, human activity releases 9.2-11.5 Pg of carbon (C) into the atmosphere every year causing Earth's climate to change (Friedlingstein et al., 2019). Limiting global warming to 1.5 ºC compared to pre-industrial levels is expected to require a reduction of CO_2 emissions by 50% before 2030 (IPCC, 2018). The soil system is one of the most important and promising solutions for climate change mitigation because it stores more than 3,195 Pg of C in the upper 3 m (Jobbágy & Jackson, 2000) amassing more C than all of the C in vegetation and the atmospheric combined (Amundson, 2001). The majority of soil C research has historically focused on the top 23 cm, even though 30-80% of OC is stored below 23 cm and despite studies showing that mean residence time of C in

subsoils can reach 20,000 years (Batjes, 1996; Billings & de Souza, 2020; Jobbágy & Jackson, 2000; Paul et al., 1997; Paul, 2016; Rumpel & Kögel-Knabner, 2011; Tian et al., In review).

Increasing soil organic C (SOC) persistence and stabilization with depth is one of the most important reasons why studies on SOM dynamics should include deep soils. SOC stability determines how long SOC persists in a given soil by limiting loss of thermodynamically unstable organic compounds from soil (Berhe & Kleber, 2013). Generally, with increased depth, SOC concentration decreases and its stability increases (Eusterhues et al. 2003; Paul et al., 1997; Scharpenseel et al. 1989). Even though key works have expressed the importance of soil depth in understanding the C cycle (Shi et al., 2020), an astounding 60% of papers published in four soil journals did not include depth in their report and the average depth studied in the 2000s is 23 cm (Yost & Hartemink, 2020). This is a major knowledge gap in our understanding of SOC dynamics as 85% of soil is estimated to be deeper than 2 m and could be deeper than 50 m (Shangguan et al., 2017). Therefore, at a minimum, we currently lack understanding of up to 90% of the soil profile. Hence, we only have a cursory understanding of the role of deep SOC stocks and its persistence that is needed for developing informed and effective set of solutions to mitigate climate change.

Climatic influence on deep soil C dynamics has not received a lot of attention. This is partly due to a long-held assumption that deep C pools do not change with time and that they are not likely to be vulnerable to changes in atmospheric warming. However, recent studies are showing that changes in temperature affects subsoil OC storage, stability, and

stabilization mechanisms, potentially altering the stocks and flux of carbon dioxide (CO_2) from deep soil to the atmosphere. There are even fewer studies looking at how changes in precipitation impact subsoil SOC storage and stabilization. Although C turnover rates are slower in deeper soils than in surface soils, recent studies have shown that deep SOC is more vulnerable to loss than previously thought (Hicks Pries, et al. 2017; Jia et al., 2019; Cornelia Rumpel & Kögel-Knabner, 2011). One soil warming study reported that the mean Q_{10} (increase of soil respiration per 10 °C increase in temperature) value was 25% higher in deep soil than surface soil, reflecting a higher sensitivity of deep soils to changes in temperature (Hicks Pries et al., 2017).A conservative global extrapolation from a in situ warming experiment to 1 m, suggest that the subsoils could lose 3.1 Pg C y^{-1} as a result of 4 °C warming (Hicks Pries, et al. 2018). These findings contribute to the growing concern that small changes in the SOC pool could have dramatic impacts on the concentration of CO_2 in the atmosphere. Unfortunately, a comprehensive analysis on the dynamics of deep soil C has not happened until now as few past studies had investigated relevant factors (*e.g.*, carbon amount, distribution, persistence mechanisms) at depths greater than 1 m (Fierer et al. 2003; Hicks Pries et al., 2017; Jia et al., 2019; Rumpel & Kögel-Knabner, 2011; Zhang et al. 2016).

Our understanding of how deep soil conditions enable storage and persistence of large amount of persistent C remains incomplete. It was long thought that oxygen limitation, low microbial biomass, and chemical 'recalcitrance' controlled deep C turnover (Jobbágy & Jackson, 2000). However, studies show that the primary control on turnover time is likely microbial access to C as deep soils are still biologically active (Brewer et al., 2019;

Preusser et al., 2019; Stone et al., 2014). However, there is less diverse bacterial and archaeal diversity than top soil layers and some taxa become proportionally more abundant with depth (Brewer et al., 2019; Schmidt et al., 2011). Recent work has shown deep soil organic matter (SOM) can be a mixture of new and old organic matter (Chabbi et al., 2009; Tian et al., 2020), that is rendered relatively stable due to burial, aggregation, its disconnection with decomposers, and chemical association with soil minerals (Marin-Spiotta et al., 2014; C Rumpel et al., 2002). C that is protected via physical and chemical association with soil minerals typically has slower turnover times than less protected pools (Jobbágy & Jackson, 2000). Improved quantification of deep C distribution into fractions, mean residence times, and chemical composition can help us to determine how C is stored for long periods of time and better understand future trajectories of belowground C storage ((IPCC) Intergovernmental Panel on Climate Change, 2014). Numerous studies have shown that climate warming is causing species to shift geographic ranges to higher latitude and altitude (Root et al., 2003). For example, western United States forests are experiencing an upward shift of warmer/drier ecosystems influencing a narrowing of climate envelopes where a range of ecological communities are adapted to (Crimmins et al., 2010). It is unknown how this shift will impact deep SOC turnover. In particular, temperate forests in the western United States store a significant amount of SOC (Homann et al., 2007). Despite occupying 25% of the land surface, conifer forests in California and Arizona account for ~45% of the regional SOC (Rasmussen et al., 2006).

In this study, we conducted a whole soil profile accounting of C amount, distribution, stability and chemical composition with a goal of deriving mechanistic understanding of deep SOC dynamics across a range of vegetation and climates. Our goal is to improve the overall understanding of the vulnerability of SOC under anticipated climate change scenarios. We conducted this study across soil depth profiles from a series of study sites located within the transition from oak savannah to high alpine forests in the Southern Sierra Nevada Critical Zone bio-climosequence, where all of the soil state forming factors are similar, except climate and consequently vegetation (Dahlgren et al., 1997; Trumbore et al., 1996). Specifically, we investigated two critical questions:

1. How does climate drive partitioning of deep soil C into free particulate, occluded, and mineral associated OC fractions? and
2. How does climate affect persistence of SOM in topsoil compared to subsoil horizons?

Answering these questions will allow us to infer the effects that anticipated climate change will have in the Sierra Nevada and implications of upward migration of plant communities on the C persistence in the subsoil.

METHODS

This study took place in the Southern Sierra Critical Zone Observatory (SSCZO) that spans an elevation gradient of 400 to 3,000 m.a.s.l. in elevation among the Southern Sierra Nevada Mountains in California. The SSCZO site exhibits a Mediterranean-type climate. Along the SSCZO elevation gradient, as elevation increases, air temperature decreases, potential evapotranspiration demand is lowered, and precipitation increases

(Goulden et al., 2012). Vegetation and changes with elevation due to climate that controls soil physico-chemical properties and organic matter (OM) concentrations (Fig. 3-1). The oak savannah site receives all of its precipitation from rain. At higher elevations, the ponderosa pine, mixed conifer and sub-alpine sites receive precipitation as a mix of rain and snow, with higher proportion arriving as snow at highest elevation sites. The percent tree cover and height are highest at the mid-elevation sites and lowest at the oak savannah. Soils at the oak savannah are classified as Alfisols, Inceptisols and Entisols and the ponderosa pine site are classified as Alfisols. The mixed conifer site has both Inceptisols and Entisols, and soils at the highest elevation site are classified as Entisols with some likely being Inceptisols.

The SSCZO site is particularly well suited to address the research questions as it is located along an elevation transect that allows testing of the effect of climate. The space-for-time substitution approach employed in our study allows us to infer the effect of climate changes on SOC dynamics. Previous studies at the SSCZO location in nearby areas (Dahlgren et al., 1997; Harrington, 1958; Jenny et al., 1949; Trumbore et al., 1996) have documented a wealth of observations on a range of variables relevant to this study, including ecosystem C exchange, climate, soil water status along the soil profile at each elevation zone, geology, and soil development. Detailed description and properties of soils in our study sites are available in O'Geen et al., (2018).

Along the SSCZO elevation gradient (from 400 to 2700 m), as elevation increases, average annual air temperature decreases from 14.4 to 4.1 ºC, actual evapotranspiration (ET) changes from 395 749, 584, to 260 mm/year, and precipitation increases from 515

to 1080 mm/year. Gross primary productivity (GPP) follows a similar pattern to ET with the oak savannah site having 480 g C m^{-2} yr^{-1}, the ponderosa pine is 1900 g C m^{-2} yr^{-1}, and then GPP slightly decreases in the mixed conifer site to 1700 g C m^{-2} yr^{-1} and finally the sub-alpine site has a GPP of 700 g C m^{-2} yr^{-1} (Goulden et al., 2012). Vegetation changes with elevation due to climate influencing soil physico-chemical properties and OM concentrations. Soils of all sites formed from granodiorite residuum and colluvium parent materials. The concentration of OM in soil increased with elevation, reaching a peak in the mid-elevation region where our ponderosa pine and mixed conifer sites are located, and decreases thereafter (Chadwick et al., 1995; Djukic et al., 2010; Tian et al., 2020). Weathered bedrock thickness is limited by precipitation at the oak savannah and low temperature and glaciation at the high elevation subalpine forest. The bedrock thickness of the cooler and wetter mid elevation forests are not limited by climate and extend below 10 m (O'Geen et al., 2018; Tian et al., In review).

APPROACH

SAMPLING AND SOIL PHYSIO-CHEMICAL ANALYSES

Four pits were excavated and sampled by genetic horizon at each of the four sites (Fig. 3-1). Three pits per site that included samples from the soil-atmosphere interface down to the C horizon were selected for density fractionation. More detailed description of the sites and specific samples we used in this study are available in previous studies conducted at the study sites (O'Geen et al., 2018; Tian et al., 2020). Particle size analysis on bulk pit samples (40 g air dried and sieved) was performed by the hydrometer (ASTM 152H) method after treatment of soils with HCl (there is no carbonate in these systems, however,

this step was performed to match comparison of our samples with those from other sites outside of the SSCZO (Klute, 1986). Bulk density of soil was measured using the core method from three core samples in each horizon (Dane & Topp, 2020).

Soil pH was measured on air-dried and sieved soil in deionized water with a 2:1 (5 g:10 ml) mixture for thirty minutes, stirring every ten minutes and measuring the supernatant (Sparks et al., 1996). Lithium metaborate fusion was performed to determine total Fe and Al concentration in bulk soils (Robertson, 1999). The total elemental concentration was determined on an ICP-OES (Perkin-Elmer Optima 5300 DV Inductively Coupled Plasma Optical Emission Spectrometer) after soils were air dried, sieved, roots removed via floating, and crushed to a powder consistency using an agate mortar and pestle. Values are expressed as an oven dry weight using the air to oven conversion (105 ºC for 24–48 h).

CARBON AND NITROGEN ANALYSES

Bulk soil was air-dried, sieved (2-mm mesh openings), roots were removed, and soil was ball milled for 3.5 minutes with two tungsten carbide ball bearings. The light fractions (fLF and oLF, see below on separation procedure) were homogenized using an agate mortar and pestle and the heavy fraction (HF) was ball milled for 3.5 minutes. Percentage of fine-earth fraction (< 2 mm) and coarse earth fraction (> 2 mm) were measured based on air-dry mass. Gravimetric water content was determined on air-dried subsamples by drying overnight at 105 °C. We tested a subset of samples having the highest pH values with 0.01 M hydrochloric acid and in all cases, we did not notice effervescence and the

acid pretreatment did not result in a significant reduction in total C. From this we concluded that total C was equivalent to total organic C in our samples. Total C and N concentration (%) and stable isotope composition ^{13}C were determined on samples ground to pass a 180-μm sieve and analyzed by dry combustion (Costech Analytical ECS 4010 instrument, Costech Analytical Technologies, Inc., Valencia, CA).

Total OC inventory (Equation 1; C_s, kg C m^{-2}) was calculated from total OC concentration (C, g kg^{-1}), thickness of the sample layers (d_c, m) and bulk density (ρ_b, Mg/m^3), with correction for the weight percent of coarse earth fraction.

$$C_s = \sum C \times d_c \times p_b \qquad \text{Equation 1}$$

DENSITY FRACTIONATION

Density fractionation was used to separate the SOM into pools that are distinct in composition as well as mechanisms of stabilization: free light (debris outside aggregates, fLF), occluded (light fraction inside aggregates oLF), and heavy fractions (OM chemically bound to minerals, HF) using sodium polytungstate (SPT; Swanston et al. 2005; Lybrand et al., 2017; McFarlane et al., 2012). To separate the fractions, 30 g of air-dried, sieved (< 2 mm) soil was initially mixed with 1.7 g/ml of SPT for 24 hours. The fLF is first isolated by floating to the top as the supernatant and removed. To break up the aggregates and collect the oLF the remaining sample was mixed with more SPT, and dispersed using a benchtop mixer and using an ultrasonic energy at 440 J/ml with a Branson 450 Sonifier (Branson Ultrasonics, Danbury, CT, USA) probe tip 5 cm below the liquid surface (Kaiser & Berhe, 2014). The dense particles (i.e., organic matter

chemically bound to the mineral fraction, HF) was then determined from the residue at the bottom of the centrifuge tubes. All three fractions were thoroughly rinsed with 0.01 M $CaCl_2$ and DI water and the fLF and oLF were filtered and rinsed using 0.8 µm filters (Lybrand et al., 2017)

SOM COMPOSITION USING FOURIER TRANSFORMED INFRARED SPECTROSCOPY

Diffuse Reflectance Infrared Fourier Transform (DRIFT) spectroscopy was used to infer abundance of chemical functional groups. We used ratios of peak areas under regions representing abundance of specific OM functional groups across the FTIR spectrum as a proxies for extent of decomposition related processing of OM (Kaiser et al., 2012). All bulk soil and density fractions were finely ground to a powder consistency using a ball mill (SPEX Sample Prep Mixer Mill 8000C, Metuchen, NJ, USA) prior to analyses. They were then dried at 60 °C for 24 hours; oven-dried samples were kept in a desiccator prior to analyses to minimize presence of water in the samples we analyzed. We computed ratios of peak areas following methods outlined in (Hall et al., 2018). Mid-IR spectra (400 to 4000 cm^{-1}) presented in this study were recorded using an IR spectrophotometer (Bruker IFS 66v/s, Ettlingen, Germany) and a Praying Mantis DRIFT sampler (Harrick Scientific Corporation, Ossining, NY). Finely ground and oven-dried potassium bromide (Aldrich Chemical Company, Saint Louis, MO, USA, FT-IR grade) was used as a background reference for all FTIR analyses. We used 500 background scans and 500 sample scans with a 4 cm^{-1} resolution and all spectra were tangentially baseline corrected. Peak areas were calculated in reference to local baselines to remove impacts from larger spectral features and tails and all related calculations were conducted using the “approxfun” and “integrate”

functions in R version 0.98.1028 (Hall et al., 2018). Peak areas were used because peak area is less sensitive to influences of peak broadening compared to peak heights.

The FTIR spectra were analyzed to determine level of OM transformation that is derived from decomposition using a ratio of peak heights at these areas of interest. Peaks heights at 2925 and 2850 cm^{-1} (spanning 2898–2976 and 2839–2870 cm^{-1}) indicate aliphatic C–H asymmetric and symmetric stretches. Peak heights at 1648 cm^{-1} (spanning 1570–1710 cm^{-1}) indicate C=O and C=C stretch of amides, quinones, and ketones. A clearly distinguishable shoulder at 1512 cm^{-1} (spanning 1500–1550 cm^{-1}) is indicative of the aromatic C=C stretch. A pronounced peak at 1400 cm^{-1} (spanning 1360–1450 cm^{-1}) reflects the carboxylate C–O (COO) stretch. For band interpretation, functional groups of both mineral and organic substances may have vibration frequencies in overlapping wavenumbers (Demyan et al., 2012; Gerzabek et al., 2006; Hall et al., 2018; Ryals et al. 2014).

For band interpretation, it must be considered that functional groups of both mineral and organic substances may have vibration frequencies in some of the same or overlapping wave numbers. We conducted ashing experiment to ensure that the spectral features we interpreted for OM are indeed derived from OM (see Chapter 3) for more information on this).

RADIOCARBON ANALYSES

Radiocarbon analysis was conducted on all bulk soil and fractions after sealed-tube combustion of OC to CO_2 (with CuO and Ag) that was then reduced onto Fe powder in the presence of H_2 (Vogel et al., 1984). Radiocarbon values were measured in 2019 on

the 1 MeV NEC compact accelerator mass spectrometer at the Center for Accelerator Mass Spectrometry at the Lawrence Livermore National Laboratory. Radiocarbon isotopic values were corrected for mass-dependent fractionation with measured $\delta_{13}C$ values, and were reported in Δ- notation corrected for $\Delta_{14}C$ decay since 1950 (Stuiver & Polach, 1977) through normalization of the absolute activity of Oxalic Acid 1. For this purpose, we relied on organic matter $\delta_{13}C$ values that were determined at the University of California Merced using a DELTA V Plus Isotope Ratio Mass Spectrometer (Thermo Fisher Scientific, Inc.). Several secondary standards (TIRI wood, Oxalic Acid 2, ANU) and a coal background were run alongside the unknowns for quality control. Ten randomized samples were split and tested twice for $\Delta_{14}C$ to determine precision of the measurements, which was 3 ‰ on average.

We estimated turnover times of SOM in bulk soil and all the fractions using a time-dependent steady-state model (Equation 3-2). The turnover time for a given fraction or pool is the inverse of mean residence time and estimates the average time C atoms spend in a given pool before leaving that pool (Rodhe, 1992; Trumbore, 2000). The proportion of C in the fractions and their $\Delta_{14}C$ were averaged for all three pits and used to constrain the model (Marín-Spiotta et al., 2008; Torn et al., 2009). This model calculated the $\Delta_{14}C$ of each of the pools by varying turnover times to align with the measured $\Delta_{14}C$ of bulk soil (Gaudinski et al., 2000; McFarlane et al., 2013; Torn et al., 2002). Atmospheric $\Delta_{14}C$ (used to calculate F'_{atm}) was compiled from several references (Hua & Barbetti, 2004; Levin & Kromer, 2004; Stuiver et al., 1998). Values after 2003 are calculated as the global mean $\Delta_{14}CO_2$ taken from (Graven et al., 2012) assuming a 5 per mil/year decline. A three-pool

model was used to determine the fraction turnover time of all three fractions at the same time. Turnover time was estimated using the following equation (Torn et al., 2009):

$$F'_{SOM\,(t)} = \left[I \times F'_{atm\,(t-1)} + C_{(t-1)}F'_{SOM\,(t-1)}\,(1-k-\lambda)\right]/\left[C_{(t)}\right] \qquad \text{Equation 3-2}$$

where $F' = (\Delta^{14}C \times 1000^{-1}) - 1$ (or absolute fraction modern); I = inputs of carbon to a given SOM pool or fraction (g C m^{-2} y^{-1}) which are calculated by 1/turnover time; C = Stock of C for the given SOM pool (g C m^{-2}); k = Decomposition rate constant of the given SOM pool ($year^{-1}$); F'_{atm} = the $\Delta^{14}C$ value of atmospheric CO_2; F'_{SOM} = the $\Delta^{14}C$ value of the given carbon pool; λ = radioactive decay rate of $\Delta^{14}C$ ($year^{-1}$); and t = year in which calculation is being performed. Fit was determined by non-linear least squares using the solver function.

This model (Equation 3-2) makes two important assumptions. The first assumption is that the system is in steady state were the inputs are equal to the outputs. The second assumption is that the pools are homogenous in regard to the $\Delta^{14}C$ value. But it is important to note that inputs to a given SOM fraction or pool, especially in deep soils, likely have a longer lag time than surface soils and C may cycle from one fraction or depth to another as organic compounds are assimilated and transformed by microbes. Therefore, calculated turnover times are best interpreted as the residence time of C in the ecosystem rather than in the given fraction (McFarlane et al., 2013).

DATA ANALYSES

Data are presented with mean +/- standard error. ANOVA was performed on average clay %, pH, bulk density, and total Fe and Al concentrations to test if there existed statistically

significant differences in their means based on site. Pairs of means at the different depths and sites were also compared using the Tukey-Kramer HSD test, and simple linear regression was used to assess the proportion of variability in the dependent variables (clay %, pH, etc.) that depends on variability in a series of independent variables (site). For all statistical tests, a significance level of $p < 0.05$ was set a priori. All statistical tests were performed using R version 1.1.456.

Choosing a climatic variable or proxy that accurately depicts how elevation effects temperature and precipitation along a climosequence is complex because there is an increase in precipitation and decrease in temperature as you move up in elevation. Numerous soil science studies have reported mean annual temperature (MAT) and mean annual precipitation (MAP) as the key climatic variables, however these variables highly covary with each other in our sites, and these atmospheric variables are also expected to be less relevant for deep soil layers because they do not portray microclimate variables and these soils formed a long time were the climate was different than current mean annual estimates. GPP and actual evapotranspiration (ET) had the lowest covariation amongst the climate variables tested (MAT, MAP, deep water percolation (DWP=MAP-ET), ET, GPP). We choose to analyze all of their relationships to C stabilization to see their impact and compare to other studies that often report MAT and MAP with C dynamics. We used mixed effects models to assess at the relationship on how climate controls C stabilization. We used climatic variables (i.e., GPP and evapotranspiration) as the fixed effects and the independent variable of $\Delta^{14}C$ (per mil) of each topsoil and

subsoil fraction combined for all of the sites. R-squared and p-values were calculated for each fraction within either topsoil (< 30 cm depth) or subsoil (> 30 cm depth).

RESULTS

Bulk density generally increased with depth across all of the sites and ranged from 0.92 kg/m3 in the topsoil A horizon to 1.67 kg/m3 in the Cr horizon (Table 3-1). Clay % increased from the A to B horizons in all sites, and in the mid-elevation sites showed an increase from the B to C horizons. The highest and lowest elevation sites had lower clay concentration compared to mid-elevation sites. Soil pH of all sites remained within a small range of 5.20 to 6.14 and was relatively constant with depth across all of the sites (Table 3-1). Total Fe and Al in bulk soil were highest at the mid-elevation sites, showing slight increases with depth only in the soil profiles at the mid-elevation sites. At the oak savannah and sub-alpine sites total Fe and Al concentrations decreased with depth (Table3-1). Total Fe and Al exist in the Cr horizons at the mixed conifer site with 10.13 mg/g of Fe and 49.85 mg/g of Al. Simple linear regressions were performed to test if there are significant differences between site for all of the variables in Table 3-1. None of the variables varied significantly with site; with the exception of Al ($p = 0.002$, adj. $R^2 = 0.65$) and Fe ($p = 0.02$, adj. $R^2 = 0.47$, n=14) that showed statistically significant differences across the SSCZO bio-climosequence.

The concentration of C of the fLF and oLF were relatively similar with depth, while the % C in the HF showed a drastic decrease with depth across all sites (on average about 50%), especially below 30 cm soil depth (Fig. 3-2. a,f,k). The ponderosa pine site had the highest % C in the fLF and oLF (Fig. 3-2 a,f). We found higher %C in the topsoil oLF (42–47 %)

compared to the other fractions (oLF ranged from 26-36% C and HF ranges from 0.5 to 1.5% C), which stayed consistent with depth. The proportion of total C recovered in the fLF decrease with depth, for the oak savannah and mixed conifer, while the fraction of C in the HF generally increases with depth for the oak savannah and sub-alpine sites (Fig. 3-2. b,g,i). Radiocarbon concentration ($\Delta_{14}C$) increased with depth for all fractions, with the most depleted samples being found in the aggregate and mineral associated HF pools, except in the ponderosa pine site where the pattern with depth was variable (Fig. 3-2. c,h,m). The C:N ratio of the fLF and oLF increased with depth. However, in the HF, as in bulk soil, C:N ratio consistently decreased with depth (Fig. 3-2. d,i,n). The oak savannah displayed the lowest C:N in all fractions with depth. The mixed conifer site had the highest C:N typically but not always (Fig. 3-2. d,i,n). The stable C isotopic composition of $\delta_{13}C$ in the fLF and oLF across the depth profiles was observationally identical, where the $\delta_{13}C$ in the HF became heavier with depth below 25 cm. We observed a very small change in $\delta_{13}C$ of fLF and oLF with depth across all sites, except in the oak savannah site where $\delta_{13}C$ decreased with depth below the A-horizon. The oak savannah site was lighter in $\delta_{13}C$ in every fraction compared to the other sites (Fig. 3-2. e,j,o).

C PARTITIONING ACROSS FRACTIONS IN TOP VS. SUBSOIL

The largest difference in partitioning of C among the density fractions was driven by ecosystem differences between the lowest elevation oak savannah and the forested sites. Relative partitioning of the soil C in fractions showed that greater than 80% of the C in the oak savannah subsoil is in the HF pool and with increases in elevation more fLF and oLF are in the three forested systems (Fig. 3-3). The highest proportion of C in oLF, and the

largest difference between the topsoil and subsoil, was also found in the oak savannah. As elevation increases beyond the mid-elevation ponderosa pine site, we observed the proportion of C in the oLF progressively decreased. The highest proportion of fLF was observed in the subsoil at the two highest elevation. The proportion of C in the mineral associated HF fraction accounted for the largest proportion of C throughout all of the sites from the topsoil to subsoil.

PERSISTENCE OF OC IN TOPSOIL VS SUBSOIL

The $\Delta^{14}C$ values show the oak savannah site had the most depleted free light (-238‰) and heavy fractions (-570‰) out of all of the ecosystems we studied (Fig. 3-4). The most depleted oLF was in the mixed conifer subsoil at (-359‰). We observed a relatively smaller difference in $\Delta^{14}C$ of fLF in topsoil compared to the subsoil across the elevational gradient (Fig. 3-4). Generally, in the A horizon the fractions where all enriched in $\Delta^{14}C$ with modern values. In the mid-elevation sites, there was less depletion in topsoil in all fractions. However, at the highest elevation site, we observed a slight depletion in $\Delta^{14}C$ in the topsoil. Most surprisingly, we found that OC in fLF can persist in subsoils from centuries to millennia. Overall, the subsoil C in oLF and HF had a lower value (older) than topsoil. Mid-elevation sites, with highest proportion of soil C stock in subsoil, had oLF that is similarly depleted compared to HF.

Soil C distribution and $\Delta^{14}C$ data were combined in a three-pool steady-state model (Eq. 3-2) to estimate mean turnover time of the fractions. We found that SOM in all fractions was older with depth (except the sub-alpine site), with the oLF and HF being the oldest. The turnover time of the fLF ranges from 1 to 1,366 years, with the longest turnover times

recorded in the B horizons. The ponderosa pine fLF turnover time is less than 10 years in the top and subsoil and the mixed conifer site exhibited a slightly longer fLF turnover time with depth and is generally consistent with depth below the A horizon. The fLF turnover time of the oak savannah and sub-alpine site peak in the B horizon. The turnover time for the oLF ranged from 177 to 4,685 years with the longest turnover times in the deepest soil samples with peaks in the B horizon. Except in the mixed conifer and oak savannah that had the longest turnover times in the deepest sample. The HF turnover time ranged from 207 to 4,924 years, with a general observed increase in turnover time with depth with the longest times being in the deepest samples. Except for the sub-alpine site where the turnover time mirrors the fLF and oLF turnover times peaking in the B horizon.

Table 1 presents results from the mixed effects models in the all the fractions in the topsoil and subsoil and five measures of climate in order to determine the relative contribution of climate to C persistence. Out of all of the climatic variables tested, GPP and ET have the lowest p-values and largest conditional R-squared values (explains R_2 of the entire model and not just the fixed factor alone) with the topsoil fLF and HF and subsoil fLF. The strongest observed variation in C persistence in the topsoil and subsoil fLF can be explained by GPP and ET with up to 70% of the variability in subsoil fLF can be explained. The second highest correlated climatic variable to $\Delta_{14}C$ is MAT and MAP, however it has much lower conditional R-squared values compared to ET and GPP. The topsoil fLF was the only pool that correlated to MAT ($p=0.044$, $r_{2c} =0.171$). The subsoil HF was the only pool that correlated to MAP ($p=0.010$, $r_{2c}= 0.17$). The topsoil oLF was the only pool that

correlated to DWP ($p=0.049$, $r^2c=0.166$). Most of these relationships are not statistically significant.

CHEMICAL COMPOSITION OF FRACTIONS

DRIFT-FTIR spectra, that we used to determine bulk composition of SOM in the density fractions, showed peaks at 2925 cm^{-1} that correspond with aliphatic C-H vibrations (Stevenson, 1995). Topsoil peaks at 2925 cm^{-1} were sharper for the fLF and oLF compared to the HF. At the oak savannah site HF has sharper peaks at the 2925 cm^{-1} in both the topsoil and subsoil compared to the other sites, except the topsoil ponderosa pine peak (Fig. 3-6). The fLF and oLF peak at 1620 cm^{-1} corresponds with aromatic C=C stretching and/or asymmetric COO- stretching but can also indicate C=O vibrations (Stevenson, 1995). The 1620 cm^{-1} peak is observed to be higher in the fLF and oLF compared to the HF at all sites and depths (Fig. 3-6). The peak at 1512 cm^{-1} corresponds to aromatic C=C stretching vibrations and the 1390 cm^{-1} peak is the OH deformation and C-O stretching (Stevenson, 1995). The HF samples in both the topsoil and subsoil for all sites, except the ponderosa pine, exhibited a sharp peak at 1390 cm^{-1} compared to the fLF and oLF (Fig. 3-6). Peaks at 1980 and 1870 cm^{-1} are indicative of Si-O vibration of quarts mineral, while peaks at 915, 810, 690, 670 cm^{-1} represent clay and quarts minerals. Sharp peaks at 3696 and 3622 cm^{-1} that are of O-H stretching of clay minerals (Nguyen et al., 1991). The HF exhibited higher peaks and larger peak areas at 1980 cm^{-1} and 3696 cm^{-1} especially in the subsoil oak savannah and mixed conifer sites, reflecting higher relative abundance of Si-O and clay minerals compared to the fLF and oLF (Fig. 3-6).

Our DRIFT-FTIR analyses showed presence of complex and heterogeneous mixture of compounds in SOM across the fractions and depth gradients in the bio-climosequence (Fig. 3-6). To determine level of OM transformation that is associated with decomposition, we used an index of decomposition based on ratio of peak area under aromatic to aliphatic chemical constituents (Hall et al., 2018; Kelly & Goulden, 2016). Different stabilities of these functional groups of SOM were used as the basis of the energy state or strength of chemical bonds of the functional groups, such as aliphatic C–H being less stable than aromatic C = C bonds. FTIR based composition of SOM shows an increase in the area under the peak in aromatics in HF (leading to a ratio range 4-8) compared to both fLF and oLF (ratio range 1-2; Fig. 3-7). Both fLF and oLF had a similar ratio with depth and among sites with a small range between 1 and 2. In the HF, the oak savannah had a lower ratio compared to the other sites. The fLF and oLF exhibited higher peaks at both aliphatic and aromatic regions compared to the HF, with higher peak heights and larger peak areas in the aliphatic region, whereas HF exhibited higher peaks in the aromatic region and much lower peaks in aliphatic regions (Fig. 3-6).

DISCUSSION

Recent studies suggest that subsoil SOC is vulnerable to future change in climate and that the subsoil (down to 1 m) alone could respire equivalent to 30% of current fossil fuel emissions if the temperature increases by 4 ºC (Hicks Pries et al., 2017). In order to improve our understanding of how climate controls the current state of subsoil SOC, we quantified how soil C stock and stabilization mechanisms vary with depth. Across the SSCZO bio-climosequence we covered in this study, previous studies had shown that the

soils' physico-chemical properties show a systematic response to changes in climate (Dahlgren et al., 1997; Jenny et al., 1949; Pellegrini et al., 2018; Trumbore et al., 1996) making it an ideal location to answers our questions on climatic controls on deep soil C distribution and persistence.

CLIMATIC CONTROLS ON DISTRIBUTION OF SOC INTO FLF, OLF, AND HF

Worldwide, SOC stocks generally increase as MAT decreases and cool/cold, humid regions typically have C-rich soils (Hobbie et al., 2000; Post et al., 1982; Stockmann et al., 2013). Along the SSCZO bio-climosequence, GPP was highest at ponderosa pine and mixed conifer sites which were located at mid elevation and climate was most conducive to plant productivity (Dahlgren et al., 1997; Goulden et al., 2012). Our results show that there was an increase in the proportion of unprotected fLF OC in both topsoil and subsoil with increasing ET except at the highest elevation subalpine site (Fig. 3-3), following the observed pattern in GPP (Goulden et al., 2012). A similar pattern was observed in another climosequence in Arizona that transitions from a desert arid ecosystem to conifer forest (Lybrand et al., 2017). Across the elevation gradient, we observed that the HF started to account for an increasing proportion of total C with depth, while contribution of the fLF declined. Typically, studies that analyze density fractions over the entire soil profile have shown declining contributions of fLF OC to total OC with soil depth due to increases in input of OM from plants in various degrees of decomposition (Kögel-Knabner et al., 2008). We observed that the amount of fLF in the soil profiles mirrored increases in GPP (Fig. 3-1). At the subalpine site, which is colder and had lower GPP compared to the other sites, we observed that the oLF comprises the lowest proportion of

total SOC and has a shorter turnover time compared to other sites (Fig. 3-3,3-5). This aligns with previous work in our study bio-climosequence that confirmed that high plant productivity in our mid-elevation sites is driven by optimal climate for biological processes and soil weathering (Dahlgren et al., 1997; Goulden et al., 2012). Our results show that climate indirectly controls C partitioning in to the different fractions through its influence on above and below-ground sources of OM (vegetation) and extent of soil aggregation (as dictated by weathering, colloid and ionic redistribution in the soil profile, and availability of OM) that plays important role for soil C persistence.

CLIMATIC INFLUENCE C PERSISTENCE IN TOPSOIL COMPARED TO SUBSOIL

Subsoil SOC can be a mixture of new and old SOC (Chabbi et al., 2009; Rumpel & Kögel-Knabner, 2011; Tian et al., 2020) that is stabilized through physical and chemical association with soil minerals (Marin-Spiotta et al., 2014; Rumpel et al., 2002). Generally, with increased depth, SOC concentration decreases and its stability increases, as inferred from radiocarbon-based turnover rates or decomposition rates derived from incubation experiments (Eusterhues et al., 2003; Paul et al., 1997; Scharpenseel et al., 1989). This general trend with depth (SOC decreases and stability increases) was also observed in our study for all subsoil fractions, indicating that deep soils effectively store C over millennial timescales, especially in the drier oak savannah site (Fig. 3-3 and 3-4).

Much of our previous understanding of belowground C turnover was based on data collected from topsoil and bulk soil samples, overshadowing the important role of depth in persistence of SOC across all fractions. In dry conifer forests of the western United States, fLF typically consist of intact and partially degraded plant parts and pyrolyzed C,

with a relatively fast turnover time (Lybrand et al., 2017; Wagai et al., 2009). The occluded fraction is mix degraded plant parts and pyrolyzed C with a relatively long turnover time (Fig. 3-5). Longer turnover times of oLF was also seen in Arizona (Lybrand et al., 2017; Rasmussen et al., 2005). The relative stability of C in dry western US conifer forests contrasts with results from wet temperate and tropical systems, where the occluded fraction generally exhibits residence times similar to that of free light C, and mineral C fractions exhibit the longest residence times (Crow et al. 2007; Marín-Spiotta et al., 2008; McFarlane et al., 2013). Moreover, current studies, particularly ones that have a topsoil focus, indicate that the most effective storage mechanism for SOC is attachment to minerals (Hemingway et al., 2019) and some studies included the oLF as being important to persistent C (Rasmussen et al., 2005). Our results expand this understanding of C persistence in western conifer forests and oak savannah by indicating that all three topsoil fractions stored C with turnover times up to 1,500 years and the oLF and HF had consistently more depleted ^{14}C (older) signatures than fLF (Fig. 3-2,3-4). This suggests that studies that focus solely on topsoil and mineral association may skew our understanding of C persistence as they overlook long-term C persistence in the fLF and oLF.

We showed that fLF becomes more depleted in $\Delta^{14}C$ (i.e. older) (Fig. 3-2) with depth at all sites suggesting that transport and existence of particulate OM to deeper soil layers can lead to long term persistence of C, for up to millennia. Large portions of fLF exist at all sites, with $\Delta^{14}C$ ages ranging from modern in near surface layers and up to ~1,000 years old in deep soil and the longest turnover times being 1,360 years (Fig. 3-2 and 3-4).

The fLF in our study systems was composed of plant/root-like structures identified by microscopic observations (not included). This suggests that subsoil drier conditions likely limit rates of OM mineralization specifically in oak savannah. The shorter turnover rates of topsoil fLF along with slower turnover fLF in deep soil layers suggests that this typically faster cycling pool (more labile) of OM could persist for a longer time period if it was translocated to deep soil layers. However, we also show that fLF is likely most vulnerable to changes in climate in both the topsoil and subsoil, as suggested by the correlation of proportion of C in fLF with ET and GPP (Table 3-1). Our FTIR work also showed that the mostly plant/root like fLF is enriched in typically labile aliphatic compounds (compared to aromatics; Fig. 3-7) compared to the HF OC. The persistence of fLF in deep soil layers is then likely attributed to both its source of OM and reduced microbial activity with depth (Brewer et al., 2019).

Chemical binding of organic compounds to reactive soil minerals (as represented with proportion of C in HF) was most effective at the drier sites along our study bio-climosequence. We found that top- and sub-soil HF OC is most depleted in $\Delta^{14}C$ (oldest, longer turnover time) in the oak savannah and subalpine site (Fig 3-3). Specifically, in the subsoil, the mineral-OC becomes less depleted (younger, faster turnover time) as the sites increase in elevation (higher GPP, vegetation, lower MAT, higher MAP). Even though the HF stores C for similar periods of time compared to the oLF, the mineral portion of C accounts for over 50% of C at all sites (Fig. 3-1), suggesting that it is important for at least 50% C that is remaining in the profile.

Clay content is positively correlated with preservation of SOM and higher clay percentages typically leading to lower decomposition rates because the clay minerals protect SOM from decomposition (Balesdent et al., 2000; Xu et al., 2016). All of our study sites had low clay content, with the highest percent clay values observed in soils at the oak savannah and ponderosa pine sites (lower elevation sites) and in the B horizons (Table 3-1). The type of dominant association mechanisms of organic matter and minerals depends on various factors, including OM characteristics, reactivity of minerals, surface area, cation availability, presence of Fe and Al oxides (produced by weathering), pH, and redox conditions (Lehmann & Kleber, 2015; von Lutzow et al., 2006). The topsoil (0–50 cm) clay mineralogy at these sites displays a general trend with increasing elevation of increasing desilication and hydroxy-Al interlayering of 2:1 layer silicates (Dahlgren et al., 1997). As elevation increases there is more extensive weathering, which leads to lower CEC and higher concentration of Fe and Al oxides in soil that may facilitate mineral-OM associations with ligand exchange reactions that were previously shown to be associated with longer turnover times of SOM (Mikutta et al., 2007). Even though we did not explicitly test abundance of metal oxides in this study, based on previous data collected at our study sites (Dahlgren et al., 1997; O'Geen et al., 2018; Rasmussen et al., 2005) and other temperate forests (Porras et al. 2017), we can infer that OM at the lower elevation is more likely to be stabilized through ion exchange while OM is more likely stabilized by ligand exchange type reactions at higher elevations. If this holds true, it could help to explain why the temperature-limited subalpine site and water limited oak savannah site store millennia old C (Fig. 3-2) in the B horizon. Even though the pH and clay are not statistically different between sites and total Fe and Al

concentration is lower in the highest and lowest elevation sites compared to the mid-elevation sites (Table 3-1).

Mineral protection has been proposed to be the most effective storage mechanism globally because of the high activation energy required to mineralize C that is bound to minerals (Hemingway et al., 2019; Lybrand & Rasmussen, 2015). However, our data suggests that C persists longer inside aggregates (as indicated by lower values of oLF $\Delta^{14}C$) while mineral protection of C (as indicated by $\Delta^{14}C$ of the HF and proportion of HF) is strongest at the driest site. It is likely that physical association and chemical binding of organic compounds with minerals protects SOC from loss as abundance and strength of aggregates and the amount of C protected as oLF are heavily influenced by organo-mineral and mineral-mineral interactions (Oades et al., 1991; Six et al., 2000, (Lehmann et al., 2007).

The results from the mixed effect model that included the $\Delta^{14}C$ of the topsoil and subsoil fractions and several climate parameters (GPP, MAT, MAP, DWP, and ET) indicated that the persistence of the fLF significantly correlates to GPP and ET (Table 3-1). A previous study along the same bio-climosequence indicated that bulk SOM turnover in topsoil was sensitive to temperature (Trumbore et al., 1996), in agreement with our findings that show fLF in the topsoil is responsive to climate. Furthermore, subsoil fLF and HF correlate to climate, especially GPP and ET suggesting that climate change may influence the persistence of C in these pools (Table 3-2). The oLF may be more resistant to changing climate because it does not show strong variability as function of any of the climate variables we investigated, except for slight association with DWP ($p = 0.049$, $r_2 =$

0.166). This suggests that more labile fLF throughout the profile is likely to be more vulnerable to changes in climate than the other fractions. ET and GPP also significantly correlated to the topsoil HF, suggesting that only in the topsoil is mineral associated HF C vulnerable to changes in climate. In contrast, findings of this study show that topsoil and subsoil oLF and subsoil HF persistence are not closely tied to climate.

CLIMATIC CONTROLS ON PERSISTENCE OF TOPSOIL COMPARED TO SUBSOIL C

Higher aromatic:aliphatic ratios derived from FTIR indicate more OM processing (Hall et al., 2018; Ryals et al., 2014). Faster turnover times have been associated with SOM with hydrolysable chemical bonds of saccharides and aliphatic-C, and the more persistent fraction is made up of aromatic or other macromolecules derived from lignin, lipids, waxes, suberins, cutins and pyrogenic OC (von Lutzow et al., 2006). Our FTIR results showed there is an increase in aromatics in the HF compared to both fLF and oLF (Fig. 3-7). Overall, the most significant relationships are between the topsoil and subsoil fLF persistence and ET and GPP, aligning with our $\Delta^{14}C$ results and estimated turnover time (fLF being younger, faster cycling time). Likely associated with higher GPP and belowground root abundance (not measured). The fLF and oLF are similar in the entire spectra to one another for all sites and depths (Fig.3-6). Both the fLF and oLF have a similar aromatic:aliphatic ratio across all depths and sites. Interestingly, even though oLF is not highly processed, it is depleted in $\Delta^{14}C$ suggesting that chemical composition is not always a good indication of persistence (Fig. 3-3 and 3-4).

The spectra for all sites show similar patterns from the topsoil to the subsoil. Aliphatic-C intensities are higher in the topsoil and decrease with depth indicating less processing in

the topsoil (Fig. 3-7). Decreases in peaks assigned to aliphatic methyl, polysaccharides, and alcohol functional groups from the topsoil to subsoil are likely due to preferential degradation of these compound types by soil microbes compared with condensed aromatic structures, at least in the short-term (Hsu & Lo, 1999; Paul, 2016; von Lutzow et al., 2006). This pattern matches the decrease in the C:N ratio with depth, indicating that it is a useful proxy for decomposition (Fig. 3-2). Subalpine and ponderosa pine sites have varying intensities in the topsoil compared to the other two sites, that is likely due to differences in clay content (aromatic OM selectively sorbs to clay minerals (Mikutta et al., 2007), vegetation type, Al and Fe content, and soil genesis (Falloon & Smith, 2006); Table 1).

We expected the C:N ratio to decline from fLF to oLF reflecting oxidation of organic C compounds by heterotrophic microbes, while N is relatively conserved in the microbial biomass owing to microbial N demand (their biomass has a much lower C:N ratio than plant biomass). However, this is not the trend we observed in both aromatic:aliphatic and C:N ratios with depth across the bio-climosequence (Fig. 3-1,3-6). (Wagai et al., 2009) compiled density separations and found that most soils had a higher C:N ratios in oLF than fLF, with differences in C:N of up to 10–20 units in some forest soils consistent with our results. HF had consistently lower C:N ratios implying that post-sonication, HF is dominated by microbially processed compounds and/or N-rich compounds, such as peptides, with little inclusion of high C:N fresh plant detritus. Lower C:N in the oak savannah site compared to the forested sites possibly exists because forest soils contain source materials with wider ranges of chemical compositions or different avenues that

SOM gets into soil: as litter deposition in forests and as root cell exudation in grasslands (Dietz et al., 2020). This trend was also noted in a meta-analysis of grassland and forested soils (Wagai et al., 2009). We observed a observable difference between the of C:N ratio, $\delta^{13}C$, and ^{14}C of the oak savannah compared to the forested sites likely driven by differences in rate of OM decomposition (consistent to findings of (Wagai et al., 2009)).

Past studies in this area suggested that major portions of the oLF is derived from selective preservation of char or other persistent biomolecules that are typically lighter in $\delta^{13}C$ (Badeck et al., 2005). One study cited that the reason for older OC in the oLF is due to abundance of char in this fraction (Lybrand et al., 2017). However, our FTIR results do not suggest that OC in this fraction are enriched in char, as was also the case in (Lavallee et al., 2019).

FATE OF SUBSOIL C AFTER CLIMATE CHANGE

Climate change has and is expected to shift distribution of precipitation types with significant implications for a range of ecosystem processes. Along the SSCZO bio-climosequence (Dahlgren et al., 1997; O'Geen et al., 2018) the expected change in climate includes shifting of the winter rain-snow transition zone to higher elevations with accompanying upward movement of the upper tree line by 300-500 m (Dahlgren et al., 1997). Dahlgren et al., (1997) suggested that the change caused by this shift would cause a net loss of SOM and no appreciable net change in rates of carbonic acid weathering. Our data show that that climate change and consequent shifting of the rain-snow transition zone and upper tree line could unfold via climate's impact on multiple key processes that play major role in soil C cycling. Our results show how vegetation (GPP)

exerts important influence on C partitioning into the three fractions (C free from association with minerals, C that stabilization through formation of physical associations with soil minerals, and C that is chemically bound to the surfaces of soil minerals). Furthermore, the variability in soil C turnover rates that we found in this study suggest that if vegetation changes it will likely shift the partitioning and turnover times of OC throughout the soil system. In lower elevations (oak savannah and ponderosa pine) that are expected to become drier/hotter, we can expect larger shift towards mineral protection and less C stored in the soil overall that is older (with slower transit time). Due to cooler temperatures, less biota (micro and macro), substrate availability (more roots, less fLF), and increased association with minerals, the subsoil may have much longer turnover times. In the highest elevation subalpine site weathering may be intensified with warming and shift of precipitation from that dominated by snow to rain, increasing the thickness of saprock and concentration of Fe and Al oxides leading to higher rate of C stabilization in soil over longer periods of times. Our results indicate that topsoil fLF, HF and the subsoil fLF are likely to change in response to changes in ET and GPP possibly indicating that with future changes in temperature and precipitation the fLF pool is likely to be most susceptible to climate change in the subsoil. We expect the changes in C stored in fLF to be highest in the lowest and highest elevation sites.

CONCLUSIONS

Our results show major differences in SOC partitioning and persistence that are driven, at least partially, by climate. We showed that lower-elevation, moisture-limited ecosystems store highly persistent and microbially processed C that it associated with minerals in the

topsoil and subsoil. We also found that with increases in elevation there is non-linear increases in soil C driven by interactions among ET, GPP, and decomposition rates along elevational transect. Our data indicate that the fLF and oLF OC proportion increased with elevation, suggesting mineral protection is important for long term storage in locations with lower ET/GPP. In contrast, aggregation plays important role in OC persistence in locations with higher ET/GPP. We demonstrate that even unprotected OC can persist over long periods of time and that physical association of OM with minerals in soil can play an important role in long-term stabilization of subsurface OC across the bioclimatic gradient. Moreover, our results show that C in fLF in both the topsoil and subsoil is likely to be vulnerable to changes in climate. We conclude that deep SOC stock and persistence as a function of climate cannot be easily predicted from observations of near-surface soil C dynamics. Deep soil OC inventory and persistence varies as a function of direct and indirect influences of climate on soil physical and chemical properties, including regolith thickness. Along the SSCZO elevation gradient, climate exerts strong influences on weathering and vegetation ultimately influencing partitioning and persistence of OC throughout the soil profile, specifically the more labile fLF portion.

ACKNOWLEDGEMENTS

Funding: U.S. National Science Foundation, through the Southern Sierra Critical Zone Observatory, Grant/Award number: EAR-1331939; and UC Lab Fees Research Fellowship, Award number: LGF-18-488060/SCW1447 from DOE-BER-TES

REFERENCES

Amundson, R. (2001). The carbon budget in soils. *Annual Review of Earth and Planetary Sciences*, *29*(1), 535–562. doi:10.1146/annurev.earth.29.1.535

Badeck, F.-W., Tcherkez, G., Nogués, S., Piel, C., & Ghashghaie, J. (2005). Post-photosynthetic fractionation of stable carbon isotopes between plant organs--a widespread phenomenon. *Rapid Communications in Mass Spectrometry*, *19*(11), 1381–1391. doi:10.1002/rcm.1912

Balesdent, J., Chenu, C., & Balabane, M. (2000). Relationship of soil organic matter dynamics to physical protection and tillage. *Soil and Tillage Research*, *53*(3–4), 215–230. doi:10.1016/S0167-1987(99)00107-5

Batjes, N. H. (1996). Total carbon and nitrogen in the soils of the world. *European Journal of Soil Science*, *47*(2), 151–163. doi:10.1111/j.1365-2389.1996.tb01386.x

Berhe, A. A., & Kleber, M. (2013). Erosion, deposition, and the persistence of soil organic matter: mechanistic considerations and problems with terminology. *Earth Surface Processes and Landforms*, *38*(8), 908–912. doi:10.1002/esp.3408

Billings, S. A., & de Souza, L. F. T. (2020). Earth's soil harbours ancient carbon. *Nature Geoscience*. doi:10.1038/s41561-020-0614-1

Brewer, T. E., Aronson, E. L., Arogyaswamy, K., Billings, S. A., Botthoff, J. K., Campbell, A. N., … Fierer, N. (2019). Ecological and genomic attributes of novel bacterial taxa that thrive in subsurface soil horizons. *MBio*, *10*(5). doi:10.1128/mBio.01318-19

Chabbi, A., Kögel-Knabner, I., & Rumpel, C. (2009). Stabilised carbon in subsoil horizons is located in spatially distinct parts of the soil profile. *Soil Biology and Biochemistry*, *41*(2), 256–261. doi:10.1016/j.soilbio.2008.10.033

Chadwick, O. A., Nettleton, W. D., & Staidl, G. J. (1995). Soil polygenesis as a function of Quaternary climate change, northern Great Basin, USA. *Geoderma*, *68*(1–2), 1–26. doi:10.1016/0016-7061(95)00025-J

Crimmins, T. M., Crimmins, M. A., & David Bertelsen, C. (2010). Complex responses to climate drivers in onset of spring flowering across a semi-arid elevation gradient. *Journal of Ecology*, *98*(5), 1042–1051. doi:10.1111/j.1365-2745.2010.01696.x

Crow, S. E., Swanston, C. W., Lajtha, K., Brooks, J. R., & Keirstead, H. (2007). Density fractionation of forest soils: methodological questions and interpretation of incubation results and turnover time in an ecosystem context. *Biogeochemistry*, *85*(1), 69–90. doi:10.1007/s10533-007-9100-8

Dahlgren, R. A., Boettinger, J. L., Huntington, G. L., & Amundson, R. G. (1997). Soil development along an elevational transect in the western Sierra Nevada, California. *Geoderma*, *78*(3–4), 207–236. doi:10.1016/S0016-7061(97)00034-7

Dane, J. H., & Topp, C. G. (Eds.). (2020). *Methods of Soil Analysis, Part 4: Physical Methods* (illustrated.). John Wiley & Sons.

Demyan, M. S., Rasche, F., Schulz, E., Breulmann, M., Müller, T., & Cadisch, G. (2012). Use of specific peaks obtained by diffuse reflectance Fourier transform mid-infrared spectroscopy to study the composition of organic matter in a Haplic Chernozem.

European Journal of Soil Science, *63*(2), 189–199. doi:10.1111/j.1365-2389.2011.01420.x

Dietz, S., Herz, K., Gorzolka, K., Jandt, U., Bruelheide, H., & Scheel, D. (2020). Root exudate composition of grass and forb species in natural grasslands. *Scientific Reports*, *10*(1), 10691. doi:10.1038/s41598-019-54309-5

Djukic, I., Zehetner, F., Tatzber, M., & Gerzabek, M. H. (2010). Soil organic-matter stocks and characteristics along an Alpine elevation gradient. *Journal of Plant Nutrition and Soil Science*, *173*(1), 30–38. doi:10.1002/jpln.200900027

Eusterhues, K., Rumpel, C., Kleber, M., & Kögel-Knabner, I. (2003). Stabilisation of soil organic matter by interactions with minerals as revealed by mineral dissolution and oxidative degradation. *Organic Geochemistry*, *34*(12), 1591–1600. doi:10.1016/j.orggeochem.2003.08.007

Falloon, P., & Smith, P. (2006). Simulating SOC changes in long-term experiments with RothC and CENTURY: model evaluation for a regional scale application. *Soil Use and Management*, *18*(2), 101–111. doi:10.1111/j.1475-2743.2002.tb00227.x

Fierer, N., Allen, A. S., Schimel, J. P., & Holden, P. A. (2003). Controls on microbial CO2 production: a comparison of surface and subsurface soil horizons. *Global Change Biology*, *9*(9), 1322–1332. doi:10.1046/j.1365-2486.2003.00663.x

Friedlingstein, P., Jones, M. W., O'Sullivan, M., Andrew, R. M., Hauck, J., Peters, G. P., Zaehle, S. (2019). Global carbon budget 2019. *Earth System Science Data*, *11*(4), 1783–1838. doi:10.5194/essd-11-1783-2019

Gaudinski, J. B., Trumbore, S. E., Davidson, E. A., & Zheng, S. (2000). Soil carbon cycling in a temperate forest: radiocarbon-based estimates of residence times, sequestration rates and partitioning of fluxes. *Biogeochemistry*, *51*(1), 33–69. doi:10.1023/A:1006301010014

Gerzabek, M. H., Antil, R. S., Kogel-Knabner, I., Knicker, H., Kirchmann, H., & Haberhauer, G. (2006). How are soil use and management reflected by soil organic matter characteristics: a spectroscopic approach. *European Journal of Soil Science*, *57*(4), 485–494. doi:10.1111/j.1365-2389.2006.00794.x

Goulden, M. L., Anderson, R. G., Bales, R. C., Kelly, A. E., Meadows, M., & Winston, G. C. (2012). Evapotranspiration along an elevation gradient in California's Sierra Nevada. *Journal of Geophysical Research*, *117*(G3). doi:10.1029/2012JG002027

Graven, H. D., Guilderson, T. P., & Keeling, R. F. (2012). Observations of radiocarbon in CO_2 at La Jolla, California, USA 1992-2007: Analysis of the long-term trend. *Journal of Geophysical Research*, *117*(D2). doi:10.1029/2011JD016533

Hall, S. J., Berhe, A. A., & Thompson, A. (2018). Order from disorder: do soil organic matter composition and turnover co-vary with iron phase crystallinity? *Biogeochemistry*, *140*(1), 93–110. doi:10.1007/s10533-018-0476-4

Harrington, F. (1958). Influence of Parent Matrial and Climate on Texture and Nitrogen.

Hemingway, J. D., Rothman, D. H., Grant, K. E., Rosengard, S. Z., Eglinton, T. I., Derry, L. A., & Galy, V. V. (2019). Mineral protection regulates long-term global preservation of natural organic carbon. *Nature*, *570*(7760), 228–231. doi:10.1038/s41586-019-1280-6

Hicks Pries, C. E., Castanha, C., Porras, R. C., & Torn, M. S. (2017). The whole-soil carbon flux in response to warming. *Science*, *355*(6332), 1420–1423. doi:10.1126/science.aal1319

Hicks Pries, C. E., Castanha, C., Porras, R., Phillips, C., & Torn, M. S. (2018). Response to Comment on "The whole-soil carbon flux in response to warming". *Science*, *359*(6378). doi:10.1126/science.aao0457

Hobbie, S. E., Schimel, J. P., Trumbore, S. E., & Randerson, J. R. (2000). Controls over carbon storage and turnover in high-latitude soils. *Global Change Biology*, *6*(S1), 196–210. doi:10.1046/j.1365-2486.2000.06021.x

Homann, P. S., Kapchinske, J. S., & Boyce, A. (2007). Relations of mineral-soil C and N to climate and texture: regional differences within the conterminous USA. *Biogeochemistry*, *85*(3), 303–316. doi:10.1007/s10533-007-9139-6

Hsu, J.-H., & Lo, S.-L. (1999). Chemical and spectroscopic analysis of organic matter transformations during composting of pig manure. *Environmental Pollution*, *104*(2), 189–196. doi:10.1016/S0269-7491(98)00193-6

Hua, Q., & Barbetti, M. (2004). Review of tropospheric bomb^{14}C data for carbon cycle modeling and age calibration purposes. *Radiocarbon*, *46*(3), 1273–1298. doi:10.1017/S0033822200033142

IPCC. (2018). Global Warming of 1.5 °C an IPCC special report on the impacts of global warming of 1.5 °C above pre-industrial levels and related global greenhouse gas emission pathways, in the context of strengthening the global response to the threat of climate

change, sustainable development, and efforts to eradicate poverty (p. 32). Geneva, Switzerland: (IPCC) *Intergovernmental Panel on Climate Change*.

IPCC. (2014). Intergovernmental Panel on Climate Change (Ed.). (2014). *Climate Change 2013 - The Physical Science Basis* (1st ed., p. 1535). Cambridge, UK and New York, NY, USA: Cambridge University Press. doi:10.1017/CBO9781107415324

Jenny, H., Gessel, S. P., & Bingham, F. T. (1949). Comparative study of decomposition rates of organic matter in temperate and tropical regions. *Soil Science*, *68*(6), 419–432. doi:10.1097/00010694-194912000-00001

Jia, J., Cao, Z., Liu, C., Zhang, Z., Lin, L., Wang, Y., … Feng, X. (2019). Climate warming alters subsoil but not topsoil carbon dynamics in alpine grassland. *Global Change Biology*, *25*(12), 4383–4393. doi:10.1111/gcb.14823

Jobbágy, E. G., & Jackson, R. B. (2000). The verttical distribution of soil organic carbon and its relation to climate and vegetation. *Ecological Applications*.

Kaiser, M., & Asefaw Berhe, A. (2014). How does sonication affect the mineral and organic constituents of soil aggregates?-A review. *Journal of Plant Nutrition and Soil Science*, *177*(4), 479–495. doi:10.1002/jpln.201300339

Kaiser, M., Berhe, A. A., Sommer, M., & Kleber, M. (2012). Application of ultrasound to disperse soil aggregates of high mechanical stability. *Journal of Plant Nutrition and Soil Science*, *175*(4), 521–526. doi:10.1002/jpln.201200077

Kelly, A. E., & Goulden, M. L. (2016). A montane Mediterranean climate supports year-round photosynthesis and high forest biomass. *Tree Physiology*, *36*(4), 459–468.

doi:10.1093/treephys/tpv131

Klute, E. A. (1986). *Methods Of Soil Analysis. Part 1. Physical And Mineralogical Methods (sssa Book Series No 5) (sssa Book Series No 5)* (2nd ed., p. 1358). American Society Of Agronomy-soil Science Society Of America.

Kögel-Knabner, I., Guggenberger, G., Kleber, M., Kandeler, E., Kalbitz, K., Scheu, S., … Leinweber, P. (2008). Organo-mineral associations in temperate soils: Integrating biology, mineralogy, and organic matter chemistry. *Journal of Plant Nutrition and Soil Science*, *171*(1), 61–82. doi:10.1002/jpln.200700048

Lavallee, J. M., Conant, R. T., Haddix, M. L., Follett, R. F., Bird, M. I., & Paul, E. A. (2019). Selective preservation of pyrogenic carbon across soil organic matter fractions and its influence on calculations of carbon mean residence times. *Geoderma*, *354*, 113866. doi:10.1016/j.geoderma.2019.07.024

Lehmann, J., Kinyangi, J., & Solomon, D. (2007). Organic matter stabilization in soil microaggregates: implications from spatial heterogeneity of organic carbon contents and carbon forms. *Biogeochemistry*, *85*(1), 45–57. doi:10.1007/s10533-007-9105-3

Lehmann, J., & Kleber, M. (2015). The contentious nature of soil organic matter. *Nature*, *528*(7580), 60–68. doi:10.1038/nature16069

Levin, I., & Kromer, B. (2004). The Tropospheric$^{14}CO_2$ Level in Mid-Latitudes of the Northern Hemisphere (1959–2003). *Radiocarbon*, *46*(3), 1261–1272. doi:10.1017/S0033822200033130

Lybrand, R. A., Heckman, K., & Rasmussen, C. (2017). Soil organic carbon partitioning

and Δ14C variation in desert and conifer ecosystems of southern Arizona. *Biogeochemistry*, *134*(3), 261–277. doi:10.1007/s10533-017-0360-7

Lybrand, R. A., & Rasmussen, C. (2015). Quantifying climate and landscape position controls on soil development in semiarid ecosystems. *Soil Science Society of America Journal*, *79*(1), 104–116. doi:10.2136/sssaj2014.06.0242

Marin-Spiotta, E., Chaopricha, N. T., Plante, A. F., Diefendorf, A. F., Mueller, C. W., Grandy, A. S., & Mason, J. A. (2014). Long-term stabilization of deep soil carbon by fire and burial during early Holocene climate change. *Nature Geoscience*, *7*(6), 428–432. doi:10.1038/ngeo2169

Marín-Spiotta, E., Swanston, C. W., Torn, M. S., Silver, W. L., & Burton, S. D. (2008). Chemical and mineral control of soil carbon turnover in abandoned tropical pastures. *Geoderma*, *143*(1–2), 49–62. doi:10.1016/j.geoderma.2007.10.001

McFarlane, K. J., Torn, M. S., Hanson, P. J., Porras, R. C., Swanston, C. W., Callaham, M. A., & Guilderson, T. P. (2013). Comparison of soil organic matter dynamics at five temperate deciduous forests with physical fractionation and radiocarbon measurements. *Biogeochemistry*, *112*(1–3), 457–476. doi:10.1007/s10533-012-9740-1

Mikutta, R., Mikutta, C., Kalbitz, K., Scheel, T., Kaiser, K., & Jahn, R. (2007). Biodegradation of forest floor organic matter bound to minerals via different binding mechanisms. *Geochimica et Cosmochimica Acta*, *71*(10), 2569–2590. doi:10.1016/j.gca.2007.03.002

O'Geen, A. T., Safeeq, M., Wagenbrenner, J., Stacy, E., Hartsough, P., Devine, S., …

Bales, R. (2018). Southern sierra critical zone observatory and kings river experimental watersheds: A synthesis of measurements, new insights, and future directions. *Vadose Zone Journal*, *17*(1), 180081. doi:10.2136/vzj2018.04.0081

Paul, E A, Follett, R. F., Leavitt, S. W., Halvorson, A., Peterson, G. A., & Lyon, D. J. (1997). Radiocarbon dating for determination of soil organic matter pool sizes and dynamics. *Soil Science Society of America Journal*, *61*(4), 1058. doi:10.2136/sssaj1997.03615995006100040011x

Paul, E. A. (2016). The nature and dynamics of soil organic matter: Plant inputs, microbial transformations, and organic matter stabilization. *Soil Biology and Biochemistry*, *98*, 109–126. doi:10.1016/j.soilbio.2016.04.001

Pellegrini, S., Agnelli, A. E., Andrenelli, M. C., Barbetti, R., Lo Papa, G., Priori, S., & Costantini, E. A. C. (2018). Using present and past climosequences to estimate soil organic carbon and related physical quality indicators under future climatic conditions. *Agriculture, Ecosystems & Environment*, *266*, 17–30. doi:10.1016/j.agee.2018.07.015

Porras, R. C., Hicks Pries, C. E., McFarlane, K. J., Hanson, P. J., & Torn, M. S. (2017). Association with pedogenic iron and aluminum: effects on soil organic carbon storage and stability in four temperate forest soils. *Biogeochemistry*, *133*(3), 333–345. doi:10.1007/s10533-017-0337-6

Post, W. M., Emanuel, W. R., Zinke, P. J., & Stangenberger, A. G. (1982). Soil carbon pools and world life zones. *Nature*, *298*(5870), 156–159. doi:10.1038/298156a0

Preusser, S., Poll, C., Marhan, S., Angst, G., Mueller, C. W., Bachmann, J., & Kandeler,

E. (2019). Fungi and bacteria respond differently to changing environmental conditions within a soil profile. *Soil Biology and Biochemistry*, *137*, 107543. doi:10.1016/j.soilbio.2019.107543

Rasmussen, CRAIG, Southard, R. J., & Horwath, W. R. (2006). Mineral control of organic carbon mineralization in a range of temperate conifer forest soils. *Global Change Biology*, *12*(5), 834–847. doi:10.1111/j.1365-2486.2006.01132.x

Rasmussen, Craig, Torn, M. S., & Southard, R. J. (2005). Mineral assemblage and aggregates control carbon dynamics in a california conifer forest. *Soil Science Society of America Journal*, *69*(6), 1711. doi:10.2136/sssaj2005.0040

Robertson, G. P. (1999). *Standard Soil Methods For Long-term Ecological Research (long-term Ecological Research Network Series)* (1st ed., p. 480). New York: Oxford University Press.

Rodhe, H. (1992). 4 modeling biogeochemical cycles. In *Global Biogeochemical Cycles* (Vol. 50, pp. 55–72). Elsevier. doi:10.1016/S0074-6142(08)62687-X

Root, T. L., Price, J. T., Hall, K. R., Schneider, S. H., Rosenzweig, C., & Pounds, J. A. (2003). Fingerprints of global warming on wild animals and plants. *Nature*, *421*(6918), 57–60. doi:10.1038/nature01333

Rumpel, C, Kögel-Knabner, I., & Bruhn, F. (2002). Vertical distribution, age, and chemical composition of organic carbon in two forest soils of different pedogenesis. *Organic Geochemistry*, *33*(10), 1131–1142. doi:10.1016/S0146-6380(02)00088-8

Rumpel, Cornelia, & Kögel-Knabner, I. (2011). Deep soil organic matter—a key but

poorly understood component of terrestrial C cycle. *Plant and Soil*, *338*(1–2), 143–158. doi:10.1007/s11104-010-0391-5

Ryals, R., Kaiser, M., Torn, M. S., Berhe, A. A., & Silver, W. L. (2014). Impacts of organic matter amendments on carbon and nitrogen dynamics in grassland soils. *Soil Biology and Biochemistry*, *68*, 52–61. doi:10.1016/j.soilbio.2013.09.011

Scharpenseel, H. W., Becker-Heidmann, P., Neue, H. U., & Tsutsuki, K. (1989). Bomb-carbon, 14C-dating and 13C — Measurements as tracers of organic matter dynamics as well as of morphogenetic and turbation processes | Semantic Scholar.

Schmidt, M. W. I., Torn, M. S., Abiven, S., Dittmar, T., Guggenberger, G., Janssens, I. A., … Trumbore, S. E. (2011). Persistence of soil organic matter as an ecosystem property. *Nature*, *478*(7367), 49–56. doi:10.1038/nature10386

Shangguan, W., Hengl, T., Mendes de Jesus, J., Yuan, H., & Dai, Y. (2017). Mapping the global depth to bedrock for land surface modeling. *Journal of Advances in Modeling Earth Systems*, *9*(1), 65–88. doi:10.1002/2016MS000686

Shi, Z., Allison, S. D., He, Y., Levine, P. A., Hoyt, A. M., Beem-Miller, J., … Randerson, J. T. (2020). The age distribution of global soil carbon inferred from radiocarbon measurements. *Nature Geoscience*. doi:10.1038/s41561-020-0596-z

Sparks, D. L., Page, A. L., Helmke, P. A., Loeppert, R. H., Soltanpour, P. N., Tabatabai, M. A., … Sumner, M. E. (Eds.). (1996). *Methods of soil analysis: part 3 chemical methods. Soil pH and soil acidity.* (J.M. Bigham., pp. 475–490). Madison, WI, USA: Soil Science Society of America, American Society of Agronomy.

doi:10.2136/sssabookser5.3

Stevenson, F. J. (1995). Humus chemistry: genesis, composition, reactions, second edition . *Journal of Chemical Education*, *72*(4), A93. doi:10.1021/ed072pA93.6

Stockmann, U., Adams, M. A., Crawford, J. W., Field, D. J., Henakaarchchi, N., Jenkins, M., … Zimmermann, M. (2013). The knowns, known unknowns and unknowns of sequestration of soil organic carbon. *Agriculture, Ecosystems & Environment*, *164*, 80–99. doi:10.1016/j.agee.2012.10.001

Stone, M. M., DeForest, J. L., & Plante, A. F. (2014). Changes in extracellular enzyme activity and microbial community structure with soil depth at the Luquillo Critical Zone Observatory. *Soil Biology and Biochemistry*, *75*, 237–247. doi:10.1016/j.soilbio.2014.04.017

Stuiver, M., & Polach, H. A. (1977). Discussion; reporting of C-14 data. *Radiocarbon*.

Stuiver, M., Reimer, P. J., & Braziunas, T. F. (1998). High-Precision Radiocarbon Age Calibration for Terrestrial and Marine Samples. *Radiocarbon*, *40*(3), 1127–1151. doi:10.1017/S0033822200019172

Tian, Z., Moreland, K., O'Geen, A., McFarlane, K., Hartsough, P., Hart, S., … Berhe, A. A. (In review). Deep in the critical zone: weathered bedrockrepresents a large and potentially active pool of soil carbon.

Torn, M S, Swanston, C. W., Castanha, C., & Trumbore, S. E. (2009). Storage and turnover of organic matter in soil. In N. Senesi, B. Xing, & P. M. Huang (Eds.), *Biophysico-Chemical Processes Involving Natural Nonliving Organic Matter in*

Environmental Systems (pp. 219–272). Hoboken, NJ, USA: John Wiley & Sons, Inc. doi:10.1002/9780470494950.ch6

Torn, M. S., Lapenis, A. G., Timofeev, A., Fischer, M. L., Babikov, B. V., & Harden, J. W. (2002). Organic carbon and carbon isotopes in modern and 100-year-old-soil archives of the Russian steppe. *Global Change Biology*, *8*(10), 941–953. doi:10.1046/j.1365-2486.2002.00477.x

Trumbore, S.E. (2000). Age of soil organic maytter and soil respiration:radiocarbon contrainsts on belowground C dynamics. *Ecological Applications*.

Trumbore, S. E., Chadwick, O. A., & Amundson, R. (1996). Rapid exchange between soil carbon and atmospheric carbon dioxide driven by temperature change. *Science*, *272*(5260), 393–396. doi:10.1126/science.272.5260.393

Vogel, J. S., Southon, J. R., Nelson, D. E., & Brown, T. A. (1984). Performance of catalytically condensed carbon for use in accelerator mass spectrometry. *Nuclear Instruments and Methods in Physics Research Section B: Beam Interactions with Materials and Atoms*, *5*(2), 289–293. doi:10.1016/0168-583X(84)90529-9

von Lutzow, M., Kogel-Knabner, I., Ekschmitt, K., Matzner, E., Guggenberger, G., Marschner, B., & Flessa, H. (2006). Stabilization of organic matter in temperate soils: mechanisms and their relevance under different soil conditions - a review. *European Journal of Soil Science*, *57*(4), 426–445. doi:10.1111/j.1365-2389.2006.00809.x

Wagai, R., Mayer, L. M., & Kitayama, K. (2009). Nature of the “occluded” low-density fraction in soil organic matter studies: A critical review. *Soil Science and Plant Nutrition*,

55(1), 13–25. doi:10.1111/j.1747-0765.2008.00356.x

Xu, X., Shi, Z., Li, D., Rey, A., Ruan, H., Craine, J. M., … Luo, Y. (2016). Soil properties control decomposition of soil organic carbon: Results from data-assimilation analysis. *Geoderma*, *262*, 235–242. doi:10.1016/j.geoderma.2015.08.038

Yost, J. L., & Hartemink, A. E. (2020). How deep is the soil studied – an analysis of four soil science journals. *Plant and Soil*. doi:10.1007/s11104-020-04550-z

Zhang, H., Wang, E., Zhou, D., Luo, Z., & Zhang, Z. (2016). Rising soil temperature in China and its potential ecological impact. *Scientific Reports*, *6*, 35530. doi:10.1038/srep35530

FIGURES

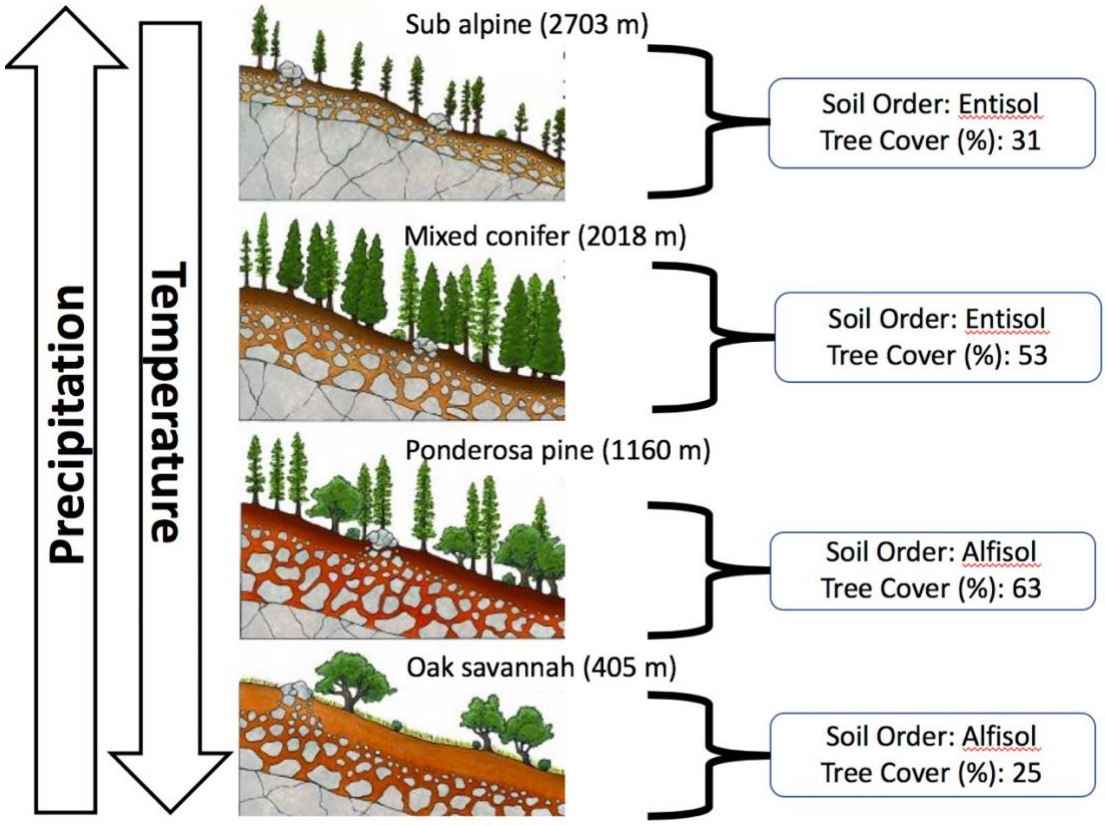

Figure 0-1. Conceptual model of the SSCZO, showing elevation and climate gradient, with regolith properties, vegetation, and temporal feedbacks in the study site.

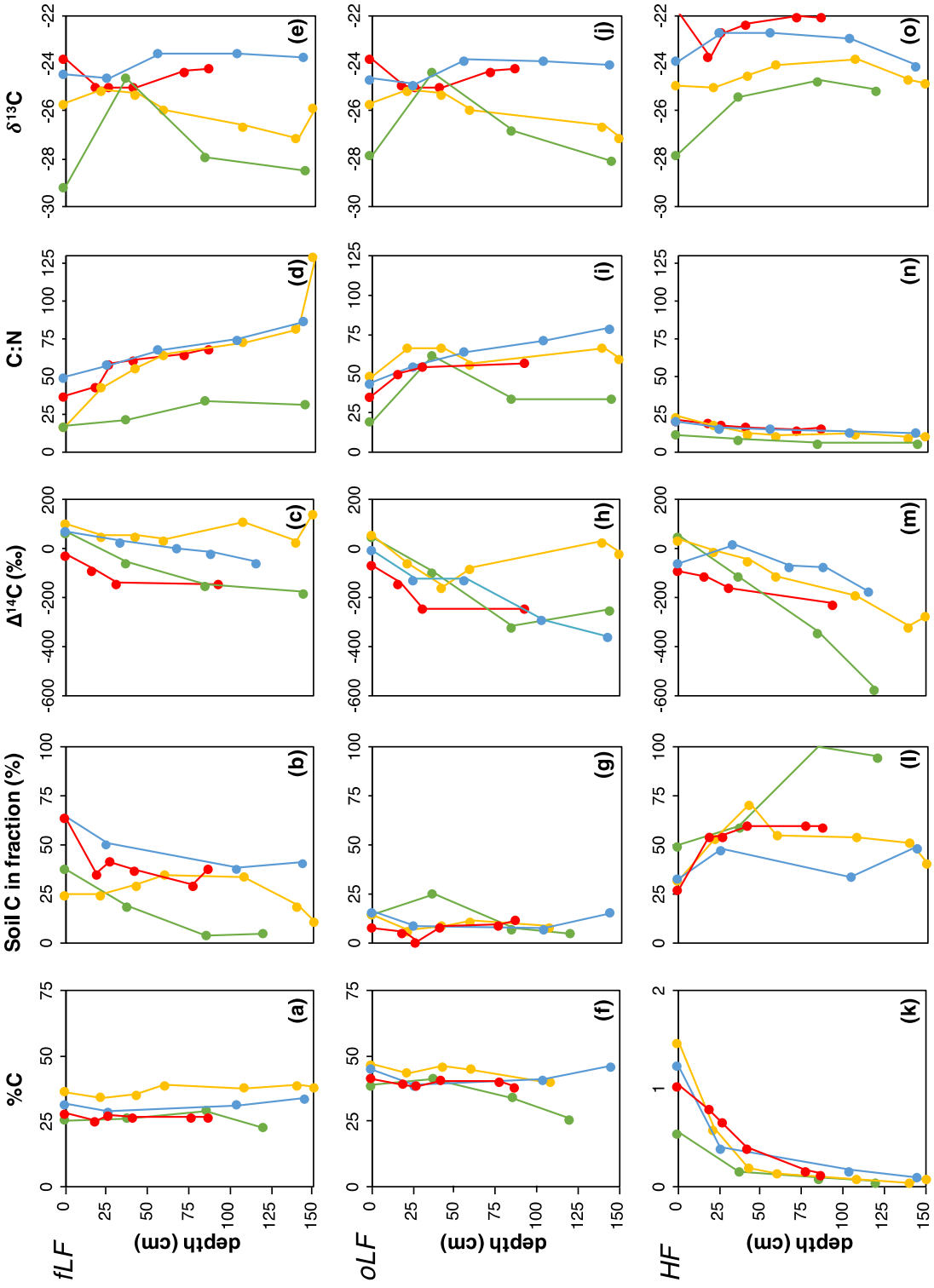

Figure 0-2. Mean percent C, soil C distribution in each fraction, Δ14C, C:N, and the □13C in (a-e) fLF, (e-h), oLF, and (k-o) HF. n=3 for each point in every fraction.

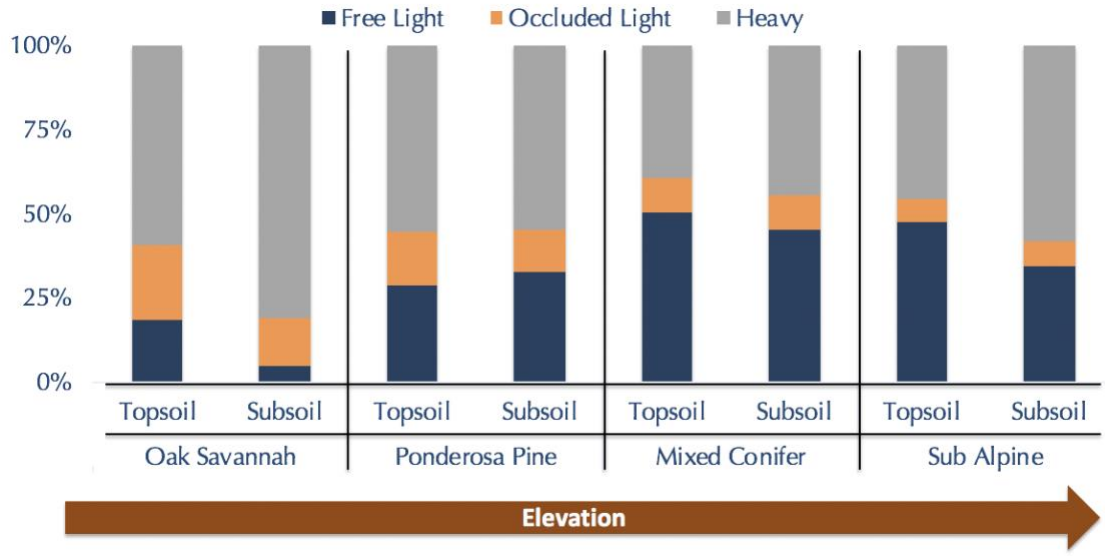

Figure 0-3. Mean proportion of C in each fraction in the topsoil (0-30 cm) and subsoil (30-150 cm) for each site. Means were normalized to 100 to account for any loss during the fractionation (less than 15% compared to bulk soils).

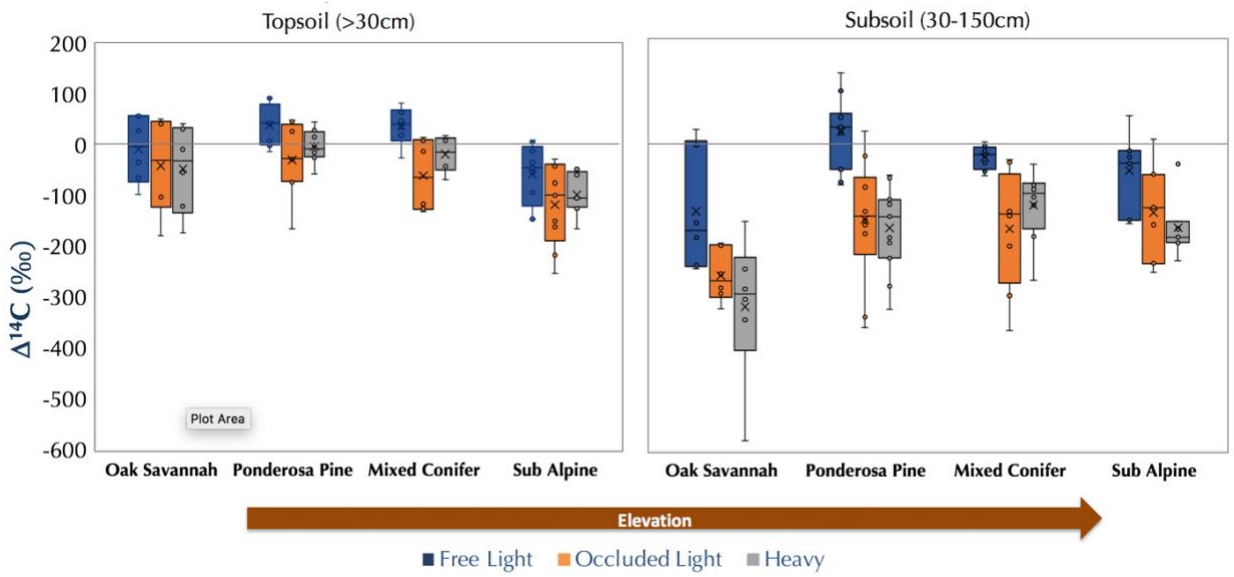

Figure 0-4. $\Delta^{14}C$ (‰) in each fraction across the sites. The line indicates C that would be considered modern. The x represents the mean and the o are the individual data points.

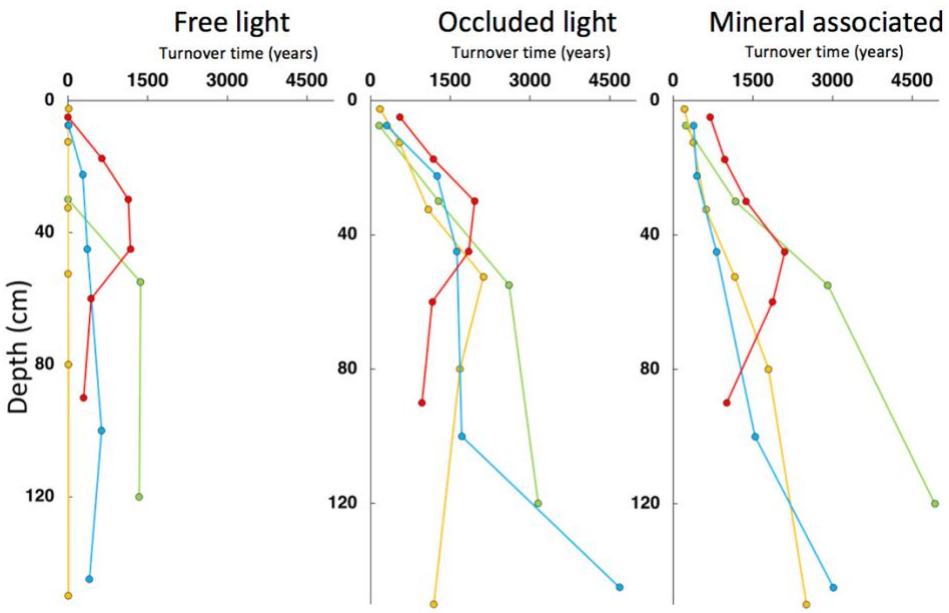

Figure 0-5. Estimated mean turnover time of the fractions with depth. Reported turnover times are the means of the three pits sampled at each site. Elevations are in the legend.

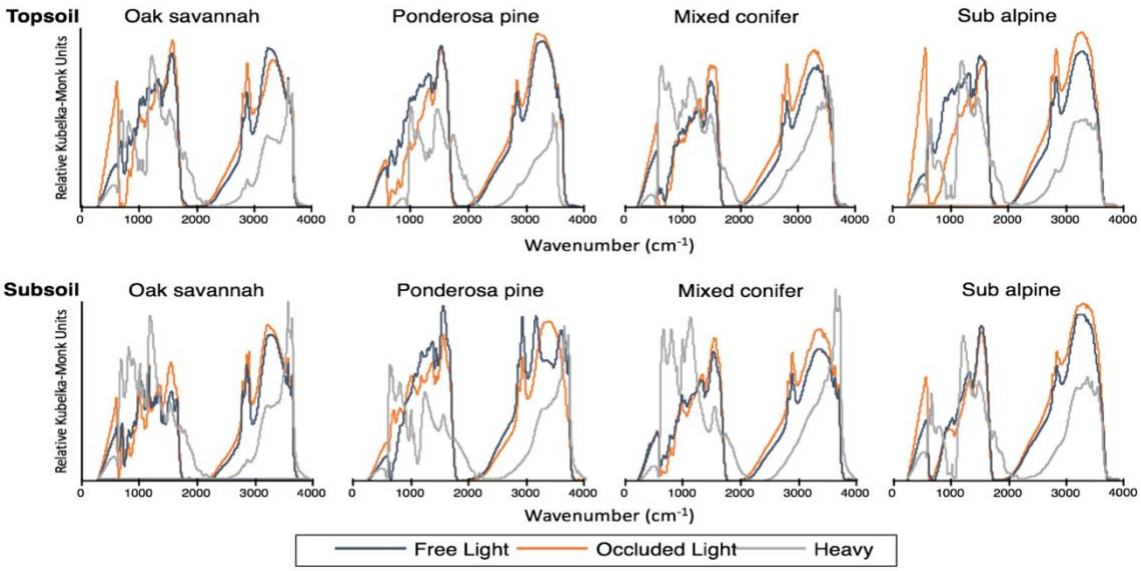

Figure 0-6. Representative FTIR-DRIFT spectra of the topsoil (A horizon) and subsoil (BC horizon) fractions for all sites chosen by the uppermost sample and the deepest sample.

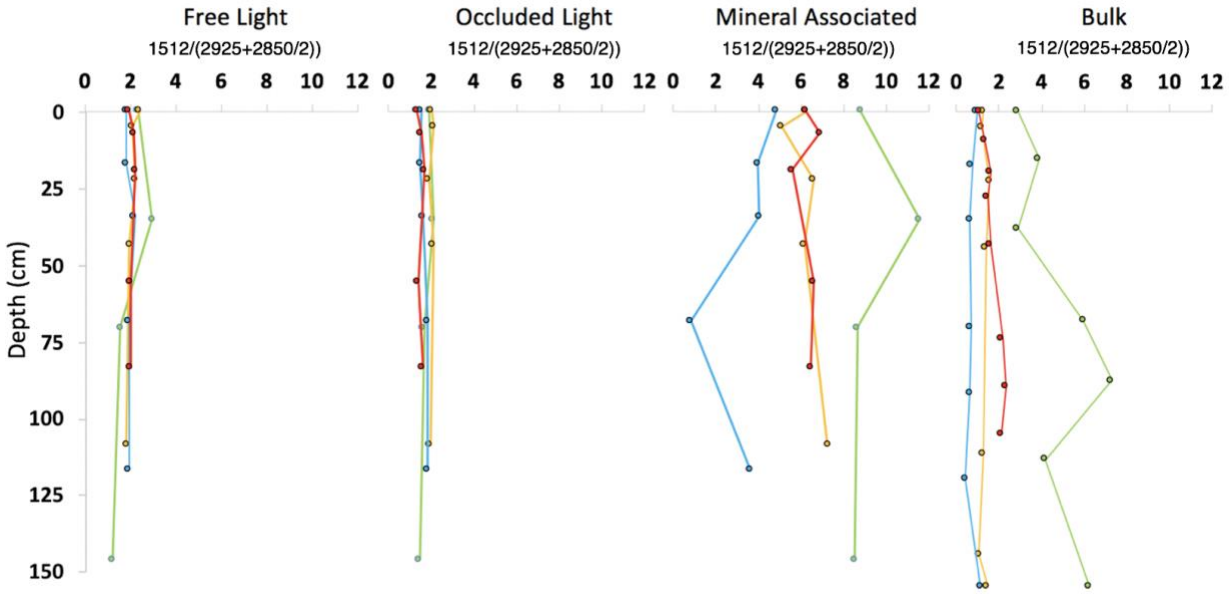

Figure 0-7. Mean aromatic:aliphatic ratio (1512 cm^{-1}/(2925 cm^{-1}+2850 cm^{-1}/2)) with depth of the fractions and bulk soils. n = 3 for fraction samples and n = 4 for bulk samples.

TABLES

Table 0-1. Mean bulk sample bulk density, clay %, pH, total Fe and Al concentrations from each master horizon along the climosequence. Means are of each soil pit and from each master horizon. The error term represents standard error. n for A horizon is 6–10, n for B horizon is 7–12, n for C horizon is 3–6, and n for Cr horizon is 4–5. n/a values indicate that the soil profile at the subalpine system did not have Cr horizon. Data rounded to smallest error. *Total Fe and Al obtained from Morgan Barnes.

Site	Master Horizon and Cr	Bulk Density (g/cm^3)	Clay %	pH (DI)	Total Fe (mg/g)	Total Al (mg/g)
Oak savannah	A	1.46 ± 0.10	5.53 ± 0.81	5.38 ± 0.57	7.54 ± 3	41.57 ± 4
	B	1.63 ± 0.13	9.83 ± 5.06	5.70 ± 0.77	4.53 ± 3	38.54 ± 5
	C	1.64 ± 0.14	4.31 ± 0.94	6.14 ± 0.97	5.65 ± 7	37.08 ± 9
	Cr	1.67 ± 0.06	2.72 ± 2.52	5.81 ± 0.78	4.17 ± 4	37.52 ± 6
Ponderosa pine	A	0.92 ± 0.33	5.40 ± 1.86	5.50 ± 0.38	8.17 ± 1	41.54 ± 3
	B	1.02 ± 0.46	6.84 ± 1.93	5.29 ± 0.56	7.35 ± 2	37.58 ± 12
	C	1.45 ± 0.18	10.97 ± 6.38	5.72 ± 0.85	8.53 ± 1	48.27 ± 6
	Cr	1.42 ± 0.00	8.50 ± 5.86	5.57 ± 0.65	7.97 ± 1	45.17 ± 4
Mixed conifer	A	0.98 ± 0.22	3.26 ± 2.82	5.55 ± 0.08	3.73 ± 5	42.10 ± 2
	B	1.39 ± 0.13	6.08 ± 1.93	5.34 ± 0.27	9.96 ± 2	43.28 ± 4
	C	1.41 ± 0.09	6.91 ± 1.96	5.25 ± 0.45	9.20 ± 2	45.86 ± 6
	Cr	1.54 ± 0.13	5.44 ± 2.10	5.22 ± 0.18	10.13 ± 1	49.85 ± 4
Subalpine	A	1.25 ± 0.10	3.23 ± 0.61	5.25 ± 0.30	3.64 ± 1	32.15 ± 4
	B	1.42 ± 0.14	4.27 ± 1.73	5.60 ± 0.29	3.44 ± 0	32.36 ± 2
	C	1.33 ± 0.09	3.66 ± 0.68	5.69 ± 0.25	3.91 ± 1	34.40 ± 2
	Cr	n/a	n/a	n/a	n/a	n/a

Table 3-2. Mixed effect model results between $\Delta^{14}C$ and climate variables (Elevation, MAT, MAP, DWP, ET) with conditional R-squared and P-value ($p < 0.05$, * $p < 0.01$, **). Topsoil n = 25, subsoil n = 38. Topsoil was grouped by A horizons and typically fell above 30 cm. Subsoil was classified as the B and BC horizons going down to 150 cm.

		GPP		**MAT**		**MAP**		**DWP**		**ET**	
		R^2C	P-value	R^2C	P-value	R^2C	P-value	R^2C	P-value	R^2C	P-value
Topsoil	fLF	0.260	0.011*	0.17	0.04*	0.15	0.78	0.16	0.24	0.31	0.004**
Subsoil	fLF	0.675	0.024*	0.70	0.91	0.69	0.33	0.83	0.70	0.70	0.05*
Topsoil	oLF	0.026	0.555	0.16	0.21	0.12	0.11	0.17	0.04*	0.08	0.18
Subsoil	oLF	0.268	0.421	0.26	0.46	0.25	0.29	0.26	0.43	0.27	0.66
Topsoil	HF	0.238	0.012*	0.08	0.17	0.05	0.83	0.20	0.07	0.31	0.003**
Subsoil	HF	0.088	0.071	0.08	0.08	0.17	0.01**	0.09	0.07	0.02	0.43

CHAPTER 4: CLIMATIC CONTROLS ON SOIL NITROGEN STOCK, DISTRIBUTION, COMPOSITION, AND PERSISTENCE IN DEEP VERSUS NEAR SURFACE SOIL LAYERS

ABSTRACT

Nitrogen (N) is a major plant essential nutrient in soil that regulates plant growth, microbial community dynamics, terrestrial sequestration of atmospheric carbon dioxide, and persistence of organic compounds in soil. However, major knowledge gaps remain about how climate change may impact N accumulation and persistence, in particular in deep soil layers. In order to gain a better understanding whole soil profile N stock and the controls on N accumulation and persistence, we investigated the concentration, distribution of soil N, and estimated persistence of soil N along a bio-climosequence in the southern Sierra Nevada in California. We found that climate exerts both a direct and indirect control on soil N accumulation and persistence. Analysis of the entire soil profile illustrated that in the cooler/wetter mixed conifer site held 37% of profile N in weathered bedrock, accounting for more than the entire drier/hotter oak savannah soil system N. This indicates that the effect of climate on deep weathered bedrock N storage might be indirect, primarily through climate and subsequently biota's influence on thickness of the weathered bedrock. Statistical analyses of effect of climate on amount and distribution of soil N in density fractions indicated that the majority of N in soil, which is mineral-associated and persistent, is not influenced by the climate proxies tested. Soil N in topsoil and subsoil unprotected, and occluded fractions stock increased with elevation. Both the unprotected and occluded fractions of N are strongly influenced by climate, suggesting a direct climatic effect on these more labile pools of soil N. Modeled turnover rate of N in the soils across the bio-

climosequence showed that drier/hotter climates have a shorter turnover time compared to mid-elevation sites with climates that are cooler/ wetter. Our results also suggest that climate likely, indirectly influences N cycling across the entire critical zone from the top of the trees down into soil through a variety of other biological and chemical processes.

INTRODUCTION

Nitrogen (N) is a major plant essential nutrient that controls microbial functioning, plant growth, and the cycling of soil organic matter (SOM; (Chapin et al., 2011; Houlton & Morford, 2015; LeBauer & Treseder, 2008). The concentration, and availability of N in both its organic and inorganic forms is closely related to biological productivity in terrestrial and aquatic systems. The majority of N in soils is found in the form of organic biomolecules and its distribution parallels that of soil organic carbon (C) (Berhe & Torn, 2017; Weil & Brady, 2016). Globally, soils store up to 50% of N below 30 cm (to 100 cm) (Batjes, 1996). But, our understanding of soil N dynamics in deep soil layers is limited as the average maximum depth of previous studies in the top four soil journals is 23 cm (Yost & Hartemink, 2020). This is concerning because the estimated average soil thickness is 2 m, meaning we are missing a massive portion of the soil system (Shangguan et al. 2017). Recently, controls on availability of soil N and how it is likely to affect C sequestration in a world with a changing climate has been a focus of growing number of studies (Craine et al., 2015; van Groenigen et al., 2015; Wieder et al., 2015). Consequently, there is now a pressing need to improve our understanding of whole soil profile N dynamics, including variables controlling subsoil N stocks, distribution, stability, and climate sensitivity.

Climate is one of the fundamental variables that controls soil N dynamics, including total N input, rate of N fixation, N abundance, and contribution of rock weathering to soil N (Houlton & Morford, 2015; Jenny, 1928). Changes in climate are expected to significantly influence overall soil nutrient cycling with consequent effects on N cycling (Conant et al., 2011), and hence the structure, functioning and diversity of terrestrial

ecosystems (Sistla & Schimel, 2012). Among different climatic parameters, soil temperature and moisture stand out as key drivers that control soil N cycling (Bell et al. 2008), where lower soil moisture has been shown to lead to reduced N mineralization, availability, and increase ammonia oxidation (Manzoni et al., 2012; Niboyet et al., 2011). Studies investigating the impacts of warming temperature on N show contrasting results: For instance, a meta-analysis (Rustad et al., 2001) and a lab incubation (MacDonald et al., 1995) reported that with warming N mineralization rates increased by 46%, with highest impacts observed in forested ecosystems.

(Hart, 2006) found that even small increases in mean annual temperature can greatly impact soil N cycling. On the other hand, Niboyet et al., (2011) found little influence of warming on the nitrite and ammonia oxidation. In addition to this uncertainly, lack of studies that have explicitly quantified climate sensitive of soil N below 50 cm means there are major gaps in our ability to extrapolate these findings to whole soil profile scale N response to changing climate.

Recent studies have shown that persistent N in soil tends to be made up of mixture of intact plant-derived biomolecules and microbially processed organic matter (Kleber et al., 2011). Aggregation and sorptive interaction of organic compounds with reactive soil minerals have been shown to be responsible for stabilization of N over century and longer timescales (Berhe & Torn, 2017). Nitrogen-containing compounds can adsorb directly onto mineral surfaces via H-bonding, van der Waals, hydrophobic interactions, and through cation bridging (Bingham & Cotrufo, 2016) and ammonium ions can sorb onto mineral surfaces or become fixed within the crystal structure of silicate minerals such as micas (Hall, 1999). Binding of N-containing organic compounds to the surfaces of

minerals prevents their vertical translocation within the soil profile with moving water or as particulate matter and reduces the vulnerability of the N containing organic compounds to mineralization (Kögel-Knabner et al., 2008).

Historic conceptual and process based models of N are based upon the understanding that N enter ecosystems solely from the atmosphere via biological fixation of N_2, and wet and dry deposition (Delwiche, 1970; Fowler et al., 2013; Galloway et al., 2004; Houlton & Morford, 2015). But, recent studies have shown that weathering of bedrock can contribute large amount of N to soil that becomes available to plants via mycorrhizal associations (Dynarski et al., 2019; Houlton & Morford, 2015). The availability of N in soil and its form is governed by the extent of weathering and mineralogical properties of soil along with its subsequent incorporation in OM and association with soil minerals (Berhe & Torn, 2017).

To further our understanding of how projected climate change can influence subsoil N accumulation and stabilization, we set out to conduct a complete accounting of soil N stocks including topsoil, subsoil, and weathered bedrock (part of the soil profile where the parent material maintains the original rock texture but is porous and friable) and derive mechanistic insights on the controls of whole soil N accumulation and persistence. The major objective of this research was to determine how climate affects accumulation and stabilization mechanisms of near surface compared to deep soil N. Specifically we asked two targeted questions:

(1) Does climate affect the accumulation of N in soil and weathered bedrock? and

(2) How does climate influence the distribution of N in soil and the mechanisms of N stabilization?

Results derived from our study along the bio-climosequence in the Southern Sierra Nevada Critical Zone Observatory in California are critical for our ability to infer the effect of climate on soil N dynamics across a range of environmental conditions (i.e., soil thicknesses, physical and chemical properties, vegetation and soil types).

METHODS

SITES DESCRIPTION

The SSCZO sites are well suited to answer questions related to climate changes because the bio-climosequence has soils developed under similar state factors of soil formation except climate and consequently vegetation. All the sites experience a Mediterranean climate, with cool, moist winters, and warm, dry summers. As elevation increases from 400 to 2700 m, the mean annual temperature decreases (14.4 to 4.1 ºC) and the mean annual precipitation increases (515 mm/year to 1080 mm/year). Actual evapotranspiration (ET) is highest in the mid-elevation sites (749 and 584 mm/year) and lowest at the lowest elevation (395 mm/year) and highest elevation (260 mm/year) sites. The ET pattern has a positive correlation with the gross primary productivity (GPP). The oak savannah site GPP is 480 g C m^{-2} yr^{-1}, the ponderosa pine is 1900 g C m^{-2} yr^{-1}, and then the GPP slightly decreases in the mixed conifer site to 1700 g C m^{-2} yr^{-1}, and the subalpine has a GPP of 700 g C m^{-2} yr^{-1} (Goulden et al., 2012). The parent material for all of the sites is residuum granodiorite with igneous-felsic intrusive lithology, and is hypothesized to be of comparable age except the highest elevation site where bedrock was scoured by glaciers during the last glacial maximum (Giger & Schmitt, 1983). Plant productivity and weathering are limited by low precipitation in the lowest elevation oak

savannah ecosystem, and by low temperature and historic glaciation in the high elevation subalpine forest ecosystem causing changes in the thickness of the weathered bedrock (O'Geen et al., 2018; Tian et al., In review).

SOIL AND REGOLITH SAMPLING

A total of thirty-six regolith profiles were analyzed: three Geoprobe (a hydraulic coring device, model DT22) cores and four pits excavated by a backhoe were sampled at the oak savannah site (405 m); five Geoprobe cores, five hand augers, and five pits were sampled at the ponderosa pine (1160 m); five Geoprobe cores, one hand auger, and four pits were sampled at the mixed-conifer forest site (2015 m); and four pits were excavated by hand or excavator at the subalpine forest site (2700 m). Soil pits were sampled by genetic horizons. Regolith is characterized as weathered bedrock that retains the relative positions of mineral grains of the parent bedrock. A Geoprobe sampler was used from soil surface to depth of refusal. The total depth measured at the oak savannah was 270 cm, the ponderosa pine deepest depth was 467 cm, the mixed conifer depth was 1067 cm, and the sub alpine site deepest depth was 115 cm. Weathered bedrock was identified as having brittle consistency and rock fabric (Graham et al., 2010). With hand augers, the depth of transition from soil to weathered bedrock was identified in the field by a change in color and consistency.

Particle size analysis on bulk pit samples (40 g air dried and sieved) was performed by the hydrometer (ASTM 152H) method. Bulk density of soil and weathered bedrock was measured using the core method (Dane & Topp, 2020). Three core samples were taken in each horizon from three soil profiles and averaged. They were oven-dried at 105 °C until

there was no mass change (24-48 hours) and the >2 mm fraction and roots were removed. Bulk density of lower weathered bedrock was measured by cutting an exact volume from the bottom 5-cm of each core, which was sampled by the Geoprobe at 1 m depth intervals and oven-dried at 105 °C. Soil pH was measured on air-dried and sieved soil in deionized water with a 2:1 (5 g:10 ml) mixture for thirty minutes, stirring every ten minutes (Sparks et al., 1996). The pH meter used was an Accumet Basic, Model AB15, Fisher Scientific with an Ag/AgCl electrode.

ABOVEGROUND VEGETATION SAMPLING

Foliage from dominant vegetation at each of our study sites were collected in 2018 to determine the plant N and C concentrations. Leaf samples were collected from the upper 1/3 of the canopy of all plants, cut by a pole clippers or by climbing. Leaf samples were air-dried prior to being ground to pass a 180-μm sieve and analyzed for total C and N concentration (%) using dry combustion (Costech Analytical ECS 4010 instrument, Costech Analytical Technologies, Inc., Valencia, CA). At the oak savannah site, we sampled overstory tree species *Quercus douglasii, Quercus wislizenii, Pinus sabiniana,* and understory species *Bromus diandrus, Bromus hordeaceus, , Aveca barbata, Croton setiger,* and *Ceanothus leucodermis*. At the ponderosa pine site we sampled overstory tree species *Quercus chrysolepis, Quercus kelloggii, Pinus ponderosa,* and understory species *Arctostaphylos biscida, Ribes montigenum,* and *chamaebatia foliolosa.* At the mixed conifer site, we sampled overstory *Quercus kelloggii, Pinus jeffreyi,* and understory species *Arctostaphylos patula, Ribes montigenum, Lupinus,* and *Ceanothus velutinus.* At the subalpine site we sampled overstory *Pinus contorta* and understory

Eriogonum ovalifolium, and *Lupinus.* Results of elemental and isotopic composition of foliage are grouped by site.

CARBON AND NITROGEN ANALYSES

Soil and weathered bedrock materials were air-dried, gently crushed by a rolling pin, and sieved (2-mm mesh openings). Percentage of fine-earth fraction (< 2 mm) and coarse earth fraction (> 2 mm) were measured based on air-dry mass. Coarse earth fraction was assumed to have no OC. Gravimetric water content was determined on air-dried subsamples by drying overnight at 105 °C. Total C and N concentration (%) of the fine-earth fraction was determined on samples ground to pass a 180-μm sieve and analyzed by dry combustion (Costech Analytical ECS 4010 instrument, Costech Analytical Technologies, Inc., Valencia, CA).

Total N inventory (N_s, kg C m^{-2}) was calculated from total N concentration (N, g kg^{-1}), thickness of the sample layers (d_c, cm) and bulk density (ρ_b, mg/m^3), with correction for the weight percent of the coarse earth fraction (Eq. 4-1).

$$N_s = \sum N \times d_c \times p_b \times 100 \qquad \text{Equation 4-3}$$

DENSITY FRACTIONATION

Density fractionation was used to separate the SOM into pools that are distinct in composition and to infer dominant mechanisms of SOM stabilization: light (debris outside aggregates, LF), occluded (light fraction inside aggregates oLF), and heavy fractions (OM bound to minerals, HF) using sodium polytungstate (Lybrand et al., 2017; McFarlane et al., 2013; Swanston et al., 2002). 30 g of air-dried, sieved (<2mm) soil was

initially mixed with 1.7 g/ml of SPT for 24 hours. The fLF is first isolated by floating to the top as the supernatant and removed and rinsed. To break up the aggregates and collect the oLF the remaining sample was dispersed with ultrasonic energy at 440 J/ml with a Branson 450 Sonifier (Branson Ultrasonics, Danbury, CT, USA) probe tip 5 cm below the liquid surface. This fraction can also include OM that coated minerals making it not float to the top for the fLF. The dense particles, mineral fraction (HF), formed a pellet at the bottom. All three fractions were extensively rinsed with 0.01 M $CaCl_2$ and DI water and the fLF and oLF were filtered and rinsed using 0.8 um filters (Lybrand et al., 2017). All samples lost less than 15% of the bulk N after fractionation.

RADIOCARBON ANALYSIS

Radiocarbon analyses was conducted on soil samples after sealed-tube combustion of OC to CO_2 (with CuO and Ag) that was then reduced onto Fe powder in the presence of H_2 (Vogel et al. 1984). Radiocarbon values were measured in 2018 and 2019 on the Van de Graaff FN accelerator mass spectrometer at the Center for Accelerator Mass Spectrometry at the Lawrence Livermore National Laboratory. Organic matter $\delta_{13}C$ values were determined at the University of California, Merced using a DELTA V Plus Isotope Ratio Mass Spectrometer (Thermo Fisher Scientific, Inc.). Radiocarbon isotopic values were corrected for mass-dependent fractionation with measured $\delta_{13}C$ values and were reported in Δ- notation corrected for $_{14}C$ decay since 1950 (Stuiver & Polach, 1977).

SOIL N ACCUMULATION MODEL

To estimate the rate of N accumulation in bulk soil, the radiocarbon analysis and % total N was used in a first-order kinetic model of N accumulation (Berhe et al. 2008; Berhe & Torn, 2017; Hilton et al. 2013; Jenny, 1994; Trumbore & Harden, 1997) where:

$$\frac{dN_{inv}}{dt} = I - k * N_{inv} \quad \text{Equation 4-4}$$

N_{inv} is the N inventory in the bulk soil profile (kg m^{-2}); I is the net N input to a soil pool from combined processes of atmospheric deposition, biological N fixation, and deposition of eroded topsoil (kg m^{-2} $year^{-1}$), I does not account for N that leaves the soil profile soon after it enters the system; and k is the coefficient for first-order loss of N from soil through all particulate, dissolved and gaseous pathways ($year^{-1}$). Equation (4-2) is solved subject to the initial conditions $N_{inv} = N_0$ at t = 0 at the start of N accumulation in the soil profile. Hence, assuming that $N_0 = 0$ at the beginning of soil development, equation (4-2) is solved as:

$$N_{inv}(t) = \frac{I}{k}[1 - \exp(-kt)] \quad \text{Equation 4-5}$$

For each site, all four pits and the geoprobe samples (after the deepest pit sample ~3m geoprobe samples were used to extend the profile to bedrock to 5 m) were used in calculations of N_{inv}. Samples were only used to 5 m at the mid-elevation sites to avoid skewing of the turnover time from the abundance of older radiocarbon ages from 5 to 10 m. When testing the model, the mean residence times of the mixed conifer site were skewed by thousands of years due to the use of samples past 5 m that have radiocarbon

ages up to 20,000 years therefore, we only used samples to 5 m. The soil N_{inv} and the ^{14}C radiocarbon ages from each pit and geoprobe samples were used to derive cumulative N and estimated turnover rate of the N in each profile (Berhe et al., 2008; Berhe & Torn, 2017). For each soil profile, the N_{inv} in each horizon and then geoprobe samples (thickness ~50-70 cm) were amassed at each depth increment to estimate the N accumulation between successive time stages. Because there is no tracer that allows us to trace N cycling specifically, here we used radiocarbon ages to approximate N residence time in soil. This decision is based on our data and numerous other past studies that have shown that more than 95% of N in soils is organic and most organic N is covalently bonded to carbon-based SOM (Allison, 1973; Batjes, 1996; McGill & Cole, 1981). In addition, we found that the concentration of the bulk sample C and N are strongly correlated at (R^2=0.84 p=0.049, n=400), as was previously shown in other past studies (Berhe & Torn, 2017). For each pit, the N that is accumulated between the successive time stages is amassed into a total profile N accumulation, as estimated from radiocarbon based ages of each soil layer. The total profile N inventory vs. years of accumulation (t) was used to estimate *I* and *k* by fitting the data with equation (4-3) using the solver function in Excel (MS Office 2011). Model fit was assessed by non-linear least squares. This is a first-order approximation of N accumulation and residence time using the solver function to fit the data over time. The accumulation starts from the bottom up because of the assumption that the deepest soil formed first and the organic matter associated with the soil layers on top formed later (Riebe et al. 2017).

DATA ANALYSES

Data are presented with mean +/- standard error. ANOVA was performed on average clay %, pH, bulk density, and Fe and Al concentrations to test if they significantly varied by site. Pairs of means at the different sites were compared using the Tukey-Kramer HSD test and simple linear regression was used to assess the proportion of variability in these variables. For all statistical tests, an a priori significance level of $p < 0.05$ was used. All statistical tests were performed using R version 1.1.456.

We used a random mixed effects model to assess at the relationship on how climate controls N concentration. We used climatic variables (GPP, evapotranspiration, mean annual temperature, mean annual precipitation, and deep water percolation) as the fixed effects and the independent variable of TN (mg N/g) of each fraction. R-squared and p-values were calculated for each fraction within topsoil (> 30 cm) or subsoil (< 30 cm).

RESULTS

Table 4-1 summarizes results from physical characterization of soils across the bio-climosequence we studied. Across the elevational gradient, bulk density generally increased with depth for all sites and ranged from 0.92 kg/cm3 in the topsoil A horizon to 1.67 kg/cm3 in the Cr horizon (Table 4-1). The soils were generally coarsely textured with clay below 11%. Clay % increased from the A to B horizons (average 1.6%) in all sites, and from the B to C horizons (average 2.5%) in the mid-elevation sites. At the other two sites, clay % decreased from the B to C horizon (average decrease if 2.2%). Soils across the study system were acidic, ranging from 5.20 and 6.14, with little variability in pH across depth or elevation gradients. There was no clear or consistent trend in pH

change with depth for all of the sites (Table 4-1). ANOVA and linear regression determined that there is no statistically significant difference between sites for bulk density, clay %, and pH.

TOTAL NITROGEN STORAGE IN SOIL AND WEATHERED BEDROCK

The concentration and total inventory of N were highest in soils that typically extended to depths greater than 1.5 m in all sites. However, weathered bedrock (the portion of the soil profile that retains structural parent rock fabric after having been weathered into a friable substrate *in situ* and has substantial porosity) accounted for a large proportion of total TN inventory at mid-elevation sites (Fig. 4-1). In soil, TN inventory increased with elevation to a maximum of 0.75 kg N m^{-2} at the mixed conifer forest (2015 m) but decreased to 0.25 kg N m^{-2} at the subalpine forest (2700 m; Fig. 4-1). Soil TN increased (relative to weathered bedrock) at the subalpine forest (2700 m), because this site did not have deep regolith (Fig. 4-1). The proportion of TN inventory in weathered bedrock had a similar trend to that of soil OC; the OC proportion in weathered bedrock from 4% in the oak savannah, 23% in the ponderosa pine and 37% in mixed-conifer forest (Fig. 4-1). The regolith alone of the mixed-conifer forest (2015 m) stored 0.432 kg N m^{-2} compared to soil profiles in oak savannah (405 m) that stored 0.387 kg N m^{-2} and the weathered bedrock stored 0.015 kg N m^{-2} (Fig. 4-1).

NET N ACCUMULATION OVER TIME ALONG THE BIO-CLIMOSEQUENCE

The rate of N accumulation varied considerably between sites. During the early years of model simulation, the rate of N accumulation is fastest at the ponderosa pine and sub alpine sites and occurs within a few hundred years. The ponderosa pine and sub alpine

site, reaches steady state N stock in about 500 years, compared to the oak savannah that reaches steady state right before 5,000 years and the mixed conifer reaches steady state between 7,500 to 10,000 years.

Results from our model runs show that the rate of soil N accumulation is distinctly different in the hotter oak savannah and ponderosa pine site compared to the wetter/cooler higher elevation forested sites. The whole profile averaged mean residence time of N in our study sites was calculated and increased in elevation from 64 years for the oak savannah to a maximum of 652 years for the mixed conifer, and then decreased to 117 years for the sub alpine (Table 4-2). The modeled rate of N input in the mixed conifer site was 5-50 times higher than the oak savannah site and ponderosa pine site. The general trend indicates that a drier and hotter climate (low elevation) have a faster turnover time and climates that are cooler and wetter have slower turnover times (Table 4-2).

N PARTITIONING ACROSS FRACTIONS IN TOP VS. SUBSOIL

All fractions exhibit a decrease in % N from the topsoil to the subsoil. Both fLF and oLF decrease in %N drastically (average 0.5%) from 0 to 25 cm and stayed consistent after that depth. Comparatively, the heavy fraction decreases most with depth from 0 to 50 cm (Fig 4-6. a,f,k). The N in each fraction decreases substantially with depth for both the fLF and oLF with more N in the topsoil fLF compared to the topsoil oLF. The proportion of total N that was recovered in the fLF and oLF decreased with depth, for both fLF and oLF, while the fraction of N in the HF generally increases with depth (Fig 4-6. b,g,i). Radiocarbon concentration ($\Delta^{14}C$) increases with depth for all fractions with the most depleted samples being found in the aggregate and mineral associated pools (Fig 4-6.

c,h,m). The stable N isotopic composition of $\delta_{15}N$ in the light fraction across the depth profiles at all sites mirror each other, where the $\delta_{15}N$ in all fractions gets heavier from the A to B horizon and from the B to C horizon the fractions become lighter (Fig 4-2. e,j,o).

The proportion of N in the mineral-associated HF fraction accounts for the largest proportion (over 50%) of N across all of the sites and with depth (Fig. 4-3). Relative partitioning of the soil N in fractions varied from greater than 95% of the N in the oak savannah below 1 m being located in the HF pool, to more partitioning of both the fLF and oLF in the three forested systems (Fig. 4-3). The highest proportion of N in the oLF and the largest difference, between the top and subsoil, was also found in the mid-elevation sites. In the highest elevation site, we observed progressive decreases in proportion of N in oLF. With depth, N in the fLF and oLF decreases in at every site. As elevation increases, there is greater proportion of N into the fLF and oLF.

Table 4-3 presents mixed effect model results for N distribution in the different fractions with elevation and five climate variables or proxies in order to determine the relative contribution of climate in explaining variability of N partitioning in top compared to sub-soil layers within the fractions. The most variation in the dependent variables tested was using the independent variables topsoil fLF and oLF were GPP and MAP explaining 57-68% of the variation in $\delta_{14}N$ (Table 4-3). Topsoil and subsoil fLF were the only fractions that variation could be explained by MAT, with up to 68% of the variation being accounted for by MAT in the topsoil and 26% of the variation in subsoil fLF. The topsoil oLF was the only fraction that significantly correlated with ET, with 28% of the variation being explained by ET ($p=0.008$). The HF did not significantly correlate to any of the climate proxies in the topsoil and subsoil (Table 4-3).

In the topsoil layers, we compared the $\delta^{15}N$ values in above- and below-ground vegetation, fLF, oLF, and HF to determine if the OM in each pool shows any evidence of progressive processing associated with $\delta^{15}N$ fractionation due to oxidative decomposition. We observed a trend of $\delta^{15}N$ going from lower to higher as we move from the A to B horizons and then as the profile transitions from the B to C horizon the $\delta^{15}N$ gets lighter (Fig 4-6. e,j,o). For example, the most drastic examples of this trend are in the mixed conifer site for all three of the fractions; the average topsoil $\delta^{15}N$ is 1.9 ‰ and then increases to 6.3‰ in the B horizon and then decreases to -1.5‰ (Fig 4-3., o). Foliar $\delta^{15}N$ values have the lightest mixture of $\delta^{15}N$ isotopes compared to roots, density fractions, weathered rock, and bulk (Fig 4-5).

DISCUSSION

ALLOCATION OF N IN SOIL AND WEATHERED BEDROCK ACROSS THE BIOCLIMATIC GRADIENT

The regolith (including soils and parent rock) represents the literal foundation for terrestrial life. Regolith provides physical substrate, a water-air-nutrient reservoir, and is the primary source of most of the essential elements for primary producers. Over time the parent material is weathered as a function of the five state factors of soil formation: climate, time, parent material, relief and biota that regulate the input of material and efflux of byproducts, via a combination of abiotic and biotic weathering processes (Pope, 1995). The mid-elevation sites in the SSCZO extends down to more than 10 m depth, illustrating that the conditions are optimal for extensive weathering of the bedrock (Tian et al., In review). Recent studies are highlighting that, in addition to biological fixation of

atmospheric N_2, this weathering of parent material can contribute to soil N stocks and availability (Houlton & Morford, 2015).

Our results show that, in the southern Sierra Nevada elevation gradient, soil total N inventory was highest at the mid-elevation sites (ponderosa pine and mixed conifer forest) where GPP is not limited by climate (Fig. 4-1; (Goulden & Bales, 2014; Kelly & Goulden, 2016)). Our findings are consistent with previous studies using a bio-climosequence that have shown that soil development and weathering rates are maximized in warm and wet sites, such as the mid-elevation ponderosa pine and mixed conifer forests we studied (Dahlgren et al., 1997; Egli et al., 2003; Jenny, 1980; Rasmussen et al., 2007). Total N concentration was low in weathered bedrock at all sites suggesting that the effect of climate on deep regolith N storage might be primarily influenced by its effect on soil thickness, not necessarily concentration of N in the regolith. This low concentration of N in weathered bedrock mirrors the trends seen in the relative concentrations of C inventory in soil compared to weathered bedrock in the same study sites, where weathered bedrock C represents 8 to 30 percent of the profile C inventory (Tian et al., In review), compared to the 0 - 37% profile N being accounted by weathered bedrock that we found in this study.

Despite the overall low N concentrations in weathered bedrock in our study bio-climosequence, we found significant differences between sites in the amount and relative proportion of N in soils versus weathered bedrock. At the mixed conifer site, total N inventory in weathered bedrock was greater than the total N stocks of the other sites throughout the entire soil profile (soil plus weathered bedrock; i.e., regolith Fig. 4-1). The higher N inventories of the weathered bedrock of the ponderosa pine and mixed conifer

forests was largely due to high regolith thicknesses that averaged 2.45 m in the ponderosa pine site compared to 7.55 m in the mixed conifer forest. Climate, through its influence in presence of thick regolith in the mid-elevation sites enables weathered bedrock to contribute a considerable amount of N to the total soil profile N inventory. Our results suggest that climates that are either too cold (highest elevation sub-alpine ecosystem) or too hot and dry (lowest elevation oak savannah ecosystem) are not conducive to large scale weathering of bedrock and hence in these regolith's, weathered bedrock's contribution to the total soil N inventory is low to none. Our findings highlight that the link between climate and total profile N inventory in soil is likely indirect, mediated primarily through the effect of climate on soil weathering.

DIFFERENTIAL RATES OF ACCUMULATION AND MRT OF N ALONG THE BIO-CLIMOSEQUENCE

Results from our model simulations on N accumulation in the soil profiles at the four sites illustrate that the rate of soil N accumulation and profile-averaged mean residence time of N is distinctly different in the hotter oak savannah and ponderosa pine site compared to the wetter/cooler higher elevation forested sites. The ponderosa pine and sub alpine site reach steady state N accumulation around 500 years in the soil profiles, compared to the oak savannah site that reached steady state N accumulation right before 5,000 years and the mixed conifer that reached steady state between 7,500 to 10,000 years (Fig. 4-2). The modeled rate of N input into the forested sites was 5-50 times higher than the oak savannah site. The general trend indicates that a drier and hotter climate (low elevation) have a shorter turnover time and climates that are cooler, and wetter have longer N residence times in soil until it's the temperature limits primary production like

in the sub alpine site (Table. 4-2). Previous work in a similar site as the mixed conifer, in the Sierra Nevada's, estimated that the mean residence time of N of the forest floor was 7 years and the mineral soil below that had a residence time of 34 years. The authors suggest that this is due to microbial immobilization of N that is substantial within this forest floor layer and that a greater proportion of the total organic N pool is mineralized annually within the forest floor compared to the surface mineral soil (Hart & Firestone, 1991). This suggests that N is coming into the mineral soil system and a larger proportion of the N stays in the mineral soil as opposed to the faster cycling forest floor. These results suggest that climate influences N turnover rate, time to steady state, and persistence.

CLIMATIC INFLUENCE ON THE DISTRIBUTION OF N IN SOIL FRACTIONS

Results from the density fractionation show that most N throughout the profiles and ecosystems we studied is mineral-associated (Fig. 4-3). Across the sites, the mineral-associated N accounts for over 50% of total N and in some cases, such as soil >1 m in the oak savannah, accounts for over 95% of total N. This is consistent with the density fractionation data from grassland sites in Northern California reported by Berhe and Torn (2017) where 90% of N was in the mineral associated pool with parent material types of chert, greenstone, and Franciscan sandstone. The majority of soil organic nitrogen (SON) tends to be in the form of amides and amide containing compounds such as proteins, which are more likely to be charged molecules, increasing their affinity for mineral attachment (von Lutzow et al., 2006). It was previously proposed that N-containing organic compounds sorb mainly electrostatically were the hydrophobic interaction between protein and clay minerals govern adsorption compensating for electrostatic

repulsion (Sollins et al., 2006). Exchange between cations on the surfaces of layer silicates (permanent charge) and organic cations usually occurs between pH 5 and 6 (soils from all our sites have values within this range) suggesting that part of the persistent N in the HF is sorbed via electrostatic interactions contributing to the persistent N pool (Table. 4-1; (Jones, 1999; Oades, 1989).

Despite the major importance of mineral-associated N discussed above, we found important trends in the relative proportion of the light fractions (fLF and oLF) between sites that vary with climate, indicating that accumulation of mostly N in the fLF and oLF is sensitive to changes in climate. As elevation increases, we observed more partitioning of N into the fLF and oLF, mimicking C trends at these sites (Rasmussen et al. 2005; Tian et al., In review). This is partly due to the higher GPP at the higher elevation sites where there are greater inputs from aboveground plant and root sources (Goulden et al., 2012). Furthermore, the mixed effect model results indicate that variability in the topsoil and subsoil fLF and oLF can be explained by most of the climate parameters, especially GPP and MAP. Trends in the models (lower R^2 in subsoil) suggest that less variability in the subsoil fLF and oLF can be explained by climate indicating more persistent N in the subsoil that is not as vulnerable to changes in climate compared to topsoil fractions (Table. 4-3). The indication that climate directly influences the N accumulation in the fLF and oLF helps to understand why the lower elevation (hotter/drier) sites have a faster turnover time compared to the higher elevation sites (Table 4-2). This also suggests that the higher elevation sites have more N in the fLF and oLF because of higher GPP resulting in greater N cycling as GPP increases.

We observed increases in N:C ratios in soil with depth in the mineral associated and soils with more depleted (older) ^{14}C in deep layers suggesting more effective retention of N compared to C (Fig. 4-5; (Berhe & Torn, 2017)). Previous studies suggested that this bulk soil N:C trends with depth, in particular if combined with increasing DON concentration (not measured in this study), could indicate enrichment of more microbially-derived N in deeper soil layers while the topsoil primarily consists of plant-derived compounds (Kaiser & Kalbitz, 2012; Ros et al., 2009). This understanding is also supported by the Fourier Transformed Infrared spectroscopy (FTIR) at these sites where we found more microbially processed organic matter in the mineral associated pool compared to the fLF and oLF (Moreland et al., In Prep, Chapter 3). The N:C and FTIR results suggest that the more active cycling N pool is more labile in composition and the more labile N is vulnerable to changes in climate (especially in the topsoil). Whereas the mineral associated N pool is more processed N sorbed with minerals that is not vulnerable to changes in climate. Overall, this suggest that the more labile N in the fLF and oLF may be vulnerable to changes in climate.

VARIABILITY OF ISOTOPIC COMPOSITION OF N WITH DEPTH AND ELEVATION

Stable isotopic ratios of N ($\delta^{15}N$) is commonly used to help understand N cycling processes in ecosystems (Craine et al., 2015). Many processes in the N cycle alter the $^{15}N/^{14}N$ ratios of SOM, and the $\delta^{15}N$ of bulk soil reflects a mixture of litter input, root input, rock sources, and kinetic isotopic fractionation during biotic and abiotic transformations of N in soil (Craine et al., 2015; Houlton et al., 2018; Robinson, 2001). Previous works that measured the $\delta^{15}N$ of soils showed a significant increase in $\delta^{15}N$ between topsoil and subsoil (Amundson et al., 2003; Berhe & Torn, 2017; Natelhoffer &

Fry, 1988). This depth trend was attributed to kinetic fractionation during the microbial degradation of polymeric N-containing biomolecules at depth and the preferential utilization of low $\delta^{15}N$ material in microbial processes. The enrichment of $\delta_{15}N$ with depth trend matches what we observed in our data (Fig 4-3. e,j,o): topsoil values approximately match that of live aboveground foliage and increase through the B horizon. In addition, our results also indicate that deeper in the profile, $\delta_{15}N$ decreases to a value similar to the topsoil $\delta_{15}N$ values (Fig 4-3. e,j,o). This reversal was not seen in the majority of previous studies, which designated the topsoil to be 0-10 cm and subsoil to be 10-20 cm or 10-50 cm. However, Nadelhoffer and Fry (1988) acknowledged that the shallow depths of their study limited their understanding of whole profile dynamics. Because this deeper soil trend was not seen in key earlier studies, current models have focused solely on describing the increase in $\delta_{15}N$ with depth and have not addressed the potential mechanisms controlling soil $\delta_{15}N$ in deeper soils (Amundson & Baisden, 2000; Baisden et al., 2002). Our findings highlight important differences in $\delta_{15}N$ with depth that warrant reassessment of some of the fundamental mechanisms that were presumed to govern this pattern.

Recent studies on soil $\delta_{15}N$ have led to major evolution of our interpretation of the reasons behind increase in $\delta_{15}N$ with depth from the A to B horizon overturning the previous explanation that the $\delta_{15}N$ of SOM increased with depth because of fractionation during microbial degradation of peptides (Macko & Estep, 1984; Macko et al. 1987; Philben et al., 2018). Philben et al. (2018) suggest that N isotopic fractionation only occurs when there is transamination (removal of terminal amine) and does not occur during catabolism (peptide hydrolysis). Because enzymatic peptide hydrolysis is the

primary mechanism of peptide degradation, the observed increase in $\delta^{15}N$ with increasing degradation would not be expected to occur. Instead, Philben et al. (2018) hypothesize that the reason for the $\delta^{15}N$ increase with depth likely stems from the preferential uptake of low $\delta^{15}N$ material by mycorrhizae at depth, which acts to increase the $\delta^{15}N$ of residual soil N. Previously, Hobbie et al. (2009) showed that soil $\delta^{15}N$ is on average 4.5‰ higher in ecosystems dominated by ectomycorrhizal symbioses than in ecosystems dominated by arbuscular mycorrhizal symbioses, likely due to arbuscular mycorrhizal mainly taking up soluble compounds that are available and ectomycorrhiza releasing enzymes to degrade complex SOM. Thus, providing further evidence that mycorrhizea are an important factor controlling the $\delta^{15}N$ of soil ecosystems (Chalot & Brun, 1998).

Mycorrhizae (not quantified in this study) could then at least partially explain observed differences in subsoil $\delta^{15}N$ between sites. In the oak savannah site, the average bulk $\delta^{15}N$ is 4.6‰ and ranges from 7.5‰ to 8.5‰ in the forested sites. The oak savannah site is dominated by grass species often associated with arbuscular mycorrhiza (oaks can have arbuscular and ectomycorrhizal associations (Dickie et al. 2009)). The forested sites are dominated by species often associated with ectomycorrhiza, which are associated with higher soil $\delta^{15}N$ values (Hobbie & Ouimette, 2009). The differences in soil $\delta^{15}N$ between sites can potentially be further influenced by climatic factors. MAP and MAT significantly correlate with bulk soil $\delta^{15}N$ and foliar $\delta^{15}N$ in several review papers, where soil and foliar $\delta^{15}N$ is higher in warmer tropical ecosystems and lower in colder regions (Amundson et al., 2003; Handley et al., 1999). However, this is opposite to the trend we observed across our sites, where the highest foliar values are in the coldest and wettest

sites, suggesting that mycorrhizal type may be a factor in determining soil $\delta^{15}N$ values. We speculate that since the types of mycorrhizae that are present in soils change with climate, climate may impose indirect controls on $\delta^{15}N$ composition throughout the entire system (trees, roots, soil, weathered bedrock) through its effect on plant species distribution and mycorrhizae type.

The lower $\delta^{15}N$ values in the C horizon we observed in this study could also suggest an important mechanism by which mycorrhizae may increase soil $\delta^{15}N$ in the B horizon. We observed a lower abundance of roots (and consequently mycorrhizae, however infection rates can vary dramatically) in the C horizon compared to the A and B horizons. This would suggest that there is likely not as much mycorrhizal uptake at this depth, leading to significantly less fractionation and resulting in isotopic values more similar to the A horizon. An alternate explanation for the decrease in $\delta^{15}N$ from the B to C horizons could be dissolved organic nitrogen (DON), which is the most mobile fraction of OM in the soil system (Glatzel et al. 2003). The DON fraction (not measured) constitutes an important pool of N and its flux controls many processes in the soil system. The DON from the topsoil could be transported down the profile and become immobilized by attachment to clay minerals that increase in abundance with depth in these systems. Another alternative explanation could be ^{15}N-depeted N as product of enzymatic hydrolysis, ammonification, nitrification, or denitrification that is then translocated by leaching, gaseous losses, or uptake of the ^{15}N-depleted N by plants (Hobbie & Ouimette, 2009). Overall, without measuring the mycorrhizae type and abundance and inorganic/organic forms of N with depth, it is difficult to understand why the trend with depth exists and justifies further investigation.

N isotope compositions of granites indicates a relatively wide range of $\delta_{15}N$ values (+1 to +10‰), reflecting heterogeneity of the N sources and complex metamorphic–magmatic processes (Bebout et al., 1999; Boyd et al., 1993). Data on $\delta_{15}N$ of granites is rare and the two reported here are different in composition from the igneous granodiorite that exist in the southern Sierras. The weathered rock values in our study are closest to the mineral associated $\delta_{15}N$ values in both the topsoil and subsoil for most of the sites (Fig.4- 4) indicating that some of the $\delta_{15}N$ in the bulk, weathered bedrock, and heavy fraction could be coming from the weathered rock.

CONCLUSIONS

Climate exerts both a direct and indirect control on soil N accumulation and persistence. Our bulk soil and weathered bedrock results evaluating the entire profile N from topsoil to bedrock suggest that the effect of climate on deep weathered bedrock N storage might be primarily through its effect on thickness, not necessarily concentration of N in the regolith. The density fractionation results suggest that the mineral associated pool contributes substantially to the persistence of N, especially in the subsoil and is only indirectly influenced by climate via weathering. Overall, our findings suggest that N in the mineral associated pool will not be vulnerable to changes in climate and will continue to contribute to the persistent soil N pool. The amount of topsoil and subsoil unprotected, and occluded N variability can be explained by GPP and MAP indicating that changes in climate can likely influence how much N is partitioned into these pools. Subsoil N in the fLF and oLF contains more persistent N and is only slightly less influenced by climate compared to the topsoil fLF and oLF. The modeled rate of N turnover and input indicated

that a drier and hotter climate (low elevation) have a shorter turnover time and climates that are cooler, and wetter have longer N residence times in soil that are driven mainly by smaller regolith N pools. Lastly, we speculate that climate indirectly influences $\delta^{15}N$ cycling from the top of the trees down to soil likely through its control over mycorrhiza type abundance.

ACKNOWLEDGEMENTS

Funding: U.S. National Science Foundation, through the Southern Sierra Critical Zone Observatory, Grant/Award number: EAR-1331939; and UC Lab Fees Research Fellowship, Award number: LGF-18-488060/SCW1447 from DOE-BER-TES

FIGURES

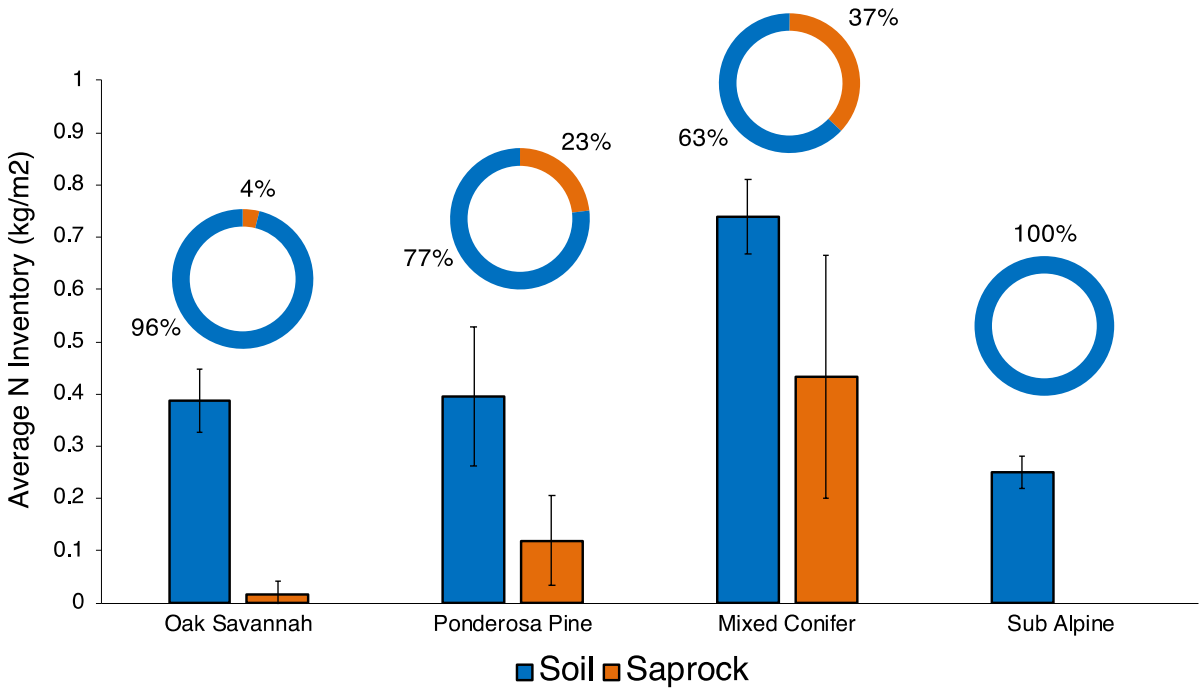

Figure 4-1. Allocation of N in soil and weathered bedrock across the bioclimatic gradient only using geoprobe data. (a) Bar charts represent the total N pool (error bars represent standard deviations) in soil and weathered bedrock. Pie charts represent the proportion of N inventory of soil to weathered bedrock among the four study sites: oak savannah, ponderosa pine, mixed-conifer forest, and subalpine forest. Standard deviation is represented as the error bars.

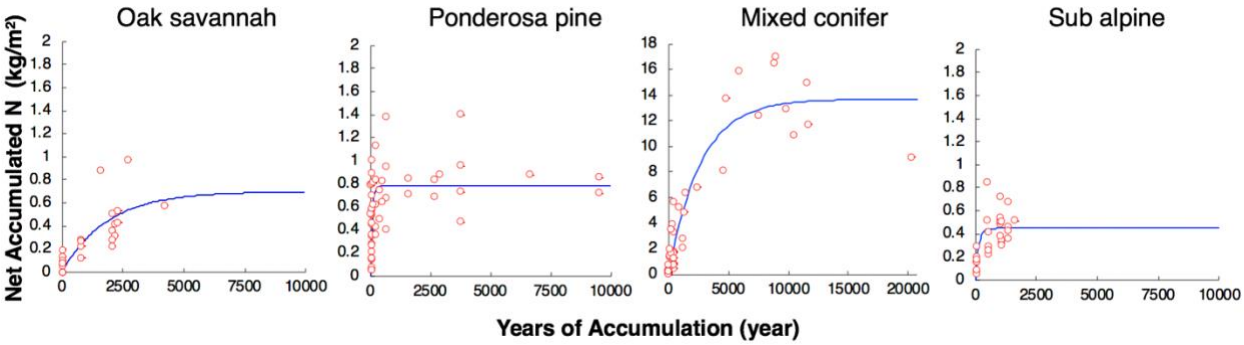

Figure 4-2. Model results vs. the measured values of net accumulation of N over time for all four sites. Samples include pit and geoprobe down to 5 m. Years of accumulation were calibrated with radiocarbon ages of bulk samples in each horizon and geoprobe samples. Note scale for mixed conifer site on both axis is increased.

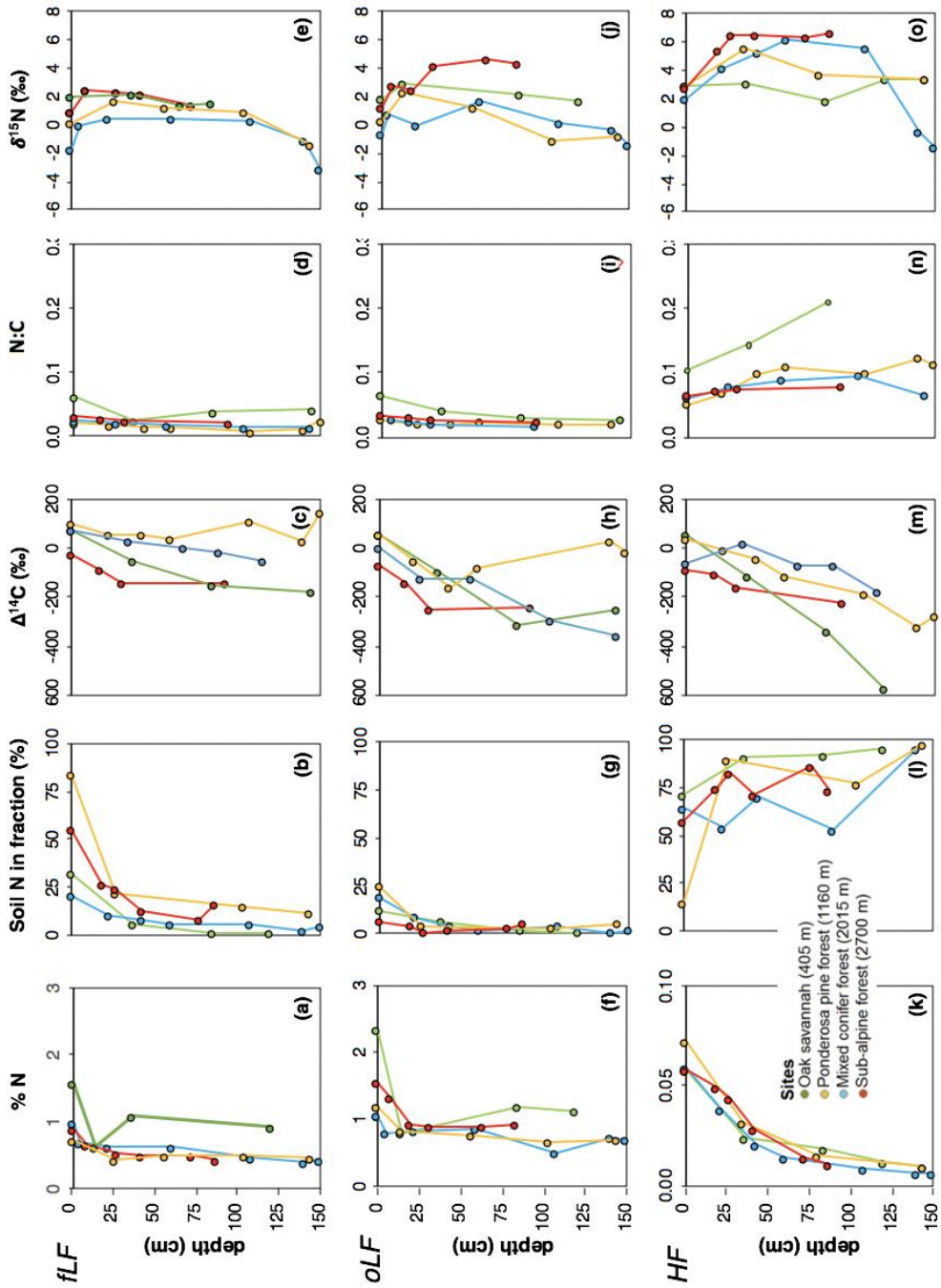

Figure 4-3. Average percent N, soil N distribution in each fraction, Δ14C, C:N, and the $\delta^{15}N$ in (a-e) fLF, (e-h) oLF, and (k-o) HF. n=3 for each point in every fraction, except some of the deepest samples were n=1. *Note that panel k has a different axis scale than the fLF and oLF (panels a and f).

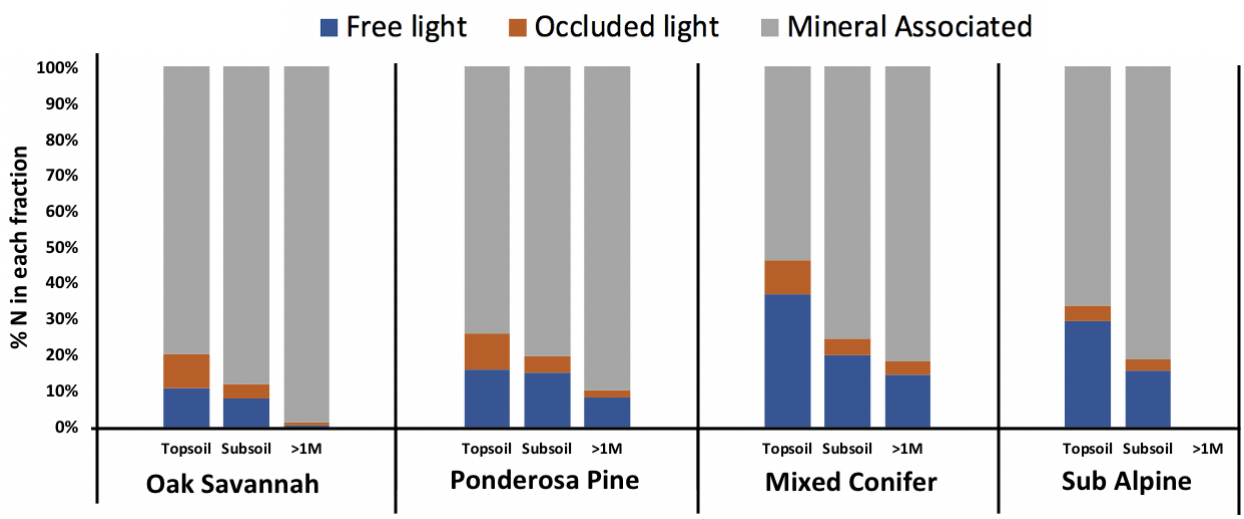

Figure 4-4. Average proportion of N in each fraction in the topsoil (0-30-cm), subsoil (30-100-cm), and below 100 cm for each site. Averages were normalized to 100 to account for any N loss during fractionation (>less than 15% lost).

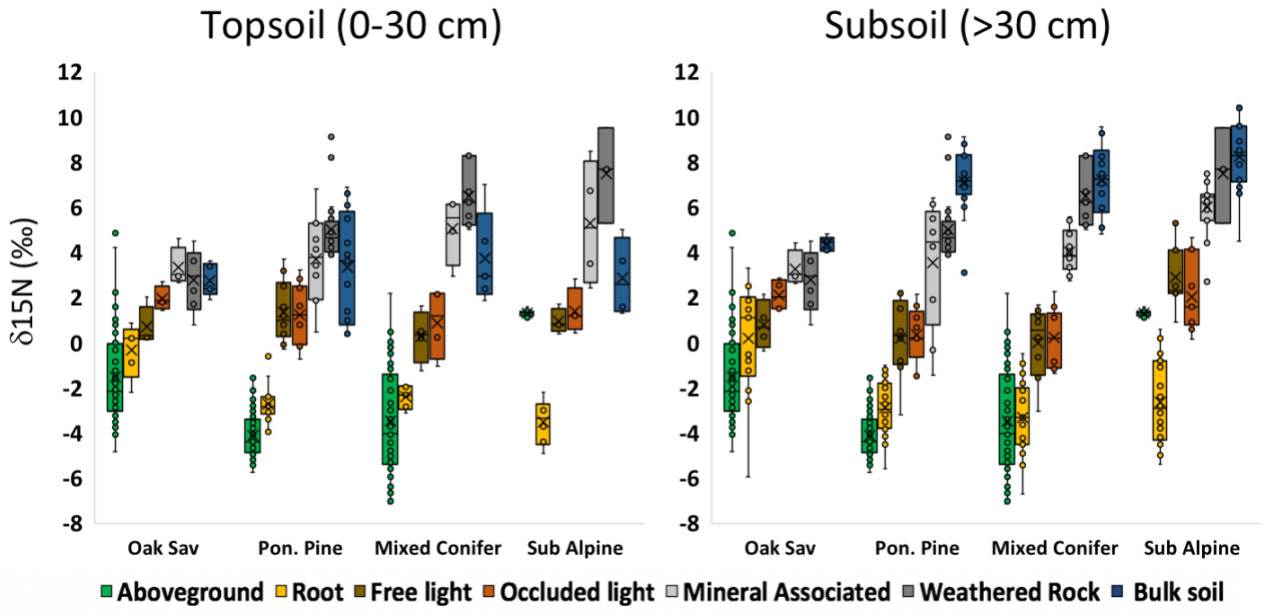

Figure 4-5. Boxplots of topsoil and subsoil δ15N of live aboveground foliage, roots, fLF, oLF, HF, weathered bedrock, bulk soil with all data grouped together.

TABLES

Table 4-1. Average bulk density, clay % and pH from each master horizon along the climosequence. Averages are of each soil pit and from each master horizon. The error term represents standard error. n for A horizon ranges from 6-10, n for B horizon ranges from 7-12, n for C horizon ranges from 3-6, and n for Cr horizon ranges from 4-5. Cr in sub alpine site not present because there was no Cr material present.

Site	Master Horizon and Cr	Bulk Density (Mg/m^3)	Clay (%)	pH (DI)
Oak Savannah	A	1.46 ± 0.10	5.53 ± 0.81	5.38 ± 0.57
	B	1.63 ± 0.13	9.83 ± 5.06	5.70 ± 0.77
	C	1.64 ± 0.14	4.31 ± 0.94	6.14 ± 0.97
	Cr	1.67 ± 0.06	2.72 ± 2.52	5.81 ± 0.78
Ponderosa Pine	A	0.92 ± 0.33	5.40 ± 1.86	5.50 ± 0.38
	B	1.02 ± 0.46	6.84 ± 1.93	5.29 ± 0.56
	C	1.45 ± 0.18	10.97 ± 6.38	5.72 ± 0.85
	Cr	1.42 ± 0.00	8.50 ± 5.86	5.57 ± 0.65
Mixed Conifer	A	0.98 ± 0.22	3.26 ± 2.82	5.55 ± 0.08
	B	1.39 ± 0.13	6.08 ± 1.93	5.34 ± 0.27
	C	1.41 ± 0.09	6.91 ± 1.96	5.25 ± 0.45
	Cr	1.54 ± 0.13	5.44 ± 2.10	5.22 ± 0.18
Sub Alpine	A	1.25 ± 0.10	3.23 ± 0.61	5.25 ± 0.30
	B	1.42 ± 0.14	4.27 ± 1.73	5.60 ± 0.29
	C	1.33 ± 0.09	3.66 ± 0.68	5.69 ± 0.25
	Cr	n/a	n/a	n/a

Table 4-2. Average total profile soil N inventory (N*inv*) and modeled values of whole soil profile-integrated net input of N to the soil N pool (I_N), modeled coefficient for first-order N loss from for the soil profile (k), and modeled mean residence time of N (MRT_N) in soil profiles at each site.

Site	N*inv* (kg/m^2)	I_N (kg/m^2 $year^{-1}$)	*k* ($year^{-1}$)	MRT_N (year)	Sum of squares of errors
Oak savannah	0.5	6.4E-03	1.5E-02	64	0.0013
Ponderosa pine	0.9	1.1E-02	1.4E-02	70	0.0007
Mixed conifer	4.7	7.5E-03	6.9E-04	652	0.5100
Sub alpine	0.6	3.8E-03	8.5E-03	117	0.0100

Table 4-3. Mixed effect model results between N in fractions (mgN/g) and climate variables and proxies (GPP, mean annual temperature, mean annual precipitation, deep water percolation, and evapotranspiration) with conditional R-squared (includes random and mixed effects) and P-value (* p<.05, ** p<.01, *** p<.001). Topsoil n = 25, Subsoil n = 38. Topsoil was grouped by A horizons and typically fell above 30 cm and subsoil was classified as the B and BC horizons going down to 150 cm.

		GPP		**MAT**		**MAP**		**DWP**		**ET**	
		R^2C	P-value	R^2C	P-value	R^2C	P-value	R^2C	P-value	R^2C	P-value
Topsoil	fLF	0.654	<0.01**	0.681	0.051*	0.662	<0.01***	0.682	0.042*	0.680	0.171
Subsoil	fLF	0.261	0.146*	0.263	0.054*	0.251	<0.01**	0.26	0.041*	0.252	0.701
Topsoil	oLF	0.574	<0.01***	0.332	0.141	0.663	<0.01***	0.493	0.053*	0.283	<0.01**
Subsoil	oLF	0.528	0.010	0.561	0.072	0.542	<0.01**	0.561	0.051*	0.554	0.191
Topsoil	HF	0.136	0.065	0.001	0.873	0.221	0.173	<0.01	0.963	0.141	0.065
Subsoil	HF	0.242	0.579	0.221	0.241	0.018	0.512	0.221	0.232	0.232	0.980

REFERENCES

Allison, F. E. (1973). Soil Organic Matter And Its Role In Crop Production, *Volume 3 (developments In Soil Science)* (p. 639). Amsterdam: Elsevier Science.

Amundson, R., Austin, A. T., Schuur, E. A. G., Yoo, K., Matzek, V., Kendall, C., … Baisden, W. T. (2003). Global patterns of the isotopic composition of soil and plant nitrogen. *Global Biogeochemical Cycles*, *17*(1), n/a-n/a. doi:10.1029/2002GB001903

Amundson, R., & Baisden, W. T. (2000). Stable isotope tracers and mathematical models in soil organic matter studies. In O. E. Sala, R. B. Jackson, H. A. Mooney, & R. W. Howarth (Eds.), *Methods in ecosystem science* (pp. 117–137). New York, NY: Springer New York. doi:10.1007/978-1-4612-1224-9_9

Baisden, W. T., Amundson, R., Brenner, D. L., Cook, A. C., Kendall, C., & Harden, J. W. (2002). A multiisotope C and N modeling analysis of soil organic matter turnover and transport as a function of soil depth in a California annual grassland soil chronosequence. *Global Biogeochemical Cycles*, *16*(4), 82-1-82–26. doi:10.1029/2001GB001823

Baisden, W. T., Amundson, R., Cook, A. C., & Brenner, D. L. (2002). Turnover and storage of C and N in five density fractions from California annual grassland surface soils. *Global Biogeochemical Cycles*, *16*(4), 64-1-64–16. doi:10.1029/2001GB001822

Batjes, N. H. (1996). Total carbon and nitrogen in the soils of the world. *European Journal of Soil Science*, *47*(2), 151–163. doi:10.1111/j.1365-2389.1996.tb01386.x

Bebout, G. E., Cooper, D. C., Bradley, A. D., & Sadofsky, S. J. (1999). Nitrogen-isotope record of fluid-rock interactions in the Skiddaw aureole and granite, English Lake District. *American Mineralogist*, *84*(10), 1495–1505. doi:10.2138/am-1999-1002

Bell, C., McIntyre, N., Cox, S., Tissue, D., & Zak, J. (2008). Soil microbial responses to temporal variations of moisture and temperature in a chihuahuan desert grassland. *Microbial Ecology*, *56*(1), 153–167. doi:10.1007/s00248-007-9333-z

Berhe, A. A., Harden, J. W., Torn, M. S., & Harte, J. (2008). Linking soil organic matter dynamics and erosion-induced terrestrial carbon sequestration at different landform positions. *Journal of Geophysical Research*, *113*(G4). doi:10.1029/2008JG000751

Berhe, A. A., & Torn, M. S. (2017). Erosional redistribution of topsoil controls soil nitrogen dynamics. *Biogeochemistry*, *132*(1–2), 37–54. doi:10.1007/s10533-016-0286-5

Bingham, A. H., & Cotrufo, M. F. (2016). Organic nitrogen storage in mineral soil: Implications for policy and management. *The Science of the Total Environment*, *551–552*, 116–126. doi:10.1016/j.scitotenv.2016.02.020

Boyd, S. R., Hall, A., & Pillinger, C. T. (1993). The measurement of δ15N in crustal rocks by static vacuum mass spectrometry: Application to the origin of the ammonium in the Cornubian batholith, southwest England. *Geochimica et Cosmochimica Acta*, *57*(6), 1339–1347. doi:10.1016/0016-7037(93)90070-D

Chalot, M., & Brun, A. (1998). Physiology of organic nitrogen acquisition by ectomycorrhizal fungi and ectomycorrhizas. *FEMS Microbiology Reviews*, *22*(1), 21–44. doi:10.1111/j.1574-6976.1998.tb00359.x

Chapin, F. S., Matson, P. A., & Vitousek, P. M. (2011). *Principles of Terrestrial Ecosystem Ecology*. New York, NY: Springer New York. doi:10.1007/978-1-4419-9504-9

Conant, R. T., Ryan, M. G., Ågren, G. I., Birge, H. E., Davidson, E. A., Eliasson, P. E.,

… Bradford, M. A. (2011). Temperature and soil organic matter decomposition rates - synthesis of current knowledge and a way forward. *Global Change Biology*, *17*(11), 3392–3404. doi:10.1111/j.1365-2486.2011.02496.x

Craine, J. M., Elmore, A. J., Wang, L., Augusto, L., Baisden, W. T., Brookshire, E. N. J., … Zeller, B. (2015). Convergence of soil nitrogen isotopes across global climate gradients. *Scientific Reports*, *5*, 8280. doi:10.1038/srep08280

Dahlgren, R. A., Boettinger, J. L., Huntington, G. L., & Amundson, R. G. (1997). Soil development along an elevational transect in the western Sierra Nevada, California. *Geoderma*, *78*(3–4), 207–236. doi:10.1016/S0016-7061(97)00034-7

Dane, J. H., & Topp, C. G. (Eds.). (2020). *Methods of Soil Analysis, Part 4: Physical Methods* (illustrated.). John Wiley & Sons.

Delwiche, C. C. (1970). The nitrogen cycle. *Scientific American*, *223*(3), 137–146.

Dickie, I. A., Dentinger, B. T. M., Avis, P. G., McLaughlin, D. J., & Reich, P. B. (2009). Ectomycorrhizal fungal communities of oak savanna are distinct from forest communities. *Mycologia*, *101*(4), 473–483. doi:10.3852/08-178

Dynarski, K. A., Morford, S. L., Mitchell, S. A., & Houlton, B. Z. (2019). Bedrock nitrogen weathering stimulates biological nitrogen fixation. *Ecology*, *100*(8), e02741. doi:10.1002/ecy.2741

Egli, M., Mirabella, A., Sartori, G., & Fitze, P. (2003). Weathering rates as a function of climate: results from a climosequence of the Val Genova (Trentino, Italian Alps). *Geoderma*, *111*(1–2), 99–121. doi:10.1016/S0016-7061(02)00256-2

Fowler, D., Coyle, M., Skiba, U., Sutton, M. A., Cape, J. N., Reis, S., … Voss, M. (2013). The global nitrogen cycle in the twenty-first century. *Philosophical Transactions of the Royal Society of London. Series B, Biological Sciences*, *368*(1621), 20130164. doi:10.1098/rstb.2013.0164

Galloway, J. N., Dentener, F. J., Capone, D. G., Boyer, E. W., Howarth, R. W., Seitzinger, S. P., … V�osmarty, C. J. (2004). Nitrogen cycles: past, present, and future. *Biogeochemistry*, *70*(2), 153–226. doi:10.1007/s10533-004-0370-0

Giger, D. R., & Schmitt, G. J. (1983). *Soil survey of the Sierra National Forest area,California.* . United States Department of Agriculture (USDA) Forest Service Publication, Clovis. Retrieved from https://www.nrcs.usda.gov/wps/portal/nrcs/surveylist/soils/survey/state/?stateId=CA

Glatzel, S., Kalbitz, K., Dalva, M., & Moore, T. (2003). Dissolved organic matter properties and their relationship to carbon dioxide efflux from restored peat bogs. *Geoderma*, *113*(3–4), 397–411. doi:10.1016/S0016-7061(02)00372-5

Goulden, M., & Bales, R. (2014). Mountain runoff vulnerability to increased evapotranspiration with vegetation expansion. *Proceedings of the National Academy of Sciences of the United States of America*, *111*(39), 14071–14075. doi:10.1073/pnas.1319316111

Goulden, M. L., Anderson, R. G., Bales, R. C., Kelly, A. E., Meadows, M., & Winston, G. C. (2012). Evapotranspiration along an elevation gradient in California's Sierra Nevada. *Journal of Geophysical Research*, *117*(G3). doi:10.1029/2012JG002027

Graham, R., Rossi, A., & Hubbert, R. (2010). Rock to regolith conversion: Producing

hospitable substrates for terrestrial ecosystems. *GSA Today*, 4–9. doi:10.1130/GSAT57A.1

Hall, A. (1999). Ammonium in granites and its petrogenetic significance. *Earth-Science Reviews*, *45*(3–4), 145–165. doi:10.1016/S0012-8252(99)00006-9

Handley, L. L., Austin, A. T., Stewart, G. R., Robinson, D., Scrimgeour, C. M., Raven, J. A., … Schmidt, S. (1999). The 15N natural abundance (δ15N) of ecosystem samples reflects measures of water availability. *Functional Plant Biology*, *26*(2), 185. doi:10.1071/PP98146

Hart, S. C. (2006). Potential impacts of climate change on nitrogen transformations and greenhouse gas fluxes in forests: a soil transfer study. *Global Change Biology*, *12*(6), 1032–1046. doi:10.1111/j.1365-2486.2006.01159.x

Hart, S., & Firestone, M. (1991). Forest floor-mineral soil interactions in the internal nitrogen cycle of an old-growth forest. *Biogeochemistry*, *12*(2). doi:10.1007/BF00001809

Hilton, R. G., Galy, A., West, A. J., Hovius, N., & Roberts, G. G. (2013). Geomorphic control on the δ_{15}N of mountain forests. *Biogeosciences*, *10*(3), 1693–1705. doi:10.5194/bg-10-1693-2013

Hobbie, E. A., & Ouimette, A. P. (2009). Controls of nitrogen isotope patterns in soil profiles. *Biogeochemistry*, *95*(2–3), 355–371. doi:10.1007/s10533-009-9328-6

Houlton, B. Z., & Morford, S. L. (2015). A new synthesis for terrestrial nitrogen inputs. *SOIL*, *1*(1), 381–397. doi:10.5194/soil-1-381-2015

Houlton, B. Z., Morford, S. L., & Dahlgren, R. A. (2018). Convergent evidence for

widespread rock nitrogen sources in Earth's surface environment. *Science*, *360*(6384), 58–62. doi:10.1126/science.aan4399

Jenny, H. (1928). Relation of climatic factors to the amount of nitrogen in soils1. *Agronomy Journal*, *20*(9), 900–912. doi:10.2134/agronj1928.00021962002000090003x

Jenny, H. (1980). *The Soil Resource* (Vol. 37). New York, NY: Springer New York. doi:10.1007/978-1-4612-6112-4

Jenny, H. (1994). *Factors Of Soil Formation: A System Of Quantitative Pedology (dover Earth Science)* (p. 320). New York: Dover Publications.

Jones, D. (1999). Biodegradation kinetics and sorption reactions of three differently charged amino acids in soil and their effects on plant organic nitrogen availability. *Soil Biology and Biochemistry*, *31*(9), 1331–1342. doi:10.1016/S0038-0717(99)00056-5

Kaiser, K., & Kalbitz, K. (2012). Cycling downwards – dissolved organic matter in soils. *Soil Biology and Biochemistry*, *52*, 29–32. doi:10.1016/j.soilbio.2012.04.002

Kelly, A. E., & Goulden, M. L. (2016). A montane Mediterranean climate supports year-round photosynthesis and high forest biomass. *Tree Physiology*, *36*(4), 459–468. doi:10.1093/treephys/tpv131

Kleber, M., Nico, P. S., Plante, A., Filley, T., Kramer, M., Swanston, C., & Sollins, P. (2011). Old and stable soil organic matter is not necessarily chemically recalcitrant: implications for modeling concepts and temperature sensitivity. *Global Change Biology*, *17*(2), 1097–1107. doi:10.1111/j.1365-2486.2010.02278.x

Kögel-Knabner, I., Guggenberger, G., Kleber, M., Kandeler, E., Kalbitz, K., Scheu, S., … Leinweber, P. (2008). Organo-mineral associations in temperate soils: Integrating biology, mineralogy, and organic matter chemistry. *Journal of Plant Nutrition and Soil Science*, *171*(1), 61–82. doi:10.1002/jpln.200700048

LeBauer, D. S., & Treseder, K. K. (2008). Nitrogen limitation of net primary productivity in terrestrial ecosystems is globally distributed. *Ecology*, *89*(2), 371–379. doi:10.1890/06-2057.1

Lybrand, R. A., Heckman, K., & Rasmussen, C. (2017). Soil organic carbon partitioning and Δ14C variation in desert and conifer ecosystems of southern Arizona. *Biogeochemistry*, *134*(3), 261–277. doi:10.1007/s10533-017-0360-7

MacDonald, N. W., Zak, D. R., & Pregitzer, K. S. (1995). Temperature effects on kinetics of microbial respiration and net nitrogen and sulfur mineralization. *Soil Science Society of America Journal*, *59*(1), 233–240. doi:10.2136/sssaj1995.03615995005900010036x

Macko, S. A., & Estep, M. L. F. (1984). Microbial alteration of stable nitrogen and carbon isotopic compositions of organic matter. *Organic Geochemistry*, *6*, 787–790. doi:10.1016/0146-6380(84)90100-1

Macko, S. A., Fogel, M. L., Hare, P. E., & Hoering, T. C. (1987). Isotopic fractionation of nitrogen and carbon in the synthesis of amino acids by microorganisms. *Chemical Geology: Isotope Geoscience Section*, *65*(1), 79–92. doi:10.1016/0168-9622(87)90064-9

Manzoni, S., Schimel, J. P., & Porporato, A. (2012). Responses of soil microbial communities to water stress: results from a meta-analysis. *Ecology*, *93*(4), 930–938.

doi:10.1890/11-0026.1

McFarlane, K. J., Torn, M. S., Hanson, P. J., Porras, R. C., Swanston, C. W., Callaham, M. A., & Guilderson, T. P. (2013). Comparison of soil organic matter dynamics at five temperate deciduous forests with physical fractionation and radiocarbon measurements. *Biogeochemistry*, *112*(1–3), 457–476. doi:10.1007/s10533-012-9740-1

McGill, W. B., & Cole, C. V. (1981). Comparative aspects of cycling of organic C, N, S and P through soil organic matter. *Geoderma*, *26*(4), 267–286. doi:10.1016/0016-7061(81)90024-0

Natelhoffer, K. J., & Fry, B. (1988). Controls on Natural Nitrogen-15 and Carbon-13 Abundances in Forest Soil Organic Matter. *Soil Science Society of America Journal*, *52*(6), 1633. doi:10.2136/sssaj1988.03615995005200060024x

Niboyet, A., Le Roux, X., Dijkstra, P., Hungate, B. A., Barthes, L., Blankinship, J. C., … Leadley, P. W. (2011). Testing interactive effects of global environmental changes on soil nitrogen cycling. *Ecosphere*, *2*(5), art56. doi:10.1890/ES10-00148.1

Oades, J. M. (1989). An introduction to organic matter in mineral soils. In J. B. Dixon & S. B. Weed (Eds.), *Minerals in soil environments* (pp. 89–159). Madison, WI, USA: Soil Science Society of America. doi:10.2136/sssabookser1.2ed.c3

O'Geen, A. T., Safeeq, M., Wagenbrenner, J., Stacy, E., Hartsough, P., Devine, S., … Bales, R. (2018). Southern sierra critical zone observatory and kings river experimental watersheds: A synthesis of measurements, new insights, and future directions. *Vadose Zone Journal*, *17*(1), 180081. doi:10.2136/vzj2018.04.0081

Philben, M., Billings, S. A., Edwards, K. A., Podrebarac, F. A., van Biesen, G., &

Ziegler, S. E. (2018). Amino acid δ15N indicates lack of N isotope fractionation during soil organic nitrogen decomposition. *Biogeochemistry*, *138*(1), 69–83. doi:10.1007/s10533-018-0429-y

Pope, G. A. (1995). Internal weathering in quartz grains. *Physical Geography*, *16*(4), 315–338. doi:10.1080/02723646.1995.10642556

Rasmussen, C., Southard, R. J., & Horwath, W. R. (2007). Soil mineralogy affects conifer forest soil carbon source utilization and microbial priming. *Soil Science Society of America Journal*, *71*(4), 1141–1150. doi:10.2136/sssaj2006.0375

Rasmussen, C., Torn, M. S., & Southard, R. J. (2005). Mineral assemblage and aggregates control carbon dynamics in a california conifer forest. *Soil Science Society of America Journal*, *69*(6), 1711. doi:10.2136/sssaj2005.0040

Riebe, C. S., Hahm, W. J., & Brantley, S. L. (2017). Controls on deep critical zone architecture: a historical review and four testable hypotheses. *Earth Surface Processes and Landforms*, *42*(1), 128–156. doi:10.1002/esp.4052

Robinson, D. (2001). δ15N as an integrator of the nitrogen cycle. *Trends in Ecology & Evolution*, *16*(3), 153–162. doi:10.1016/S0169-5347(00)02098-X

Ros, G. H., Hoffland, E., van Kessel, C., & Temminghoff, E. J. M. (2009). Extractable and dissolved soil organic nitrogen – A quantitative assessment. *Soil Biology and Biochemistry*, *41*(6), 1029–1039. doi:10.1016/j.soilbio.2009.01.011

Rustad, L., Campbell, J., Marion, G., Norby, R., Mitchell, M., Hartley, A., … GCTE-News. (2001). A meta-analysis of the response of soil respiration, net nitrogen mineralization, and aboveground plant growth to experimental ecosystem warming.

Oecologia, *126*(4), 543–562. doi:10.1007/s004420000544

Shangguan, W., Hengl, T., Mendes de Jesus, J., Yuan, H., & Dai, Y. (2017). Mapping the global depth to bedrock for land surface modeling. *Journal of Advances in Modeling Earth Systems*, *9*(1), 65–88. doi:10.1002/2016MS000686

Sistla, S. A., & Schimel, J. P. (2012). Stoichiometric flexibility as a regulator of carbon and nutrient cycling in terrestrial ecosystems under change. *The New Phytologist*, *196*(1), 68–78. doi:10.1111/j.1469-8137.2012.04234.x

Sollins, P., Swanston, C., Kleber, M., Filley, T., Kramer, M., Crow, S., … Bowden, R. (2006). Organic C and N stabilization in a forest soil: Evidence from sequential density fractionation. *Soil Biology and Biochemistry*, *38*(11), 3313–3324. doi:10.1016/j.soilbio.2006.04.014

Sparks, D. L., Page, A. L., Helmke, P. A., Loeppert, R. H., Soltanpour, P. N., Tabatabai, M. A., Sumner, M. E. (Eds.). (1996). *Methods of soil analysis: part 3 chemical methods. Soil pH and soil acidity.* (J.M. Bigham., pp. 475–490). Madison, WI, USA: Soil Science Society of America, American Society of Agronomy. doi:10.2136/sssabookser5.3

Stuiver, M., & Polach, H. A. (1977). Discussion; reporting of C-14 data. *Radiocarbon*.

Swanston, C., Caldwell, B., Homann, P., Ganio, L., & Sollins, P. (2002). Carbon dynamics during a long-term incubation of separate and recombined density fractions from seven forest soils. *Soil Biology and Biochemistry*, *34*(8), 1121–1130. doi:10.1016/S0038-0717(02)00048-2

Tian, Z., Moreland, K., O'Geen, A., McFarlane, K., Hartsough, P., Hart, S., … Berhe, A.

A. (In review). Deep in the critical zone: weathered bedrockrepresents a large and potentially active pool of soil carbon.

Trumbore, S. E., & Harden, J. W. (1997). Accumulation and turnover of carbon in organic and mineral soils of the BOREAS northern study area. *Journal of Geophysical Research*, *102*(D24), 28817–28830. doi:10.1029/97JD02231

van Groenigen, J. W., Huygens, D., Boeckx, P., Kuyper, T. W., Lubbers, I. M., Rütting, T., & Groffman, P. M. (2015). The soil N cycle: new insights and key challenges. *SOIL*, *1*(1), 235–256. doi:10.5194/soil-1-235-2015

Vogel, J. S., Southon, J. R., Nelson, D. E., & Brown, T. A. (1984). Performance of catalytically condensed carbon for use in accelerator mass spectrometry. *Nuclear Instruments and Methods in Physics Research Section B: Beam Interactions with Materials and Atoms*, *5*(2), 289–293. doi:10.1016/0168-583X(84)90529-9

von Lutzow, M., Kogel-Knabner, I., Ekschmitt, K., Matzner, E., Guggenberger, G., Marschner, B., & Flessa, H. (2006). Stabilization of organic matter in temperate soils: mechanisms and their relevance under different soil conditions - a review. *European Journal of Soil Science*, *57*(4), 426–445. doi:10.1111/j.1365-2389.2006.00809.x

Weil, R., & Brady, N. (2016). *The Nature And Properties Of Soils (15th Edition)* (15th ed., p. 1104). Columbus: Pearson.

Wieder, W. R., Cleveland, C. C., Smith, W. K., & Todd-Brown, K. (2015). Future productivity and carbon storage limited by terrestrial nutrient availability. *Nature Geoscience*, *8*(6), 441–444. doi:10.1038/ngeo2413

Yost, J. L., & Hartemink, A. E. (2020). How deep is the soil studied – an analysis of four soil science journals. *Plant and Soil*. doi:10.1007/s11104-020-04550-z

CHAPTER 5: CONCLUSION

SUMMARY

It remains unclear how the whole soil profile, from topsoil to bedrock, will respond to projected changes in climate. Over the next century, subsoils are projected to warm at roughly the same rate as surface soils with the potential to release an equivalent of 30% of annual fossil fuel derived carbon dioxide (CO_2) emission (Hicks-Pries et al. 2017). In my dissertation research, I addressed major knowledge gaps in our understanding of climatic controls on subsoil organic matter (OM) dynamics. Specifically, I investigated how climate exerts both indirect and direct controls on whole soil profile organic carbon (OC) and nitrogen (N) storage, composition, stabilization mechanisms, and persistence, making explicit comparisons between dynamics in subsoil versus topsoil.

Results from my dissertation research suggests that the effect of climate on N and OC storage is primarily through its effect on weathered bedrock thickness, and not necessarily concentration of carbon (C) or N in the regolith. My research showed that C and N in the free light fraction (fLF) in both the topsoil and subsoil is most vulnerable to changes in climate compared to the occluded light and mineral-associated C fractions. I found that subsoil mineral-associated C is also vulnerable, but to a lesser degree than fLF. Furthermore, I showed that C in the occluded fraction and the N in the mineral-associated fraction are not responsive to variability in climate, suggesting that that these pools of OM likely significantly contribute to persistent of OM in soil, even under changing climate scenarios. Findings from my dissertation research led to the logical conclusion

that climate exerts fundamental controls on amount of C and N stored in subsoil and their persistence highlighting the need to consider subsoil OM dynamics in future global soil C and climate modeling efforts.

Below I summarize the main take away message from each of my dissertation chapters.

Chapter 2: *Deep in the critical zone: weathered bedrock represents a large and potentially active pool of soil carbon*

Large uncertainty remains in our quantification of the spatial distribution of deep soil C storage and process-level understanding of climatic controls on belowground C storage. In chapter 2 of my dissertation, I presented whole-regolith C stocks, residence times, and organic matter (OM) composition, including C stores in deep weathered bedrock, for diverse set of soils along a bio-climatic gradient in the Sierra Nevada of California. I found that up to 78% of soil C is stored below a 0.3 m depth, with up to 29% of total C stored below 1.5 m. I observed significant and varying amounts of deep OC at the four climatic zones, with the highest OC storage occurring at mid-elevations where climate is most conducive to weathering and higher net primary productivity. A conservative global scaling of these results points to deep weathered bedrock storing over 200 Pg of organic carbon (OC), that is so far not accounted for in global carbon accounting. Radiocarbon, Fourier transformed infrared spectroscopy, elemental, and isotopic analyses revealed that deep soil and weathered bedrock OC is made up of mixture of both relatively fresh material and older, more decomposed OC. Collectively, this work illustrates that OC in weathered bedrock represent a massive, previously unrealized OC

pool, which is potentially susceptible to losses caused by changes in climate and the introduction of new organic matter at depth.

My findings demonstrate that regolith thickness, which is governed in part by climate, directly influences deep OC inventory and indirectly influences OC cycling. The large stock of persistent OC in weathered bedrock represents a previously unexplored pool of OC in the Earth system. This analysis provides a deeper understanding of the processes regulating OC input, storage, and turnover to improve estimations of the true capacity of the critical zone to store OC and the vulnerability of deep OC to changes in climate.

Chapter 3: *Climatic controls on deep soil organic carbon distribution and persistence*

To investigate how climate drives persistence and stabilization mechanisms of SOM in topsoil compared to subsoil layers, I performed density fractionation and analyzed the fractions (free light fraction [fLF], occluded light fraction [oLF], and heavy fraction [HF]) using elemental analysis, radiocarbon, and Fourier transformed infrared spectroscopy (FTIR). SOC persistence, partitioning into each fraction, and the C:N varied the most from the moisture-limited oak savannah to the energy-limited conifer systems. The oak savannah ecosystem we studied had the lowest C concentration, C:N ratio, most depleted $\Delta^{14}C$ value of SOM, oldest modeled turnover time in the free light and mineral associated fractions, highest aromatic:aliphatic ratio in the mineral-associated pool and stored the majority of C in the mineral associated pool. Most surprisingly, I found that SOC in the free light fractions at the lowest elevation oak savanna ecosystem can persist in subsoils from centuries to millennia. These results suggest that moisture limited ecosystems can store very persistent, microbially processed C that it associated with

minerals and the unprotected pool in both the topsoil and subsoil. The mineral associated HF exhibited decreasing C:N ratios, increased aromatics:aliphatics, and increasing $\delta_{13}C$, suggesting that microbial-derived OM may contributes higher proportions to OM in subsoil horizons than plant-derived OM in this fraction. As elevation increases, and climate changes towards lower temperature and higher precipitation, I found that more soil C partitions into the fLF and oLF, compared to the oak savannah. The mid-elevation sites had the highest proportion of soil C stocks in subsoil, the occluded light fraction had similar turnover times (if not longer) compared to the mineral associated HF pool. The oLF pool did not correlate significantly with climate proxies, suggesting that aggregation plays important role in C persistence.

I used a mixed effects statistical model to analyze how climate impacts C persistence in the topsoil and subsoil fractions and showed that actual evapotranspiration and gross primary productivity (GPP) account for a significant amount of variability in the persistence of free particulate C fraction throughout the profile and the subsoil mineral associated HF pool. The model results coupled with the faster turnover times of free light fraction indicate that this pool is most vulnerable to changes in climate in both the topsoil and subsoil. Overall, results I reported in this chapter suggest that the most active pool of C in the entire profile is the fLF, and that aggregate protected C (oLF) stores persistent C, for similar timescales as we found in HF. One of the most important findings in this chapter is the presence of actively cycling C in the subsoil that is vulnerable to changes in climate, suggesting an important mechanism for how subsoil C is likely to respond to predicted changes in climate.

Chapter 4: *Climatic controls on soil nitrogen stock, distribution, composition, and persistence in deep versus near-surface soil layers*

The third chapter focuses on climatic impacts on total N (TN) in bulk soil (including weathered bedrock) and density fraction. Concentration of TN was low in weathered bedrock (similar to C). However, weathered bedrock accounted for up to 37% of profile N in the mid-elevation site where the weathered bedrock was thickest. Climate, through its controls on regolith thickness regulated amounts of N weathered bedrock, and hence the whole soil profile N accounting. Climates that are either too cold (highest elevation) or too hot/dry (lowest elevation) are not conducive for large scale weathering of bedrock providing further proof to my conclusion on the indirect link between climate and N storage that is mediated through profile thickness.

Modeled turnover rate of N increased with elevation to a maximum at the mixed conifer site and then decreased in the highest elevation sub alpine site indicating that the mid-elevation sites with thicker weathered bedrock store more persistent N in the subsoil. The density fractionation results illustrate that, as elevation increases, N partitions more into the fLF and the oLF, mimicking C trends at these sites. These results suggest that accumulation of N in our study bio-climosequence relies on the physically protected (occluded) and free particulate pools of N, as we previously reported for C in chapter 3. Similar to the conclusions I drew for Chapter 3, I also found an indirect impact of climate on soil N stock and distribution that is mediated via climate's impact on GPP and soil weathering. The fractionation results also suggest that OM with long turnover times store N in physically protected and mineral-associated pools in soil (oLF and HF, respectively)

and the majority of the stable N in subsoil is associated with minerals in the HF. A mixed effect statistical model that was used to test climatic effects on the fraction N accumulation in the topsoil and subsoil showed that the free particulate and occluded light fraction TN significantly correlate with the climatic proxies tested, especially GPP, mean annual precipitation, mean annual temperature, and deep water percolation. The mineral associated HF pool TN did not correlate significantly with any of the climate parameters tested. My results indicate that TN is most persistent in the mineral-associated HF pool that is not impacted by climate whereas, the N contained within the free light and occlude light fractions are vulnerable to changes in climate. Lastly, the stable isotope $\delta_{15}N$ composition of soils along the southern Sierra elevation gradient suggests likely indirect influence of climate on soil N composition through its impact on mycorrhizal use of N in deep soils. Overall, I found that climate exerts both a direct and an indirect control on soil N accumulation and persistence.

FUTURE DIRECTIONS

Climate change is one of the most challenging problems facing humanity today. Millions of human lives and the health and wellbeing of countless species and ecosystems are at stake as we grapple with global climate changes that threaten the future habitability of our planet. The 2018 IPCC report stating we have to cut our emissions by half by 2030 in order to save the planet from a temperature increase of 1.5 ºC globally (IPCC, 2018). If we continue to release CO_2 and other greenhouse gases at the same rate as today, our world will be different in coming centuries. Fortunately, scientific and policy solutions for climate change mitigation and adaptation do exisit. Soils are meaningful piece to the

solution to address climate change, if they are managed right. My dissertation builds the foundation for considering deep soil carbon sequestration as part of a comprehensive approach to use natural climate change solutions as it contributes to the current knowledge base of how the entire soil profile responds to climate.

Past research mostly focused on the topsoil (30 cm), based on the assumption that deep soils do not interact with the atmosphere. However, this dissertation illustrates that subsoil C and N can be vulnerable to changes in climate and therefore dynamics of subsoil process deserve further investigation in order to improve our understanding of the amount and rate of the response of the entire soil OM stock to climate change. This work, covering samples that were collected from topsoil to bedrock contact (past 10 m), importantly illustrates the need to go below 1 m in our soil C and N studies.

Over the next century, if subsoils warm at roughly the same rate as surface soils as expected, our ability to predict the effect of the temperature increase on C cycling is so far uncertain. This is particularly true for the large amount of carbon stored in deep weathered bedrock, where ambient temperature swings are muted, and OC is isolated from high rates of microbial activity. However, results from my dissertation research clearly show that OC in weathered bedrock is a mixture of relatively young and old OM that has experienced different degrees of decomposition. If relatively younger OM is entering weathered bedrock and diluting the old OM pools (as we observed with the FTIR results from Chapters 3 and 4), then climatic factors are likely to influence not only the amount, but also the composition and persistence of OM in regolith. Specifically, temperature may exert a strong control on regolith OC storage and dynamics under a

changing climate scenario through both its effects on plant productivity and OC input into the deep regolith.

My study provides compelling evidence to justify further investigations in different ecosystems of soil and deep regolith OC sensitivity to changes in temperature critical for predictions of future response of terrestrial OC to climate. Similarly, it is important to highlight major knowledge gaps that exist in our understanding of how changes in precipitation, amount, and timing might affect flow of water and dissolved C and N through soil, further highlighting the gaps in our current understanding of deep soil's response to climate change. Many more critical questions remain unanswered about the magnitude of loss of soil C that can be expected with anticipated scenarios of climate change. Most importantly, how will different subsoil systems respond to climate change and at what rate? Hans Jenny's five state factors of soil formation can be a useful guiding framework to explore subsoil dynamics under changing climate by allowing us to focus on systems with different degrees of variability with climate and vegetation type (especially permafrost), parent material minerology (soils with varying amounts of short-order range, iron and aluminum available for sorptive stabilization of OM), microbial abundance and community composition, topography, or time (weathering extent). Secondly, my dissertation research showed that specific pools of OM show distinct degrees of vulnerability to climate change. For C the topsoil and subsoil free light and subsoil mineral associated pools showed a stronger association with GPP and ET, while for N the topsoil and subsoil free light and occluded light fraction showed significant correlation with climate. These results highlight the need for more in-depth investigation on specific compound classes in these fractions and if SOM composition contribute to

stabilization and destabilization of C and/or N in deep soil, under varying climatic conditions.

The current average depth of soil covered in most studies including SOM dynamics and carbon sequestration today is about 23 cm, while the average thickness of soil is presumed to be more than 2 m (Yost and Hartemink 2020). My dissertation research highlighted the need to dig deeper (preferably to bedrock contact) in order to derive sufficiently accurate estimations of soil organic C and N stocks and determine stability and vulnerability of soil C and N pools at depth. The previous focus of most soil and biogeochemistry studies on topsoil dynamics has skewed our understanding of how the entire soil system works. Findings from all three chapters (2 - 4) of my dissertation highlight that subsoil C or N dynamics cannot be predicted from topsoil alone. Attempts to generalize soil C and N patterns based on observations of topsoil is likely to prove inadequate and could lead to subsequently loss of political will that is needed for protection of subsoil C and N from loss. Accurate accounting for the role of subsoil is also critical from a management perspective as currently, the focus for soil management is on the top 30 cm and my study demonstrated the need for management options to sustain the current and potential subsoil SOM stocks and prioritization of subsoil C sequestration. Better accounting of deep soil C and N dynamics, and its contributions to climate change mitigation are of paramount global significance. A robust understanding of key biological, physical and chemical processes that control biogeochemical cycles of C and N along the entire soil profile is critical for accurate prediction of response of soil C and N to warming that is needed to fine tune accurate Earth system and land models

that predict our future climate and devise informed and innovative solutions to address climate change.

REFERENCES

Hicks Pries, C.E., Castanha, C., Porras, R.C. and Torn, M.S. 2017. The whole-soil carbon flux in response to warming. *Science* 355(6332), pp. 1420–1423.

IPCC 2018. Global Warming of 1.5 °C an IPCC special report on the impacts of global warming of 1.5 °C above pre-industrial levels and related global greenhouse gas emission pathways, in the context of strengthening the global response to the threat of climate change, sustainable development, and efforts to eradicate poverty. Geneva, Switzerland: (IPCC) Intergovernmental Panel on Climate Change.

Yost, J.L. and Hartemink, A.E. 2020. How deep is the soil studied – an analysis of four soil science journals. *Plant and soil*.